

2012

Method to partition between freely suspended Escherichia coli and Escherichia coli attached to clay particles

Xiao Liang
Iowa State University

Follow this and additional works at: <http://lib.dr.iastate.edu/etd>

 Part of the [Bioresource and Agricultural Engineering Commons](#), [Environmental Engineering Commons](#), and the [Environmental Sciences Commons](#)

Recommended Citation

Liang, Xiao, "Method to partition between freely suspended Escherichia coli and Escherichia coli attached to clay particles" (2012). *Graduate Theses and Dissertations*. 12382.
<http://lib.dr.iastate.edu/etd/12382>

This Thesis is brought to you for free and open access by the Graduate College at Iowa State University Digital Repository. It has been accepted for inclusion in Graduate Theses and Dissertations by an authorized administrator of Iowa State University Digital Repository. For more information, please contact digirep@iastate.edu.

**Method to partition between freely suspended *Escherichia coli* and *Escherichia coli*
attached to clay particles**

by

Xiao Liang

A thesis submitted to the graduate faculty
in partial fulfillment of the requirements for the degree of
MASTER OF SCIENCE

Major: Agricultural Engineering

Program of Study Committee:

Michelle Soupir, Major Professor

Laura Jarboe

Chenxu Yu

Iowa State University

Ames, Iowa

2012

Copyright © Xiao Liang, 2012. All rights reserved.

TABLE OF CONTENTS

LIST OF TABLES	vi
LIST OF FIGURES	vii
ACKNOWLEDGEMENTS	ix
ABSTRACT	x
CHAPTER 1 GENERAL INTRODUCTION	1
1.1 Introduction	1
1.2 Goal and objectives	2
CHAPTER 2 LITERATURE REVIEW	3
2.1 Bacteria.....	3
2.1.1 Bacteria and water quality	3
2.1.2 Fecal indicator bacteria.....	4
2.2 <i>Escherichia coli</i>	9
2.2.1 Introduction of <i>Escherichia coli</i>	9
2.2.2 Sources of <i>E. coli</i> in waters	10
2.2.3 Transport and fate of <i>E. coli</i> in the environment.....	10
2.3 Detection methods.....	13
2.3.1 Separation techniques	13
2.3.2 Dispersion techniques.....	15
2.3.3 Dilution and membrane filtration	17
2.3.4 Flow cytometry.....	17
2.3.4 Summary.....	21
CHAPTER 3 MATERIAL AND METHODS	22

3.1 Research considerations	22
3.1.1 Bacteria cultures	22
3.1.2 Soils	23
3.1.3 Selection of experimental partitioning methods	23
3.1.4 Particle ratios	26
3.2 Experimental design	27
3.2.1 Settling (or centrifugation followed by Settling).....	27
3.2.2 Flow cytometry.....	28
3.3 Calculations and statistical analysis	29
3.3.1 Percent attached calculations.....	29
3.3.2 Statistical analysis.....	29
CHAPTER 4 RESULTS AND DISCUSSIONS	32
4.1 Results	32
4.1.1 Settling method.....	33
4.1.2 Flow cytometry.....	39
4.1.3 Method comparisons.....	46
4.2 Discussion	52
4.2.1 Impacts of clay type on bacteria attachment	52
4.2.2 Impacts from particle ratios on bacteria attachment.....	53
4.2.3 Impacts of bacterial cell properties on attachment to particles	56
4.2.4 Advantages and limitations of flow cytometry.....	58
CHAPTER 5 CONCLUSIONS	61
5.1 General discussion and conclusions	61
5.2 Implications and recommendation for future research.....	62

REFERENCES	64
APPENDIX A. RESEARCH CONSIDERATIONS	76
APPENDIX A1. Absorbance values of soil samples at discrete time	76
APPENDIX A2. Bacteria count changes after centrifugation	76
APPENDIX A3. Calculations for soil concentrations by surface area	77
APPENDIX B. EXPERIMENTAL DESIGN	78
APPENDIX B1. Settling samples	78
APPENDIX B2. Flow cytometry samples	81
APPENDIX C. RAW DATA	83
APPENDIX C1. Percent attached of strain #31 in the settling method	83
APPENDIX C2. Percent attached of strain #50 in the settling method	90
APPENDIX C3. Percent attached of strain #89 in the settling method	97
APPENDIX C4. Percent attached of strain #43888 in the settling method	104
APPENDIX C5. Percent attached of strain #31 in flow cytometry	111
APPENDIX C6. Percent attached of strain #50 in flow cytometry	113
APPENDIX C7. Percent attached of strain #89 in flow cytometry	115
APPENDIX D. FLOW CYTOMETRY RESULT ANALYSIS FIGURES	117
Appendix D1. Strain #31	117
Appendix D2. Strain #50	121
Appendix D3. Strain #89	125
APPENDIX E. R CODE IN S STATISTICAL TESTS	129
APPENDIX E1. Statistical tests for data from the settling method	129
APPENDIX E2. Statistical tests for data from flow cytometry	132
APPENDIX E3. Statistical tests for method comparisons	135

APPENDIX E4. One sample t-tests	137
APPENDIX F. DATA TRANSFORMATIONS	138
APPENDIX F1. Original data distributions.....	138
APPENDIX F2. Normality tests after transformations.....	146
APPENDIX G. THREE-WAY ANOVA TEST RESULTS	156
APPENDIX G1. Results for natural log attachment ratios by flow cytometry.....	156
APPENDIX G2. Results for attachment ratios by the settling method.....	156
APPENDIX G3. Results for natural log attachment ratio difference between flow cytometry and the settling method	156
APPENDIX H. PAIRWISE COMPARISONS BETWEEN DIFFERENT SURFACE AREA RATIOS	157
APPENDIX I EXAMPLE OF ORIGINAL DOT PLOTS FROM FLOW CYTOMETRY WITH CONTROLS	160

LIST OF TABLES

Table 1. <i>E. coli</i> Criteria (Organisms/100ml of water)	7
Table 2. Clay particles with key properties	23
Table 3. Average percent attached of each variable	33
Table 4. Attachment difference between different clays in the settling method (p-values are in parentheses).....	35
Table 5. Partial pairwise comparisons of attachment ratios between different particle ratios in the settling method (only showing the comparisons without significant differences).....	37
Table 6. Attachment difference between different strains in the settling method (p-values are in parentheses)..	39
Table 7. Attachment difference between different clays in flow cytometry (p-values are in parentheses).....	42
Table 8. Pairwise comparisons of attachment ratios between different particle ratios from flow cytometry (only showing the comparisons without significant differences).....	44
Table 9. Attachment difference between different strains in flow cytometry (p-values are in parentheses).....	46
Table 10. The estimated expense for major cost of 100 samples in two methods.....	58

LIST OF FIGURES

Figure 1. Relationships between total coliform, fecal coliform, <i>E. coli</i> , and enterococci.....	8
Figure 2. Schematic of a flow cytometer (modified from Brown and Wittwer, 2000)	19
Figure 3. Flow chart of the settling method procedures	28
Figure 4. Scatter plots of attachment ratios from the settling method showing clay particle variability.	34
Figure 5. Boxplots of attachment ratios in the settling method analyzed by clay type.	36
Figure 6. Boxplots of attachment ratios from the settling method analyzed by strain.	37
Figure 7. Scatter plots of attachment ratios from the settling method.	38
Figure 8. Average percent attached of strain #31 to Hectorite	40
Figure 9. Ideal dot plot from the flow cytometry separation technique.....	40
Figure 10. Scatter plots of attachment ratios by from flow cytometry.	41
Figure 11. Boxplots of attachment ratios analyzed by clay type from samples collected using flow cytometry separation technique.	43
Figure 12. Boxplots of attachment ratios analyzed by strain from samples collected using flow cytometry separation technique.	44
Figure 13. Scatter plots of attachment ratios from the flow cytometry separation technique.	45
Figure 14. Residuals vs. fitted values for the natural log attachment ratio differences between flow cytometry and the settling method (surface area 1 and 2 removed).	47
Figure 15. Scatter plot of the natural log attachment ratio differences between flow cytometry and the settling method.	48
Figure 16A. Boxplots of natural log attachment ratio differences between flow cytometry and the settling method by clay type.	49

Figure 16B. Boxplots of natural log attachment ratio differences between flow cytometry and the settling method by strain.	49
Figure 16C. Boxplots of natural log attachment ratio differences between flow cytometry and the settling method by surface area ratio	51
Figure 17A. Histogram of <i>E. coli</i> strain #31 attachment to Montmorillonite K-10 over three different particle ratio.	55
Figure 17B. Histogram of <i>E. coli</i> strain #31 attachment to Kaolin over three different particle ratio.	55

ACKNOWLEDGEMENTS

First, I would like to thank my advisor, Michelle Soupir, for all her support and guidance throughout my M.S. programs, for creating and supporting a research environment in our laboratory. Thanks to this research environment that I have succeeded and enjoyed my experience as a master student.

I would also like to thank my committee members Laura Jarboe and Chenxu Yu for their advices and support.

Many thanks to Shawn Rigby for his efforts in flow cytometry operations and analysis and to Wei Zhang for her work in statistical analysis.

Special thanks to Amy Cervantes, Claire Hruby, Jason Garder, Joshua Claypool, Rohith Gali, and Pramod Pandey for always answering question, providing assistance in the laboratory work as well as analyzing results.

Thanks to Nathan Willey and Amanda Homan for providing assistance in laboratory work. Thanks for your diligence and responsibility.

Finally, I would like to thank my parents, for their love, support, encouragement, and patience while I lived so far away from home during my study in Iowa State University.

This research was partially funded by United States National Science Foundation.

ABSTRACT

Currently, about 29% of waters across the United States are impaired because of elevated bacterial levels (USEPA, 2009). While attachment of bacteria to particulates is one likely mode of transport through the environment, understanding of environmental transport mechanisms is lacking. Previous studies have shown that some bacteria preferentially attach to sediment but a standard procedure does not exist to separate attached and unattached bacteria. In this project, we are developing a practical and accurate method to distinguish and quantify between *E. coli* attached to clay particles and *E. coli* freely suspended in solution. Two methods to detect differences between unattached and attached *E. coli* were compared, settling (or centrifugation followed by settling) and flow cytometry. Each method was tested using three environmental strains collected from swine facilities and one research strain of *E. coli* (ATCC 43888, *E. coli* O157:H7 with Shiga-like toxin I and II removed); four clay particles: Hectorite (diameter: 1 μm , surface area: 63 m^2/g), Kaolinite (diameter: 1.25 μm , surface area: 11.2 m^2/g), Ca-Montmorillonite (diameter: 3 μm , surface area: 84 m^2/g), Montmorillonite K-10 (diameter: 6 μm , surface area: 240 m^2/g); and a range of surface area ratios (clay particle surface area to *E. coli* surface area).

From the results, *E. coli* were more likely to attach to clay particles with smaller sizes. As the surface area ratio increased from 1 to 1,000, the attachment ratio increased with greatest attachment occurring at a clay particle surface area to *E. coli* surface area ratio of 1,000, where an average of 59% of cells were attached. Moreover, the attachment ratio reached a maximum value of 99.8% for *E. coli* attachment to Kaolinite. When comparing the results of the two methods, the detected attachment ratios were always lower when using the flow cytometry method, especially for Hectorite, the smallest particle size tested in this project. The main limitation of the settling method is its inability to detect viable but non-culturable cells while the inability to discriminate live and dead cells is the main reason for the underestimated attachment fractions by flow cytometry method. Nevertheless, the increasing trend in attachment ratio from flow cytometry was similar to the results from the settling method. Our results indicate that flow cytometry is a rapid and accurate method to test the attachment ratio of *E. coli* to clay particles, but the method is still in need of further development.

CHAPTER 1 GENERAL INTRODUCTION

1.1 Introduction

Currently, 72,305 miles and 29% of impaired streams are contaminated by pathogens (USEPA, 2009), and pathogens are the leading cause of impairments in rivers and streams in United States. Waterborne human pathogens are microorganisms that are transmitted to people through drinking water or recreational water activities, including swimming, fishing, and boating. Pathogenic bacteria cause illnesses including but not limited to common gastroenteritis and diarrhea, typhoid fever, and dermatitis (Rosen, 2001; Pond, 2005). These diseases have posed a critical threat to public health. Diarrheal disease accounts for nearly 1.5 million of the 9 million children under the age of 5 who die needlessly each year across the world (UNICEF/WHO, 2009) and the infection of diarrhea is spread through contaminated food or drinking water. These diseases are not confined solely to undeveloped countries without modern water and sanitation systems. In the United States, between 1999 and 2000, there were 36 outbreaks of waterborne disease associated with drinking water and 59 outbreaks due to recreational water use (CDC, 2002). It is important to monitor waters across the United States for the presence of these pathogens in order to identify the original sources of the pathogens and the contaminated waters.

Monitoring bacteria is essential for environmental protection, but analysis of pathogens is difficult, time-consuming, expensive and potentially hazardous to workers (Myers et al., 2007). Fecal coliform was previously the most common indicator to evaluate water quality. *E. coli*, however, is accepted more extensively. *E. coli* was recommended as the primary indicators of fecal contamination in fresh waters in the U.S in 1986 by the U.S. EPA (USEPA, 1986). According to the Iowa water quality standard (USEPA, 2011), water bodies with a geometric mean of *E. coli* concentration higher than 126 CFU(colony forming units)/100 ml or with a single sample concentration higher than 235 CFU/100 ml will be considered impaired for primary and children's recreational use, and will require a plan for remediation.

Agriculture is a significant contributor of bacteria in the environment. Two major sources of bacteria in streams are from land application of manure from confined animal

systems and direct deposit by grazing animals (Soupir et al., 2006). Previous studies have shown that some bacteria preferentially attach to sediment (Gagliardi and Karns, 2000; Soupir et al., 2010; Liu et al., 2011). Bacteria attached to particulates tend to be more resistant to environmental changes such as ultraviolet radiation and such protection can increase bacterial survivals. From current knowledge, bacteria attachments in the aquatic environment could be influenced by various factors, including genetic, chemical, and physical factors, such as temperature, bacterial genotype, soil particle size, organic matter, water content, pH, and dissolved nutrients (Pachepsky et al., 2006). While attachment of bacteria to particulates is one likely mode of transport through the environment, understanding of environmental transport mechanisms is lacking. The impacts on bacterial attachments from most of these factors remain unknown. Moreover, currently, a standard procedure does not exist to separate attached and unattached *E. coli*.

1.2 Goal and objectives

The overall goal of the study was to develop a practical and accurate method to distinguish and quantify between *E. coli* attached to clay particles and *E. coli* freely suspended in solution. The specific objectives were to:

- Develop standard procedures for each suitable method; and
- Determine bacteria self-factors, such as genotype, and environmental factors, including clay type and concentrations, which impact bacteria attachment to clay particles;
- Compare flow cytometry and standard settling/centrifugation separation methods to partition between *E. coli* attached to clay particles and *E. coli* freely suspended in solution.

CHAPTER 2 LITERATURE REVIEW

2.1 Bacteria

2.1.1 Bacteria and water quality

Bacteria are a large domain of microscopic, single-celled, prokaryote microorganisms that display a wide range of metabolic types, geometric shapes and environmental habitats. There are approximately five nonillion (5×10^{30}) bacteria on earth, forming a biomass on earth, which exceeds that of all plants and animals (Hogan, 2010). Bacteria are ubiquitous in numerous environments and perform various complex actions, some of which are beneficial and some harmful. Certain bacteria, the Azotobacter on the roots of certain plants can convert nitrogen into a usable form (nitrogen fixation) (Halversen, 1927; Newton et al., 1953). A vast majority of the bacteria are rendered harmless by the protective effects of the immune system of humans. However, those that are infectious disease producing are referred to as pathogenic. Pathogenic bacteria cause illnesses including but not limited to typhoid fever, dysentery and gastroenteritis (Pond, 2005). Viruses, prion, some protozoans and fungus can also be pathogenic.

Pathogenic contamination of water has long been a concern to the public. Concern is increasing worldwide due to the outbreak of waterborne diseases. During the 1920's-1960's, *Salmonella typhi*, the bacillus which causes typhoid fever was considered a major problem in drinking water supplies (Craun, 1986) According to World Health Organization (WHO), diarrheal disease alone accounts for an estimated 4.1% of the total disability-adjusted life year (DALY) global burden of disease and is responsible for the death of 1.8 million people per year (WHO, 2004), while 88% of that burden is caused by consumption of unsafe drinking water. The infection of diarrheal is spread through contaminated food or drinking water. Diarrheal disease accounts for nearly 1.5 million of the 9 million children under the age of 5 who die needlessly each year across the world (UNIEF/WHO, 2009).

In recent years, scientists have identified a large number of pathogens responsible for waterborne disease outbreaks, and researches have focused on identifying their sources, development of resistance to water disinfection, and removal from drinking water supplies. The common bacterial infections of water diseases include *E. coli* infection, cholera, and

typhoid fever. Bathing, contact recreation, washing, and drinking can result in infection if the water is contaminated. Contact recreation and drinking uses are considered to be the two major routes of infection. *E. coli* outbreaks, most of which have been caused by a specific strain of *E. coli* bacteria such as *E. coli* O157:H7, have received much media coverage (WSDH, 2010). A number of *E. coli* O157:H7 outbreaks have been reported from recreational use of polluted waters, particularly in swimming pools that were not adequately chlorinated. Moreover, from 1982 to 2002, 15% outbreaks of *E. coli* O157:H7 were due to drinking water exposure, which resulted in 1290 illnesses (Reynolds, 2008). The acute diseases followed the infection include Hemolytic uremic syndrome with possible long-term sequelae (Pond, 2005) and *E. coli* O157 gastroenteritis.

In 1974, the U.S. Congress passed the Safe Drinking Water Act (SDWA) which requires the U.S Environmental Protection Agency (U.S. EPA) to determine the criteria of contaminants in drinking water. And both the SDWA and the Clean Water Acts (CWA) address pathogenic contamination of the United States' waterbodies. The CWA protects surface water for drinking, recreation, and aquatic food source uses while the SDWA enabled regulation of contaminations of finished drinking water and protection of source waters. In 1986, the USEPA identified that the acceptable risk levels for recreational waters at 8 illness per 100 swimmers in fresh waters and 19 per 100 in marine waters (USEPA, 1986). Since then, the USEPA has continued to modify water quality criteria for pathogens and pathogen indicators.

2.1.2 Fecal indicator bacteria

Based on above demonstrations, monitoring pathogenic microorganisms is essential. But there are some limitations on detecting all pathogens in water: (i) it is time-consuming and needs laborious analyses; (ii) large numbers of potential pathogens require many types of test and analyses; (iii) it needs large sample volumes and sample pre-concentration since pathogens are always present in relatively low concentrations; (iv) it may pose potential health hazards (Myers et al., 2007). Because of these difficulties in detecting the broad range of human pathogens, pathogen indicators are required and used to set water quality standards.

Indicators are physical, or chemical parameters whose presence at a level above specified limit may reflect a problem in the treatment process or in the integrity of the distribution system (USEPA, 2006). According to U.S. EPA, to be an ideal assessor of fecal contamination, an indicator organism should meet as many of the following criteria as possible:

- (i) The organism should be present whenever intestinal pathogens are present (USEPA, 2006; Myers et al., 2007; Payment, 2011);
- (ii) The organism could be used for all types of waters (USEPA, 2006; Myers et al., 2007);
- (iii) The organism should not be a pathogenic microorganism (to minimize the health risk to analysts) (Payment, 2011);
- (iv) The organism should have a longer survival time than the hardiest enteric pathogen (USEPA, 2006; Myers et al., 2007);
- (v) The organism should not grow/ multiply in water (USEPA, 2006; Payment, 2011);
- (vi) The organism should be found in warm-blooded animals' intestines (USEPA, 2006; Myers et al., 2007);
- (vii) The method of test the organism should be easy and inexpensive to perform (USEPA, 2006; Myers et al., 2007; Payment, 2011);
- (viii) The density of the indicator organism should have some direct relationship to the degree of fecal pollution (USEPA, 2006; Payment, 2011);

The four indicators most commonly used today are total coliforms, fecal coliforms, *Escherichia coli* (*E. coli*), and enterococci.

2.1.2.1 Total coliforms and fecal coliforms

Coliform bacteria are part of the Enterobacteriaceae and live in the lower intestines of warm-blooded animals. They are Gram-negative, oxidase-negative, non-spore forming rods, that ferment lactose with gas production at 35-37°C after 48h (WHO, 2008; Cabral, 2010). Coliforms can be found in the aquatic environment, in soil and on vegetation. Although coliform bacteria are not usually pathogenic themselves, their presence indicates fecal contamination, perhaps accompanied by disease-causing pathogens. Since the 1920s, total

and fecal coliforms are the standard microbial indicators of water quality (Reynolds, 2003). However, the usefulness of total coliforms as an indicator of fecal contamination depends on the extent to which the bacteria species found are fecal and human in origin. Therefore, total coliforms are no longer recommended as an indicator for recreational waters (USEPA, 2010).

Fecal coliform bacteria are a subgroup of coliform bacteria. They also appear in the intestinal tract of warm-blooded animals. Fecal coliforms, which are outside of a warm-blooded host, have a shorter life expectancy compared to total coliform bacteria which are associated with the digestive tract of humans or animals. The bacteria in fecal category are usually nonpathogenic, but also include pathogens such as *E. coli* O157:H7. The existence of fecal coliforms indicates fecal contamination and of the potential presence of enteric pathogens, especially bacterial pathogens. For recreational waters, fecal coliform bacteria were the primary bacteria indicator until relatively recently, when U.S. EPA began recommending *E. coli* and enterococci as better indicators of health risk from water contact (USEPA, 2010). Some states, such as New Hampshire, are still using fecal coliforms as the indicator bacteria (NHDES, 2003).

2.1.2.2 *Escherichia coli* and enterococci

The traditional indicators test should be abandoned because: (1) total coliform test can detect bacteria that have no connection with fecal pollution; (2) the detection of fecal coliforms must be carried out at 44.5°C, and positive results confirmed by identification to species levels in order to exclude false positives (Leclerc et al., 2001; Cabral, 2010). Thus, in 1986, USPEA recommended new indicator bacteria, *Escherichia coli* or *E. coli*, which is a single species within the fecal coliforms bacteria, and enterococci, a group of fecal streptococci group in the intestinal tract of warm-blooded animals.

E. coli and *Enterococci* were recommended as indicators of fecal contamination in water system in the U.S in 1986 by the U.S. EPA (USEPA, 1986). *E. coli* is the only true and reliable indicator of fecal pollution in environmental waters so far (Cabral, 2010). The *E. coli* Criteria Table for Iowa when the Class “A1”, “A2”, “A3”, or “B(CW)” uses is listed in the Table 1 (USEPA, 2011). And the Figure 1 shows the total coliform, fecal coliform, *E. coli*, and enterococci.

Table 1. *E. coli* Criteria (Organisms/100ml of water)

Use of Category	Geometric Mean	Sample Maximum
Class A1		
3/15 - 11/15	126	235
11/16 – 3/14	Does not apply	Does not apply
Class A2 (Only)		
3/15 - 11/15	630	2880
11/16 – 3/14	Does not apply	Does not apply
Class A2 and B(CW)		
Year-Round	630	2880
Class A3		
3/15 - 11/15	126	235
11/16 – 3/14	Does not apply	Does not apply
Class A1 - Primary Contact Recreational Use Class A2 - Secondary Contact Recreational Use Class A3 - Children's Recreational Use Class B(CW) – Cold Water Aquatic Life		

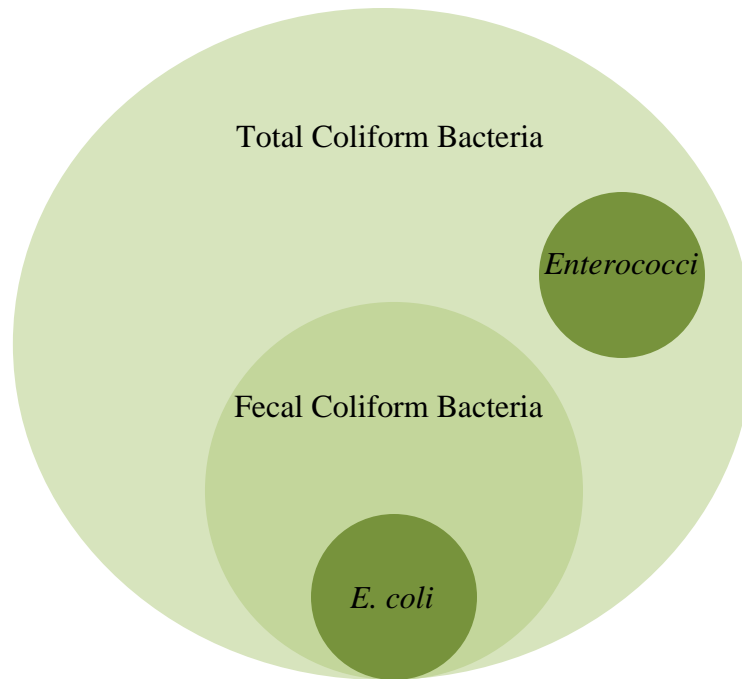


Figure 1. Relationships between total coliform, fecal coliform, *E. coli*, and enterococci. The figure showed that both *E. coli*, and enterococci are belong to total coliform bacteria, and *E. coli* are also fecal coliform bacteria, which is a subgroup of total coliform.

2.1.2.3 Limitations of pathogenic indicators

In recent years, studies have identified some limitations of using pathogenic indicators to predict the presence of enteric pathogens in water systems.

Coliform bacteria were referred to belong to the genera *Escherichia*, *Citrobacter*, *Klebsiella* and *Enterobacter*, but this group is also including other genera, such as *Serratia* and *Hafnia*. Thus, the total coliform group includes both fecal and environmental species (WHO, 2008). Total coliform counts are not an accurate measure of fecal pollution since it can detect bacteria that have no connection with fecal pollution (Cabral, 2010). Moreover, many pathogens of public health concern do not behave like fecal indicators and have no absolute indicator of their presence, only a probability of their co-occurrence (Payment, 2011). For example, fecal coliforms are not a reliable indicator during anaerobic digestion because viral pathogens tend to have a greater survivability than fecal coliforms (NHDES, 2003).

2.2 *Escherichia coli*

2.2.1 Introduction of *Escherichia coli*

Gram staining is an empirical method of differentiating bacterial species into two large groups, Gram-positive and Gram-negative, based on the chemical and physical properties of their cell walls. *Escherichia coli*, commonly abbreviated *E. coli*, is a large and diverse group of Gram-negative rod-shaped bacteria that are commonly found in the lower intestine of warm-blooded organisms. *E. coli* can grow in the media with glucose as the only organic component while wild type *E. coli* have no growth factor requirement and can transform glucose into all macromolecular components for constructing the cell through metabolism (Todar, 2011). Moreover, *E. coli* are facultative anaerobe and then can grow in the presence or absence of O₂. Under anaerobic conditions they will grow by means of fermentation or anaerobic respiration in which NO₃, NO₂ or fumarate as final electron acceptors for respiratory process (Todar, 2011). Thus, *E. coli* can adapt both the intestinal and extraintestinal environments with such characteristics.

At this time, there are over 700 genetically different types of *E. coli* that have been identified. For many years after the first description in the 19th century, *E. coli* were simply considered to be a commensal organism in the intestine. However, a strain of *E. coli* that was first shown to be the pathogen that caused an outbreak of diarrhea among infants in 1935. Diseases caused by various strains of *E. coli* include not only diarrhea but also urinary tract infections (UTIs) and neonatal meningitis. *E. coli* are responsible for 90 percent of UTIs, neonatal meningitis in 1/300 infants and an unknown number of diarrheal illnesses (Reynolds, 2008; Todar, 2009). As mentioned previously, among the pathogenic strains, *E. coli* O157:H7 from the intestinal tract of warm-blooded animals has attracted more attention. This strain is primarily spread to people by consuming unpasteurized milk or undercooked beef and can lead to severe diarrhea, Hemolytic uremic with possible sequelae, *E. coli* O157 gastroenteritis. Uropathogenic strains of *E. coli* (UPEC) are the most common cause of non-hospital-acquired urinary tract infection. This unique group can enter into the urinary tract and ascend to colonize the bladder, causing cystitis. Or these bacteria may ascend the ureter to infect the kidneys causing pyelonephritis (Vigil et al., 2011).

According to the criteria of indicator organism, *E. coli* bacteria are good indicator organisms of fecal contamination since they generally live longer than pathogens, are found in greater numbers, and are less risky to collect or culture. They can be distinguished from most other coliforms by their ability to ferment lactose at 44.5 °C in the fecal coliform test, as well as by their growth and color reaction on certain types of culture media such as mTEC plates. Monitoring for *E. coli* is an easy and cost-effective method for citizens and professionals. *E. coli* were recommended for use as an indicator of fecal contamination in water system in the U.S in 1986 by the USEPA (USEPA, 1986). Studies indicated that *E. coli* were more closely correlated with swimming-related illnesses than the total coliform bacteria, and U.S. EPA later recommended that *E. coli* be used as the indicator of choice in freshwater recreational areas.

2.2.2 Sources of *E. coli* in waters

E. coli in water can originate from the intestinal tracts of both humans (Ramchandani et al., 2005) and other warm-blooded animals, *E. coli* originating from livestock have been detected in surface waters (Ram, 2008), ground-water on or near swine farms and in runoff from research plots with highly and sparsely vegetated grassland (Soupir and Mostaghimi, 2011). Other common sources of *E. coli* in the environment include pets and wildlife, septic tanks, leaking sewer lines, wastewater treatment plants, and combined sewer overflow (CSOs). Two major sources of bacteria in streams are from land application of manure from confined animal systems and direct deposit by grazing animals (Soupir et al., 2006).

2.2.3 Transport and fate of *E. coli* in the environment

Enteric bacteria from animal waste can enter water systems via runoff from the grazed and manure-amended land (Sherer et al., 1992). The transport of *E. coli* from point and nonpoint sources to surface water is becoming a concern in the U.S. The EPA's National Water Quality Inventory report (USEPA, 2009) reported that 72,305 miles and 29% of impaired streams are contaminated by pathogens, and pathogens are the leading cause of impairments in rivers and streams in the U.S.

Manure-borne bacteria can be transported to surface water via attaching to soil and organic particles (Liu et al., 2011) or in the freely suspended, or unattached state. Pathogenic

microorganisms in land-applied human and animal wastes can also enter groundwater system by infiltration (Bolster et al., 2009). Thus, it is of great importance to understand the transport mechanism and fate for *E. coli*, which is a commonly accepted pathogenic indicator, to assist the development of best management practices. Additionally, development of partitioning method between unattached and attached bacteria can help with total maximum daily loads (TMDL) to reduce pathogen concentrations in waters (Soupir and Mostaghimi, 2003).

E. coli are released to the environment along with manure in which manure can serve as carriers, abode, and food for microbes (Pachepsky et al., 2006). The transport of bacteria in soils has been reported to enhance after attaching to manure (Gagliardi and Karns, 2000; Guber et al., 2005). At least 60% of attached *E. coli* were found to be associated with manure colloids (based on an 8 to 62 micron particle size category) regardless of soil texture (Soupir et al., 2010). Manure type is also a factor which impacts the *E. coli* concentration after releasing from manure. A study on pastureland indicated that the release plots of dairy farm (with a history of liquid dairy manure application) had significantly higher concentrations of *E. coli* than the runoff plots located at a turkey farm (which also had a history of poultry litter application). The authors also found that turkey litter treatment had the largest percentage of source *E. coli* released by a simulated rainfall event (Soupir and Mostaghimi, 2003). For the different duration after manure application (4-12 weeks), the fecal coliform concentrations released by simulated rainfall decreased approximately exponentially in response to increasing time between the manure applications and rainfall simulations (Edwards et al., 2000).

One of the factors affecting bacterial transport is attachment to soil particles (Pachepsky et al., 2008). After release from manure, microorganisms can move freely in water or attach to suspended soil and manure particles (Jeng et al., 2005; Hipsey et al., 2006; Pachepsky et al., 2008). A previous study has found that 10-20% of the fecal coliform cells adsorbed to the suspended particles in untreated stormwater runoff (Schillinger and Gannon, 1985). The fecal bacteria in stream sediment can be 10-10,000 times higher than that in water column (Davies and Bavor, 2000; Bai and Lung, 2005). Bacterial attachment to soil particles results in increased settling velocities and the sedimentation of attached bacteria may be a

critical disappearance mechanism in contaminated surface waters (Schillinger and Gannon, 1985). Bacteria in bottom sediments are also protected from the destructive action of ultraviolet radiation (Bitton et al., 1972). Therefore, *E. coli* attached to large particles may pose less threat to environment (Muirhead et al., 2005) and have a longer life expectancy.

There are several health considerations regarding the presence of bacteria in stream and lake bottom sediments. Dredging, gathering up bottom sediment in shallow seas and fresh water areas, has been shown to greatly increase concentrations of indicator bacteria by resuspending sediment (Grimes, 1975). Action of wind, currents, boats, and swimmers may also result in resuspension of bottom bacteria (Schillinger and Gannon, 1985), which could pose a health hazard in recreational areas.

The importance of *E. coli* as a pathogenic indicator has led to numerous studies investigating cell properties and the corresponding transport behavior of this organism (Bolster et al., 2009). Bacteria attachment to particles in the aquatic environment can be influenced by various factors, including both chemical and physical factors, such as temperature, predators, antibiotics, organic matter, water content, pH, and dissolved nutrients (Pachepsky et al., 2006). For example, for the range of 4°C to 37°C, the survival duration decrease corresponding to the temperature increase (Flint, 1987). Next, I will discuss some currently known properties which may impact the attachments in details.

a. Soil particle size

Previous researches had demonstrated that the soil particle size plays an important role in bacterial attachment. Bacterial attachment is greater for particles with sizes up to 330 μm than for coarse-grained sand ($\sim 1000 \mu\text{m}$) (Fontes et al., 1991). The existences of fine soil particles and high organic matter have been shown to increase *E. coli* survival (Sherer et al., 1992) in water bodies. From a study on *E. coli* attachment to five sediment fractions in fresh stormwater, it was found that 80% of attached *E. coli* were associated with the silt fraction, 18% with clay fraction, and only 2% with the sand fraction (Jeng et al., 2005). In urban storm water runoff, fecal indicator bacteria were adsorbed predominantly to fine clay particles ($< 2 \mu\text{m}$) (Muirhead et al., 2006).

b. Bacteria genes

Genotypes also impact the bacterial attachment in aquatic environment. Genes that encode various types of pili, fimbriae, and other surface proteins are responsible for bacterial attachment to other bacteria, host tissues, or other surfaces (Garcia and LeBouguenec, 1996). The expression of Ag 43, one of the adhesion genes, was found to significantly impact the bacterial attachment to quartz particles (Lutterodt et al., 2009). Moreover, Cook et al. (2011) evaluated 15 genes for 17 *E. coli* isolates following transport through saturated porous media and found that highest attachment efficiency was also associated with targeted genes including surface exclusion (*traT*) and the siderophore *iroN_{E. coli}* as well as adhesion genes (Cook et al., 2011).

c. Cell sphericity

At present, difference exists in cell sphericity have been observed to impact on bacterial attachment. In one study by Bolster et al, cell sphericity and width showed a significant relation to bacterial attachment (Bolster et al., 2009). However, no relation between attachment and cell sphericity was indicated in a study of 54 *E. coli* isolates (Foppen et al., 2010). Lutterodt et al. (2009) studied cell sphericity of 6 *E. coli* strains obtained from a soil used for cattle grazing and found cell sphericity did not significantly correlate with attaching efficiency.

2.3 Detection methods

Previous studies have shown that some bacteria preferentially attach to sediment and organic particles; however, and a variety of techniques have been used to assess attachment including centrifugation, settling, and filtration. Additionally, a variety of chemical and physical dispersion techniques are used to release attached cells from particulates for enumeration of the total concentration.

2.3.1 Separation techniques

2.3.1.1 Centrifugation

Centrifugation is a process that involves the use of the centrifugal force for the separation of mixtures with a centrifuge, in this application, used for determining the amount

of bacteria that are sediment-attached (Faegri et al., 1977; Schillinger and Gannon, 1985). Bacteria in the supernatant were considered suspended, and the difference between this concentration and the total concentration was assumed to be the attached bacteria portion (Soupir et al., 2008). However, centrifugation has some drawbacks in application. Significant losses of cell number under centrifugation exceeding 190* g as centrifugation speed and 1 min as the total centrifuge time have been observed to occur (Lunau et al., 2005). Unattached bacteria have a similar diameter as clay particles, so it can be difficult to determine proper centrifuge speed and time to partition attached and unattached bacteria (Henry, 2004).

A study of recovery of benthic bacteria with stream bed sediments used a technique called Nycodenz density gradient centrifugation to separated attached and unattached bacteria (Amalfitano and Fazi, 2008). The authors used 1ml Nycodenz as a density gradient medium placed beneath 1ml of sediment and of pre-filtered water. Tubes were centrifuged (14,000* g) for 90 min at 4°C. Next, the layers of supernatant, cells, Nycodenz cushion and sediment (described from top to bottom) were distinct when observed against a light source. Another centrifuging technique called dispersion-density-gradient centrifugation was used in a study of ammonia-oxidizing bacteria attachment to clay loam soil (Aakra et al., 2000). First, soil samples were diluted and dispersed using a blender at 22,000 rpm for 10 min. Second, a 200 ml sample of soil dilution was centrifuged at 7,000 rpm for 3 hours. In this step, 40 ml Nycodenz solution was also used as density gradient medium and placed beneath the sediment and of pre-filtered water. As a result, planktonic bacteria remained suspended and the soil containing attached bacteria had settled below the Nycodenz cushion. Gentle spinning at 500 ×g for 10 min was used to limit changes in bacterial culturability and particle size distribution due to shear and pelletization (Fries et al., 2006).

2.3.1.2 Settling

According to the Stoke's Law, particles with different size and density have different settling velocities:

$$v = \frac{gd_p^2(\rho_p - \rho_f)}{18\mu}$$

Where:

v is the particles' settling velocity (m/s) (vertically downwards if $\rho_p > \rho_f$, upwards if $\rho_p < \rho_f$),

d_p is the particle's diameter (m),

μ is the viscosity of medium (kg/m×s),

g is the gravitational acceleration (m/s²),

ρ_p is the mass density of the particles (kg/m³), and

ρ_f is the mass density of the fluid (kg/m³).

A study by Liu et al. (2010) used Stoke's equation to determine the settling time for quartz to separate free-suspended *E. coli* from quartz-attached *E. coli* (Liu et al., 2010)

2.3.1.3 Filtration

Filtration is characterized by its ability to remove particles via a sieving mechanism based on the size of the membrane pores relative to that of the particulate matter (USEPA, 2005). Qualls et al. (1983) defined the unattached bacteria as cells able to pass through an eight-micron screen (Qualls et al., 1983). Since a typical *E. coli* cell is 1.1 to 1.5µm wide by 2 to 6 µm long, the previous definition may include not only free bacteria but also those sorbed to very small particles or even small bioflocculated clumps (Soupir et al., 2008). Multiple screen filtrations can also be a useful tool. In 2008, Soupir et al. conducted a filtration system for distinguishing *E. coli* in environmental soil samples: a Mini- Sieve Microsieve set with a number 35 mesh screen was used to retain particle larger than coarse sand (>500µm); a number 230 mesh was used to retain medium, fine and very fine sand (63-500µm); an 8µm filter was used to retain fine, medium, and silt particles; a 3µm filter was used to retain clay and very fine silt particles.

2.3.2 Dispersion techniques

Techniques to detach bacteria from particulates are mainly focused on soil samples, due to agricultural and bioremediation studies (Mayr et al., 1999; Aakra et al., 2000; Caracciolo et al., 2005). The attachment of bacteria, especially pathogens to sediment makes

detection and enumeration of cells difficult. For instance, when enumerated by culture techniques, bacteria attached to sediment particles may not be randomly distributed across the surface of the media (Craig et al., 2002). Therefore, chemical and physical dispersion techniques have been developed for releasing attached and biofloculated cells from soil particles to estimate the total number of cells. Recent research is focused on cell recovery and minimizing cell loss during treatment (Amalfitano and Fazi, 2008).

2.3.2.1 Chemical techniques

Chemical agents are often used to loosen the strong hydrogen binding, van der Waals, electrostatic and chemical forces that tie cells and particles together. Previous researchers have found that Tween 20 at 0.5% concentration (Amalfitano and Fazi, 2008), Tween 80 at 0.02% concentration (BD, 2008), or Tween 85 at 0.01% concentration (Soupir et al., 2008), can all achieve satisfactory dispersing effects. Chemical dispersion agents are also used in combination with physical methods (Lindahl and Bakken, 1995).

2.3.2.2 Physical techniques

Previous physical dispersion techniques have included treatment with a waring blender, hand or orbital shaker, sonication probe, or ultrasonic bath treatment. A waring blender was used for homogenization of the sample. It shakes the sample with glass beads, or disruption of aggregates by mild ultrasonic treatment (Lindahl and Bakken, 1995). Physical entrapment of bacteria in small pores can be mechanically disrupted by horizontal and orbital shakers or ultrasonic baths (Epstein and Rossel, 1995; Kuwae and Hosokawa, 1999; Buesing and Gessner, 2003; Kalyuzhnaya et al., 2006). The procedure of shaking can last for 30 min at 720rpm (Amalfitano and Fazi, 2008) or 10 min with using hand shaker. Ultrasonic treatment can be conducted for several durations (0.5, 2, 6, 10 min) (Soupir et al., 2008). Craig et al. used sediment samples from recreational coastal sites to evaluate some physical techniques to separate micro-organisms from sediment particles, including hand shaking, treatment by sonication bath for 6 and 10 min, respectively, and by sonication probe for 15 s and 1 min, respectively. As a result, the most successful method, when the sediments consisted mainly of sand, is sonication bath for 10 min (Craig et al., 2002).

2.3.3 Dilution and membrane filtration

Dilution has been used frequently in laboratory to compensate for bacteria masking effects as well as the enumeration of bacteria. In the bacteria enumeration analyses, dilution is necessary in order to obtain concentrations within the measureable range of each analytical technique (Characklis et al., 2005). For example, the seawater samples collected from sites on the coast were diluted 50 to 250 times with particle-free seawater to obtain the final concentration (Kuwae and Hosokawa, 1999). Dilution is also necessary for chemical dispersion methods (Soupir et al., 2008) and other techniques used to partition the attached and freely suspended bacteria for soft sediment (Griebler et al., 2001).

A membrane filtration process is defined by two basic criteria:

1. The filtration system must be a pressure- or vacuum-driven process and remove particulate matter larger than 1 μm using an, engineered barrier, primarily via a size exclusion mechanism (USEPA, 2004);
2. The process must have a measurable removal efficiency of a target organism that can be verified through the application of a direct integrity test(USEPA, 2004).

For enumeration of bacteria, 0.45 μm pore size membrane filters are commonly used (Alhadidi et al., 2011; Peeva et al., 2011).

2.3.4 Flow cytometry

Flow cytometry is powerful technique for measuring and analyzing multiple parameters of individual cells (or any other particles, including nuclei, microorganisms, chromosome preparations, and latex beads) (Brown and Wittwer, 2000). The flow cytometer performs simultaneous multiparametric analysis by passing thousands of cells and particles per second through a laser beam and capturing the light as each cell/ particle emerges. Thus the flow cytometry software such as BD FACSCanto Clinical Software((BD, Franklin Lakes, NJ), can analyze the collected data statistically and report physical and/ or chemical characteristics such as phenotype, relative size, relative granularity or internal complexity, and relative fluorescence intensity (Brown and Wittwer, 2000).

2.3.4.1 Principle of flow cytometry

Fluorescent dyes such as SYTO green-fluorescent nucleic acid stains may bind or intercalate with different cellular components during sample preparation. A single wavelength of illuminating light, usually a laser, is directed onto a hydrodynamically-focused stream of fluid. As a suspended cell or particle from 0.2 to 150 microns passes through the light source at interrogation point, it will scatter light at all angles (BD, 2000). Several detectors are aimed at the point where the stream passes through the laser beam. Emitted light is scattered in all directions and is collected via optics that direct the light to a series of filters and dichroic mirrors that isolate particular wavelength bands (Brown and Wittwer, 2000). Emitted light that is scattered in the forward direction is collected by one forward scatter channel (FSC) in the line with the light beam. The FSC intensity can be used to roughly estimate the particle's size and distinguish between cellular debris and living cells. A number of side scatter channels (SSC), usually located 90 degrees from the laser's path, can collect the light approximately at 90 degree angle to the excitation line and provides information about granularity and structural complexity inside the cell. FSC and SSC are both unique for every particle in the stream, and a combination of these two can be used to differentiate different cell types in a heterogeneous sample. One or more fluorescent detectors can measure the fluorescent chemicals found in the particle or attached to the particle and can provide quantitative and qualitative data about fluorochrome-labeled cell surface receptors or intracellular molecules such as cytokines and DNA.

2.3.4.2 Flow cytometers

A flow cytometer consists of four main components:

- The fluidics system transports particles in a fluid stream to the laser beam for interrogation. It is essential that cells or particles are passed through the laser beam one at a time for definite data collection points. To accomplish this, the sample is injected into a stream of sheath fluid or saline solution (BD, 2000);
- The optics system is made up of excitation optics and collection optics. The excitation optics consists of the laser and achromatic lenses for shaping and focusing the laser beam. The collection optics consist of a lens to collect light emitted from the

particle-laser beam interaction and a system of optical mirrors and filters to route specified wavelengths of the collected light to designated optical detectors (BD, 2000);

- The electronic system process the light signal that detectors collected and convert it to a digitized value that the computer can graph. The scattered light is translated into a voltage pulse via linear or log amplification (BD, 2000);
- The interpretation system of a computer with specialized software can graphically represent the values of each parameter after analysis (Marvin).

Figure 2 shows the schematic of fluid and optical systems of a flow cytometer.

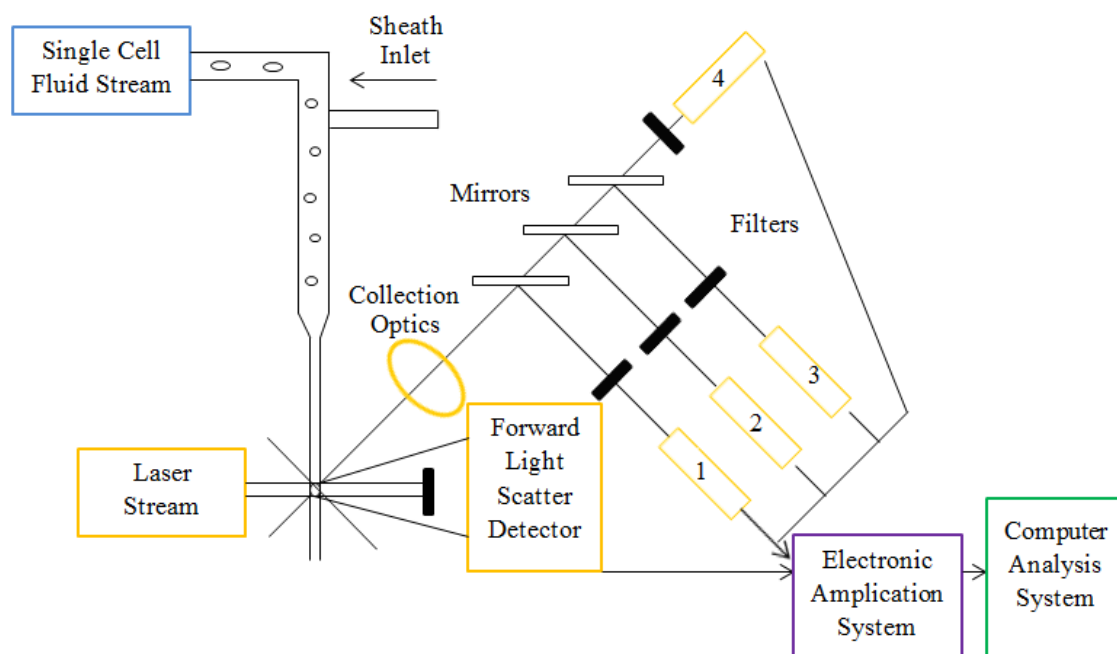


Figure 2. Schematic of a flow cytometer (modified from Brown and Wittwer, 2000)

2.3.4.3 Applications

2.3.4.3.1 Flow cytometry application in environmental research

Microbiological activity in the natural world is vital in the integrated functioning of ecosystems. For example, quantification of total bacterial numbers is basic and essential task in several areas of microbiology, including public health, biotechnology, and natural environments (Lebaron et al., 1998). But currently, the limitation of quantification is due to

unresolved problems in methodologies (Porter et al., 1997). Application of flow cytometry can be a useful tool on such work. According to the principles, flow cytometry is appropriate for analyzing aquatic samples. Flow cytometry has shown three unique technical properties of studies in the microbiology of aquatic systems: “(i) its tremendous velocity to obtain and process data; (ii) the sorting capacity of some cytometers, which allows the transfer of specific populations or even single cells to a determined location, thus allowing further physical, chemical, biological or molecular analysis; and (iii) high-speed multiparametric data acquisition and multivariate data analysis” (Vives-Rego et al., 2000). Flow cytometry was found to have more rapid and sensitive analyses when compared with epifluorescence microscopy in a purified suspension of exacted bacteria (Amalfitano and Fazi, 2008). Flow cytometry is superior to the molecular methods based on PCR because the PCR has the effects of inhibitory substances and is more time-consuming (Khan et al., 2010).

Flow cytometry has also been used to determine the final cell concentration and average biovolume after growing pathogenic bacteria (*Escherichia coli* O157, *Vibrio cholerae*, or *Pseudomonas aeruginosa*) using pure cultures as the inoculum (Vital et al., 2010). Additionally, flow cytometry also has limitations: cost, need for skilled and well-trained operators, and adequate refrigeration systems for high-powered laser and cell sorters (Vives-Rego et al., 2000).

2.3.4.3.2 SYTO green-fluorescence nucleic acid stains

Fluorescence-based microbial detection systems, including flow cytometry, are likely to be central to a number of automated microbial detection systems. Recently developed dyes, the SYTO series, are likely to become widely used in future as they are excitable at 488 or 633 nm (the most commonly available upon a fluorescent product is released on cytometers) and they appear to exhibit low background staining resulting in high Signal to Noise ratio (S/N) (Veal et al., 2000).

SYTO green-fluorescent nucleic acid stains are cell-permeant nucleic acid stains that show a large fluorescence enhancement upon binding nucleic acids of RNA and DNA in both Gram-positive and Gram-negative bacteria. SYTO dyes are compatible with many fluorescence-based instruments such as flow cytometry that use laser excitation (Invitrogen,

2008). Thus, SYTO dyes have been widely used in environmental research applications with flow cytometry.

Flow cytometry was successfully applied with SYTO 13 as a counting method for sediment cell suspension (Amalfitano and Fazi, 2008). In prokaryotic aquatic studies, SYTO dye has advantage of greater fluorescence yield than the ethidium homodimer DAPI (49,6-diamidino-2-phenylindole), which is a common stain in fluorescence microscopy (Guindulain et al., 1997). A comparison study showed that SYTO dye is more appropriate to be used to stain live bacteria in nonsaline waters than SYBR dyes (Lebaron et al., 1998). Another research finding in nucleic acid content of microparticles suggested the utility of fluorescent dyes like SYTO 13 for more sensitive quantitative assays because SYTO 13 allowed the detection of 1.5–2.9 times as many particles as did light scatter (UllaL et al., 2009).

2.3.4 Summary

Although traditional separation methods, centrifugation, filtration, and filtration are commonly used in the lab to partition between unattached and attached bacteria to particulates, they still have the following limitations. Firstly, the operations are complicated and need to be completed by skilled technicians. Additionally, long time exposure to bacteria, especially pathogenic strains, may threaten the operators' health. Secondly, the operations are time-consuming. In the settling method, the small size particles need up to several hours to settle out completely. Moreover, in this group of methods, the enumerations are operated by plate counting, which involves dilution, spread-plating, and manual colony count. This method requires at least 24 hours before the results can be interpreted and it's time-consuming and labor intensive. Thirdly, we cannot estimate the cell changes during operations. For instance, the fraction in the centrifugation method can damage the cells. Therefore, the traditional separation methods need to be substituted by a rapid and accurate technique. From this point, flow cytometry can be a potential option.

CHAPTER 3 MATERIAL AND METHODS

3.1 Research considerations

The ability of bacteria to attach to clay particles depends on several properties, including the cells, particles, and the environment. We consider each of these in the experimental design. Properties of the bacteria were varied by using different environmental and a known pathogenic strain (strain #31, #50, #89, and #43888); experiments were conducted on four different pure soil particles (Kaolin, Hectorite, Ca-Montmorillonite, and Montmorillonite K-10); and the environmental considerations such as nutrient and temperature (Luria-Bertain or Tryptic Soy medium for environmental strains and #43888, respectively; 37°C) were held constant. This study was conducted in laboratory conditions, with many of these properties controlled.

3.1.1 Bacteria cultures

In this project, three environmental strains and one pathogenic strain were used to evaluate the attachment efficiency.

The environmental isolates were collected from swine waste from five swine facilities in Iowa in 2008 and 2009. Two hundred and three isolates were obtained from the samples which had been analyzed by membrane filtration, EPA Method 1603, on modified mTEC agar (USEPA, 2002) and preserved in 25% glycerol stocks at -80°C for further investigations. Three strains were selected from these 203 isolates. In a previous study, selected strains, #31, #50, and #89 showed the highest attachment fractions (>99%) to quartz particles (Liu et al., 2011). A pathogenic strain was also considered, ATCCTM #43888, which is a genetically modified version of *E. coli* O157:H7, which does not produce either Shiga-like toxin I or II and does not possess the genes for these toxins. To eliminate the variability between the strains, only one pure culture isolate of the four was test at any one time.

Growth in a nutrients broth simulates development of cell appendages and attachment abilities more than growth on an agar media (Schillinger and Gannon, 1985). Therefore, a stock suspension of *E. coli* was grown for 24 hours at 37 °C to reach the stationary stage on the growth curve prior to all experiments in Luria-Bertain broth (BD, Franklin Lakes, NJ; Cat.

No. 244610) and Tryptic Soy broth (BD, Franklin Lakes, NJ; Cat. No. 211825), for environmental strains and serotype O157:H7, respectively.

3.1.2 Soils

Soil properties, such as particle size, organic content, nutrient availability, and pH can greatly impact the attachment of microorganisms (Muirhead et al., 2006). Four clays were selected for the project (Table 2). To cover diversity range of soil properties, the selected clay particles have different particle size, belong to three different mineral groups, and were from either commercial or natural resources.

Table 2. Clay particles with key properties

Clay Particles	Source	Average Diameter (μm)	Density (g ml^{-1})	Surface area (m^2/g)
Hectorite	San Bernaridino County, California The Clay Mineral Society, SHCa-1	1	2.2	63
Kaolin	Acoros Organics, #211740010	1.25	2.6	11.2
Ca-Montmorillonite	Gonzales County, Texas The Clay Mineral Society, STx-1b	3	2.4	84
Montmorillonite K-10	Acoros Organics, #233170050	6	2.4	240

3.1.3 Selection of experimental partitioning methods

Possible partitioning methods discussed in the previous section were settling, centrifugation, flow cytometry, and filtration combined with chemical or physical dispersion treatment. Clay has the smallest particle size among fine-grained soils. Therefore, filtration is not an appropriate method in this project since unattached bacteria (freely suspended *E. coli* with 1.1 to 1.5 μm wide by 2 to 6 μm long) are similar in size to the clay particles for this study (1 to 6 μm diameter).

Flow cytometry is rapid and powerful technique for measuring and analyzing multiple parameters of individual cells and it previously performed well when used as a technique to separate between *E. coli* attached to particles and free *E. coli* when the substrate

was polystyrene beads (6-10 μm diameter) (Tysman, unpublished data). However, flow cytometry has not been previously examined as a technique for partitioning between unattached *E. coli* and *E. coli* attached to clay particles.

3.1.3.1 Determination of settling times

In the previous studies, Stoke's equation has been used to determine the time for *E. coli* attached to quartz particles to settle out of solution (Liu et al., 2011). Preliminary calculations of the settling time for *E. coli* attached to clay particles using Stoke's equation, found that calculated times were not sufficient to achieve clear supernatants.

At this point, force balance of a single particle was considered:

$$ma = -\gamma v + mg + L(t)$$

where

m is particle mass,

γ is coefficient for Stokes' law $6\pi\eta R$, R is particle radius and η is viscosity,

(In Stokes' law, frictional force $F_d = 6\pi\eta Rv$, where v is the particle's settling velocity)

a is particle acceleration,

v is settling velocity,

g is gravitational acceleration and

$L(t)$ is Brownian motion.

Thus, the four terms in the equation originates from inertia, viscous drag, gravity and Brownian motion due to collision from solvent molecule.

This equation has an analytical solution:

$$v = v_0 \exp\left(-\frac{\gamma}{m}t\right) - \frac{1 - \exp\left(-\frac{\gamma}{m}t\right)}{\gamma/m} g + \int_0^t dt \exp\left(-\frac{\gamma}{m}(t-t')\right) \frac{L(t')}{m}$$

If we take the average of the velocity for a large amount of particles, the last term will drop out, since $L(t)$ is cause by random impacts of small molecules. We can use just Stokes'

law, and we have terminal velocity, or sediment rate of $v = mg/\gamma$, which indicates smaller particles will require in a longer time to settle. However, the Brownian motion has a stronger dependency on particle size $\sim R^3$ than gravitational term (mg) $\sim R$. Brownian motion would dominate for small particles, and random noise would dominate the sedimentation rate measure results.

Therefore, for large particles in the aquatic environment the gravity is dominant for sedimentation, while for small particles, the impacts of water molecule on particles from random directions cannot be ignored. Therefore, the settling times obtained from Stoke's Law tended to underestimate the actual settling time required.

A Spectrophotometer (HACH, Loveland, CO; model DR2800) was then used to determine sufficient settling times for clay particles to settle completely. The concentrations of clay suspensions, which were with surface area ratio 1000 (clay surface area to *E. coli*), were selected to test the settling time. Clay suspensions with clay concentration 1.25 g/L Hectorite, 7.5 g/L Kaolin, 1.0 g/L Ca-Montmorillonite, or 0.35 g/L Montmorillonite K-10 and phosphate-buffer water (HACH, Loveland, CO; Cat. No. 21431-66), mixed up to 15 ml and were placed in 15 ml centrifuge tubes on a polystyrene foam holder after shaking by hand. The absorbency values were then tested under single wave length of 400nm every 0.5 h. The suitable settling time was set based on two stable readings of absorbency value. The appropriate settling times were: 60 min for Montmorillonite K-10, 150 min for Ca-Montmorillonite, 390 min for Hectorite, and 5760 min (2 days) for Kaolinite. The absorbency values for the settling tests are provided in Appendix A1.

3.1.3.2 Determination of centrifuge speed and time

From Section 3.1.3.1, it was determined that the settling time for removal of the Kaolin clay suspension required 5760 min (2 days). To eliminate the possible variability, such as bacterial regrowth or decay that could potentially occur over a 2 day period, centrifugation was investigated prior to settling to shorten the settling time.

To determine an appropriate centrifuge speed and time, 50 ml samples with *E. coli* strain #31 with concentration 10^7 CFU ml⁻¹ and phosphate-buffered water (HACH, Loveland, CO; Cat. No. 21431-66) were used. Several combinations of centrifuge speed and time were

compared, 300 rpm for 5 min, 400 rpm for 3 min, 300rpm for 8 min, and 300rpm for 10 min in a refrigerated centrifuge (Eppendorf, Hauppauge, NY; model 5702R). After centrifugation, 1 ml of supernatant was serially diluted in 9 ml test tubes of phosphate-buffered water five times. The cell concentrations were tested using standard membrane filtration techniques (0.45 μm filter) and compared with the control group which was not centrifuged. The change was acceptable if the percent of *E. coli* concentration change was less than 5%, thus the combination of “300 rpm + 5 min” was selected. Next the settling time for Kaolin was tested following the method in Section 3.1.3.1 again, except that the sample was centrifuged at 300 rpm for 5 min before settling. As a result, the combination of “300 rpm + 5 min” shortened the settling time for Kaolin suspensions to 18 hr (1080 min). The changes in concentrations for different “centrifuge speed + time” combinations are provided in Appendix A2.

3.1.4 Particle ratios

In this project, surface area was taken into consideration as one particle factor. Surface area ratios (clay particle surface area to *E. coli* surface area) were set at 1, 2, 50, 100, 200, 500, and 1000 for the settling method and 1, 2, 5, 10, 25, 50, 100, 150, 200, 300, 400, and 500 for the flow cytometry method. Fewer surface area ratios were used in the settling method because the settling experiments were much more time-consuming. The surface area of *E. coli* was estimated to be $6 \times 10^{-12} \text{ m}^2$ and the surface area of the clay particles was calculated using the surface area values provided in Table 3-1. The calculations for *E. coli* surface area and 1:1 surface are ratio are provided in Appendix A3.

In previous researches, the surface area of clay particles was always calculated using the density and average radius with assuming particle spherical in shape. But after calculation, the surface areas for all four clays were different from the surface areas given by manufacturers. The differences can be caused by: (1) the clay particles are not spherical in shape; (2) variability exists in particle sizes even in the same clay type. Therefore, in this study, surface areas given by manufacturers were selected to calculate the surface area ratios and clay concentrations. In lab scale, the surface area of fined-grained soils can be tested by the Ethylene Glycol Monoethyl Ether method (Cerato and Lutenegeger, 2002).

3.2 Experimental design

Strain #31, #50, #89, and #43888 were used in the settling method while #31, #50, and #89 were used in flow cytometry. Each strain was transferred into a sterile 15-ml conical tube containing Lysogeny broth or Tryptic Soy broth for growth at 37°C in a isotemp incubator (Fisher Scientific, Fair Lawn, New Jersey; model 625D) for 24 hr. Samples were removed and centrifuged for 3 min at 2,000 rpm (Eppendorf, Hauppauge, NY; model 5702R) at 4 °C. The supernatant was discarded, and 10 ml of phosphate-buffered water was added to each pellet. The pellet was resuspended by vortexing at 2000 rpm. The resuspended cells were diluted to a 0.5 McFarland standard (approximately 1.0×10^8 CFU ml⁻¹) according to the Clinical and Laboratory Standards Institute (January 2006) using phosphate-buffered water.

3.2.1 Settling (or centrifugation followed by Settling)

All the four *E. coli* strains were used in this method. Diluted *E. coli* culture, clay suspensions, and phosphate-buffered water were mixed up to 50-ml volume samples. The volumes of each component are provided in Appendix A2. The samples were transferred into 250-ml Erlenmeyer flasks and shaken at 80 rpm for 10 min on orbital shaker to increase bacterial particle interactions and attachments. After shaking, the samples were transferred to 50-ml conical tubes and the tubes were placed vertically in racks to allow clay particles to settle via gravity for set times except for the samples treated with Kaolin as centrifugation required. After settling in 37°C, 25 ml of supernatant was extracted and placed in a new conical tube. After vortexing for 10 s, 3ml of supernatant was removed and diluted in 27 ml phosphate-buffered water and then 1 ml from it was serially diluted in 9 ml phosphate-buffered water four times. The final concentration was within countable range recommended for membrane filtration techniques (APHA, 1999). The remaining 25 ml were added 1 drop of Tween 85 in the tube and shaken at 300 rpm for 10 min by handshaker (Eppendorf, Hauppauge, NY; model 5702R). The serial dilution procedure was the same as for supernatant. The total *E. coli* concentration in the supernatant and remainder were enumerated using 0.45 µm membrane filter (Milipore, Bedford, MA; Cat. No. HAWG047S6) by triplication for both supernatant and remainder and recorded as the unattached fraction and remainder fraction, respectively. Luria-Bertain agar (BD, Franklin Lakes, NJ; Cat. No.

244520) and Tryptic Soy broth (BD, Franklin Lakes, NJ; Cat. No. 236950), were used to culture bacteria for environmental strains and serotype O157:H7, respectively. Figure 3 shows the flow chart of experimental procedures.

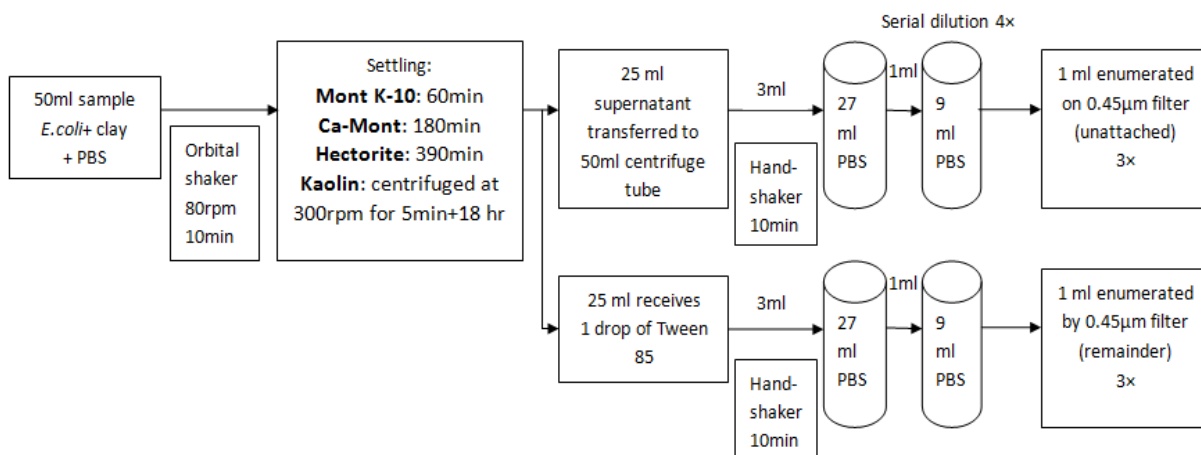


Figure 3. Flow chart of the settling method procedures
(Mont is the abbreviation for Montmorillonite)

3.2.2 Flow cytometry

E. coli concentration needs to be determined at first. 10^3 to 10^7 CFU ml⁻¹ has previously been recommended as the optimal concentration of *E. coli* in flow cytometer (Hussein et al., 2002). According to this, 10^6 CFU ml⁻¹ was selected first but the numbers of evens were too low to obtain stable attachment fractions. Therefore, in this project, 10^7 CFU ml⁻¹ was used for attached and unattached *E. coli* detected by flow cytometry. Samples were processed using FACSCanto flow cytometer (BD, Franklin Lakes, NJ).

The phosphate buffer water was filtered through 0.45 µm filter and then centrifuged at 2500 rpm for 5 minutes at 4°C three times to minimize the amount of background contamination fluorescence. SYTO dyes 11, 13, and 24 worked best on the test of *E. coli* with Kaolin and a variety of SYTO dyes and SYTO 11 was used as the dye in studying *E. coli* attachment to particulates (Tysman, unpublished data). SYTO 11 green fluorescent nucleic acid stain was selected in this study and was filtered through 0.2 µm filter and then centrifuged at 2500 rpm for 5 minutes at 4°C three times. Once the *E. coli* and soil solutions

have been made they are combined in test tubes. The complete list of the different combinations of *E. coli* strains, clay particles and surface area ratios, is provided in Appendix B1. Fixed volumes of *E. coli*, clay, phosphate-buffered water, with/without SYTO 11 were added to the tubes to create a test volume of 250 μl for each test tube (BD, Franklin Lakes, NJ; Cat. No. 352008). Additionally, for each group, 6 controls were required prior to testing: PBS only, PBS+SYTO dye, PBS+ *E. coli*, PBS+*E. coli*+ SYTO dye, PBS+ clay, and PBS+ clay+ SYTO dye. One example of original plots from flow cytometry showing all 6 controls was in Appendix I.

Next, 2 μL of SYTO 11 was added once the other components were in the test tubes. This is done right before the samples analyzed because the SYTO dye is light-sensitive. SYTO dye is added to the samples as it permeates the membrane of the *E. coli* cells and allows them to fluoresce at different wavelengths, which helps to identify the *E. coli* from background fluorescence and soil particles. Once the samples have all the components for the particular test they are run through the flow cytometer and analyzed.

3.3 Calculations and statistical analysis

3.3.1 Percent attached calculations

In settling method, the percent attached *E. coli* was computed as:

$$\text{Percent attached (\%)} = \frac{25R+25U-50U}{25R+25U} \times 100\% = \frac{R-U}{R+U} \times 100\%$$

where

U is the concentration of *E. coli* in the unattached fraction (CFU ml^{-1}),

R is the concentration of *E. coli* in the remainder fraction (CFU ml^{-1}).

In flow cytometry method, the percent attached *E. coli* can be calculated using IVD cleared BD FACSCanto system (BD, Franklin Lakes, NJ).

3.3.2 Statistical analysis

Statistical analysis of data was performed using R project software (version 2.14.1). Firstly, the settling data, flow cytometry data, and the attachments differences between using two method data were tested the normality and transformations were needed if the

distribution was not normal. Secondly, several statistical tests were applied to determine the impact on *E. coli* attachment to clay particles from each of the variables or interactions.

3.3.2.1 Data transformations

The original settling data showed slightly right-skewed distribution (Appendix F1, Figures F1-1, F1-2, and F1-3). Natural log and Box-cox ($\lambda=0.39$) transformations were applied to the settling data. Normality tests (Appendix F2, Figures F2-1, F2-2, F2-3, and F2-4) show transformations did not improve the normality sufficiently. Therefore, settling data was used in the original form when comparing variables within the settling method.

The original data from flow cytometry method were also right-skewed (Appendix F1, Figures F1-4, F1-5, and F1-6). Natural logarithm (natural log) transformation was applied to the flow cytometry data and normality tests after log transformation demonstrated perfect normality (Appendix F2, Figures F2-5, and F2-6).

The attachment fraction differences distribution were slightly right-skewed (Appendix F1, Figure F1-7, and F1-8). A uniform data format for both the settling data and flow cytometry data is required for the method comparison statistics. Natural log transformation was applied and it was found that the distribution was almost normal after removing the surface area ratio 1 and 2 from the analysis (Appendix F2, Figure F2-7, F2-8, F2-9, and F2-10). The clay concentrations for these two samples (surface area ratio 1 and 2) were extremely low compared to the concentrations typically observed in environmental waters samples. Thus, these two surface area ratios would make little sense in environmental applications.

3.3.2.2 Statistical tests

Significances was determined at the $p<0.05$ level for all statistical analysis.

One sample t-tests were conducted to determine the method variability between the settling and flow cytometry separation techniques. The null hypothesis was that the natural log attachment ratios from the two methods are equal for certain variable combinations.

Two Three-way Anova tests were conducted to test the impacts on attachment ratios from each variable (clay type, strain, or surface area ratio) and each interaction (clay type :

strain, clay type : surface area ratio, or clay type : strain : surface area ratio) for the settling method and flow cytometry method, separately. The null hypothesis was that there would be no impact on attachment ratio from each certain variable or interaction. A third Three-way Anova test was conducted to test the impact of natural log attachment ratio difference between methods from each variable (clay type, strain, or surface area ratio) and each interaction (clay type : strain, clay type : surface area ratio, or clay type : strain : surface area ratio).

Pairwise comparisons were conducted using Tukey's test for each method. The null hypothesis was that there would be no differences of impact on attachment ratio (or natural log attachment ratio) between two clays, strains or surface area ratios. Pairwise comparisons can also show the difference between expected attachment ratios of two or three certain variable interactions (clay type : strain, clay type : surface area ratio, or clay type : strain : surface area ratio).

CHAPTER 4 RESULTS AND DISCUSSIONS

4.1 Results

The experimental data described in this chapter indicates that the both settling and flow cytometry methods were successful in enumerating unattached and attached *E. coli*. The percent attached reached a maximum value of 99.8% for *E. coli* attachment to Kaolin. Moreover, from the three-way Anova (Appendix G), clay type, strain type and surface area ratio all impacted the *E. coli* attachment to clay particles. Our results indicate that flow cytometry is a rapid and accurate method to test the attachment ratio of *E. coli* to clay particles.

The results are discussed by each method. Within each method, the impacts on attachment from each of the factors and their implications are also discussed. Additionally, the two methods are compared. The average percent attached of each variable is in Table 3 while all raw data is in Appendix C.

Table 3. Average percent attached of each variable

Variable		Settling Percent attached	Flow cytometry Percent attached
Clay	Hectorite	42% a	-
	Kaolin	43% a	39% a
	Ca-Montmorillonite	26% b	11% b
	Montmorillonite K-10	21% c	5% c
Strain	#31	34% a	28% a
	#50	30% b	14% b
	#89	34% a	12% c
	#43888	35% a	-
Particle: <i>E. coli</i> ratio	1	17% a	1% a
	2	18% a	1% b
	5	-	1% c
	10	-	2% d
	25	-	5% e
	50	24% b	13% f
	100	31% c	25% g
	150	-	28% h
	200	35% c	32% i
	300	-	31% ij
	400	-	36% jk
	500	47% d	40% kl
1000	59% e	-	
Average		33%	18%

* Average percent attached was an average of all values for each variable.

* Within each column, values with the same letter are not significantly different at the $p=0.05$ level.

4.1.1 Settling method

The settling method was used to test the attachment ratios for four strains (#31, #50, #89, and #43888), four clays (Kaolin, Hectorite, Ca-Montmorillonite, and Montmorillonite K-10), and seven surface area ratios (1, 2, 50, 100, 200, 500, and 1000). The average percent attached for all variables tested by settling method was 33%. The smallest percent attached was 1.55%, which was strain #50 attached to Ca-Montmorillonite with surface area ratio 1:1, while the highest was 96.25%, which was strain #50 attached to Hectorite with surface area ratio 1000:1.

4.1.1.1 Differences in attachment to clays

In the settling method, *E. coli* was more likely to attach to Kaolin (averaged 43%) and Hectorite (averaged 42%) than to Ca-Montmorillonite (averaged 26%) or Montmorillonite K-10 (averaged 21%), which is shown Figure 4. From the results of the Tuckey's pairwise, no statistically significant difference were observed between the attachment to Kaolin and Hectorite (p -value=0.8927) (Table 4). With considering the key properties for each clay type (Table 2), we can conclude from the settling method results that *E. coli* are more likely attach to clay particles with a smaller diameter.

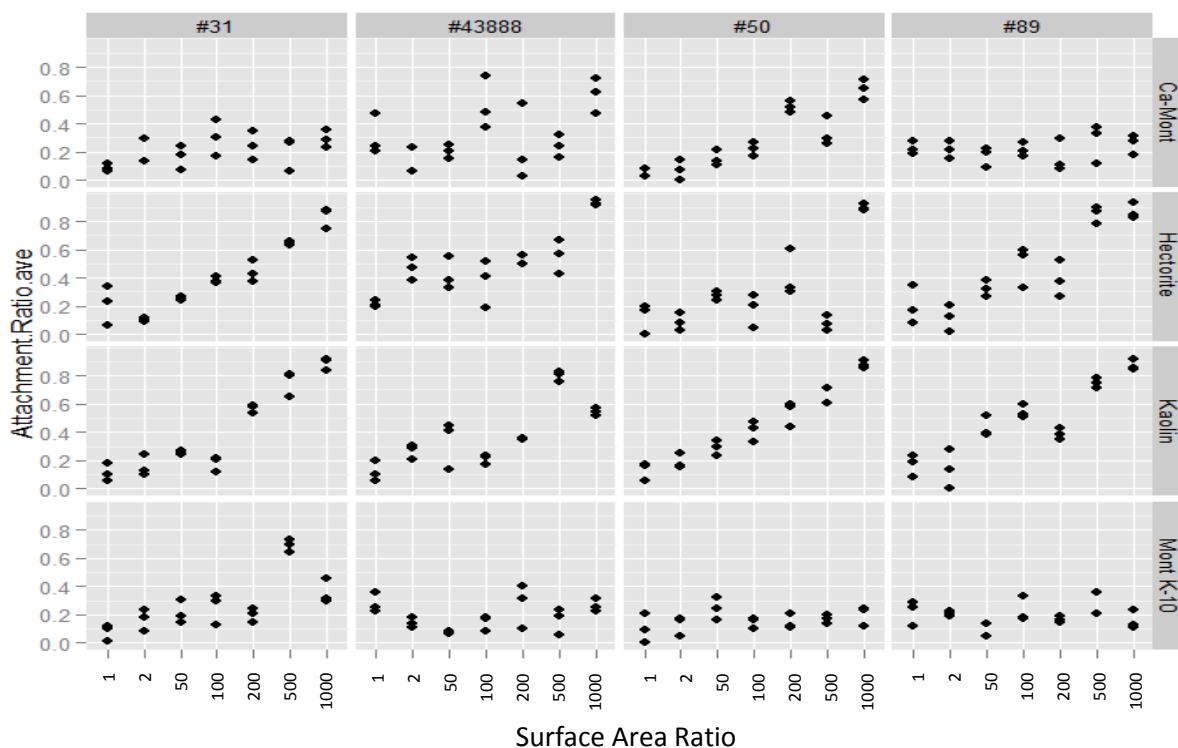


Figure 4. Scatter plots of attachment ratios from the settling method showing clay particle variability. Each plot was made for one “strain+ clay” combination by different particle: cell surface area ratios. The figure shows that *E. coli* was more likely to attach to Kaolin and Hectorite than to Ca-Montmorillonite and Montmorillonite K-10.

Table 4. Attachment difference between different clays in the settling method (p-values are in parentheses). The differences were achieved by subtracting “row” from “column”.

Clay	Hectorite	Kaolin	Ca-Mont	Mont K-10
Hectorite	-	0.009 (0.8927)	-0.156 (0.0000)	-0.209 (0.0000)
Kaolin	-0.009 (0.8927)	-	-0.166 (0.0000)	-0.219 (0.0000)
Ca-Mont	0.156 (0.0000)	0.166 (0.0000)	-	0.053 (0.0005)
Mont K-10	0.209 (0.0000)	0.219 (0.0000)	-0.053 (0.0005)	-

* “Mont” is abbreviation for “Montmorillonite” (same as below).

4.1.1.2 Impact of particle ratio on attachment

There were 7 surface area ratios (clay surface area to *E. coli* surface area) tested in the settling method: 1, 2, 50, 100, 200, 500, and 1000.

From Figure 5, we can conclude that, generally, the ascending trend of percent attached was associated with increased particle ratio (all slopes were positive). The ascending slope was sharper when the clay type was Hectorite (slope =0.0006) or Kaolin (slope =0.0006) than when the clay type was Ca-Montmorillonite or Montmorillonite K-10 (slope =0.0002 or 0.0001). From the observations of Figure 6, there were no obvious differences between the ascending slopes of different strains.

We also compared the surface area ratio impacts using Tukey’s pairwise comparison test. Percent attached of particle ratio 1 (averaged 17%) and 2 (averaged 18%) and were not significantly different from each other; as were particle ratios of 100 (averaged 31%) and 200 (averaged 35%). Once the surface area ratio increased from 500 to 1000, the percent attached increased by 27%, which was the greatest change among neighboring two surface area ratios. The partial pairwise comparisons were listed in Table 4, while the whole list was in Appendix H.

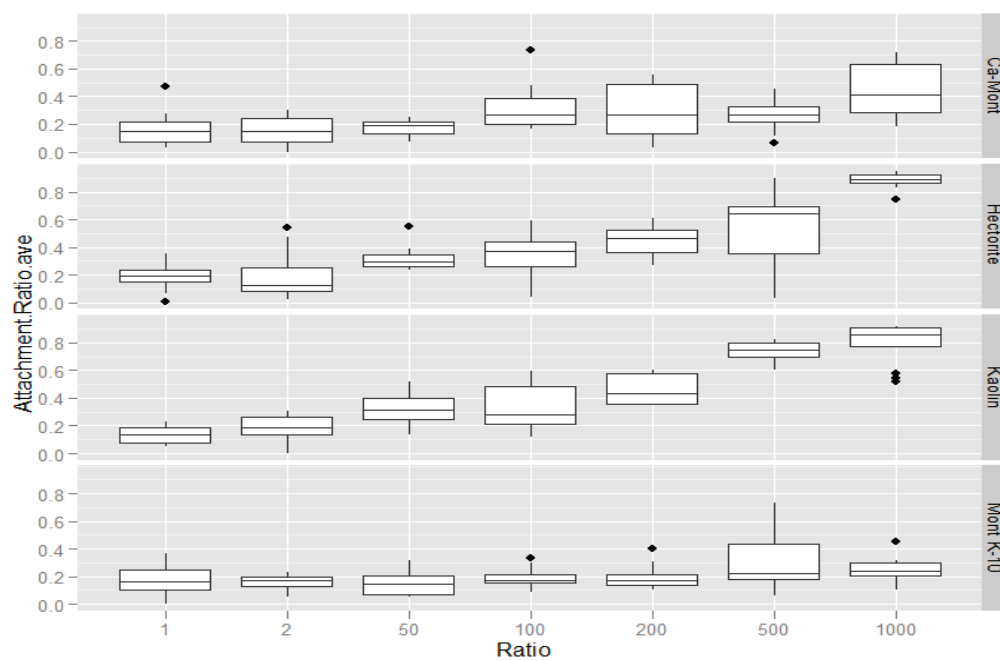


Figure 5. Boxplots of attachment ratios in the settling method analyzed by clay type. The plots show the trend for clay type by increasing surface area ratios. All slopes were positive, which indicated an ascending trend of attachment fractions was associated with increased particle ratios.

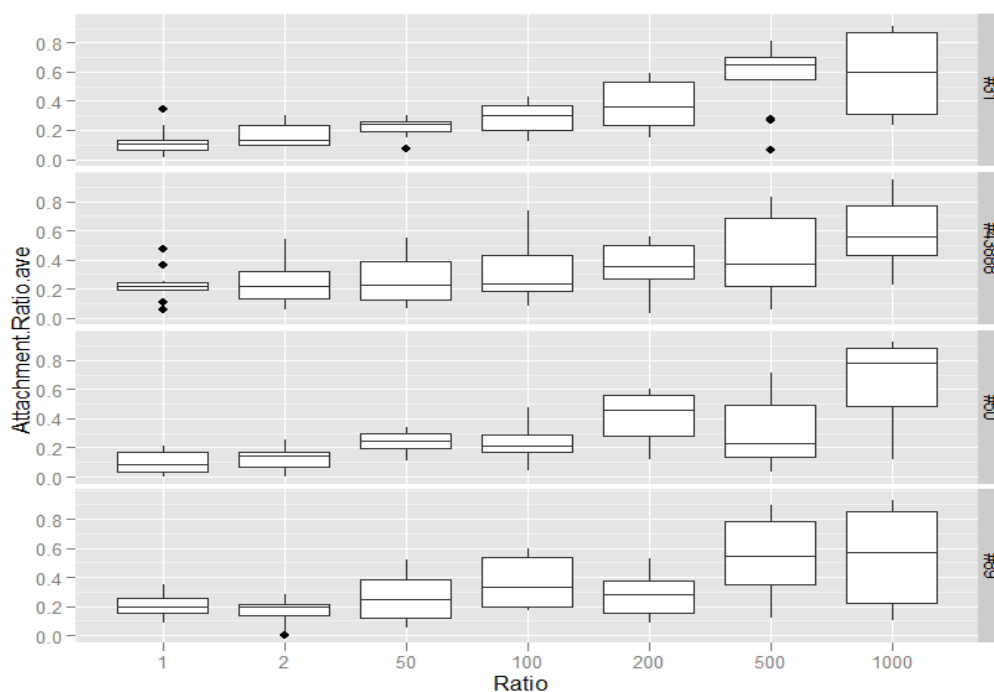


Figure 6. Boxplots of attachment ratios from the settling method analyzed by strain. Each of the plots compares attachment of each strain by different surface area ratios. All slopes were greater than 0, which indicated that the ascending trend of attachment fractions was associated with increased particle ratio.

Table 5. Partial pairwise comparisons of attachment ratios between different particle ratios in the settling method (only showing the comparisons without significant differences)

Method	Comparison	Difference	95% Confidence Interval		p-value
			Lower Limit	Upper Limit	
Settling method (untransformed)	2-1	0.01249478	-0.0390342	0.06402374	0.991177
	200-100	0.04642778	-0.0051012	0.09795675	0.107976

We can conclude that the ascending trend of attachment ratios was associated with increased particle ratio and the trend was more significant for clays with smaller particle sizes.

4.1.1.3 Differences in attachment among strains

In the settling method, we tested the attachments of three environmental *E. coli* strains from swine facilities, #31, #50, and #89, as well as #43888 as a pathogenic strain purchased from ATCC™.

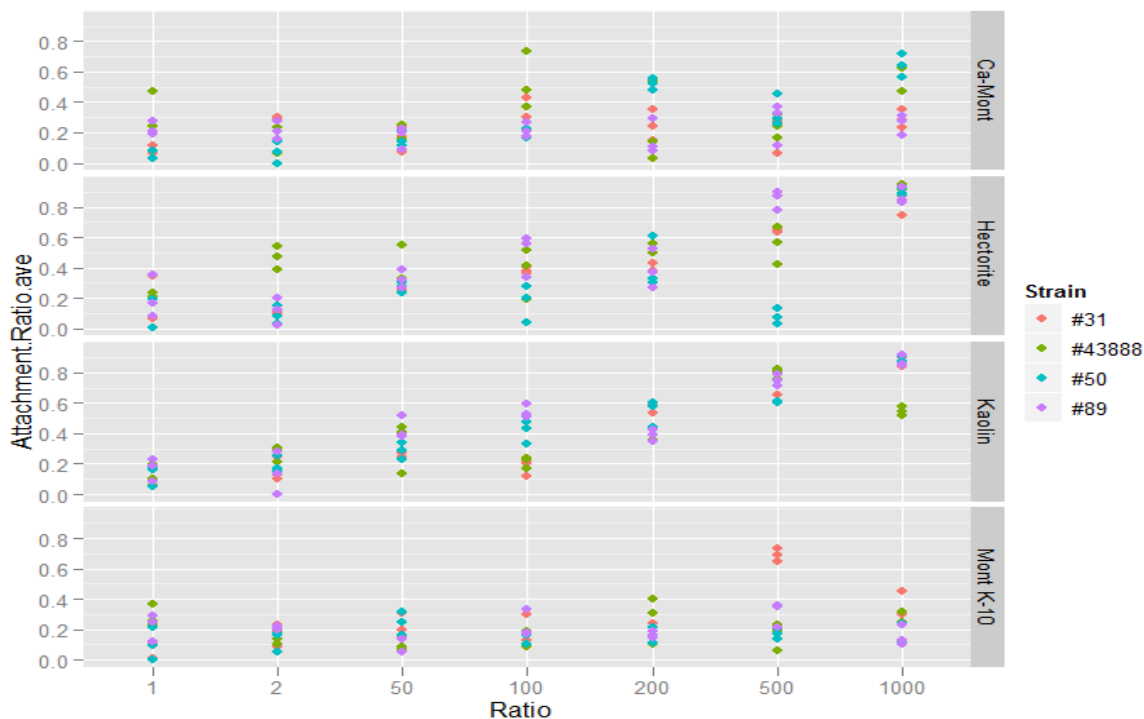


Figure 7. Scatter plots of attachment ratios from the settling method. Each plot shows the relationships between clay, surface area ratio, and strain, which is represented by colored dots.

From result analysis, it is difficult to distinct which strain had the highest attachment ratio visually (Figure 8), but the attachment ratios of #50 were consistently lower than the ratios of other three strains. The results from the pairwise comparison tests (Table 5) were consistent with observations from scatter plots in Figure 7. Strain #43888, #31, and #89 had similar attachment ratios which were greater than the attachment ratios of #50. Therefore, the genotype of the strain appears to impact the attachment.

Table 6. Attachment difference between different strains in the settling method (p-values are in parentheses). The differences were achieved by subtracting “row” from “column”.

Strain	#31	#50	#89	#43888
#31	-	-0.036 (0.0293)	0.005 (0.9828)	0.014 (0.6857)
#50	0.036 (0.0293)	-	0.041 (0.0098)	0.051 (0.0007)
#89	-0.005 (0.9828)	-0.041 (0.0098)	-	0.010 (0.8816)
#43888	-0.014 (0.6857)	0.051 (0.0007)	0.010 (0.8816)	-

4.1.2 Flow cytometry

The flow cytometry separation method tested the attachment ratios for three strains (#31, #50, and #89), four clays (Kaolin, Hectorite, Ca-Montmorillonite, and Montmorillonite K-10), and twelve surface area ratios (1, 2, 5, 10, 25, 50, 100,150, 200, 300, 400, and 500). The average percent attached tested by flow cytometry was 18%. The percent attached ranged from 0.2% to 99.8%. 99.8% was also the highest tested in this study and happened when strain #31 attached to Kaolin with surface area ratio 400:1. The dot plots and histogram were made for one triplication of every combination (Appendix D).

4.1.2.1 Differences in attachment to clays

The percent attached of *E. coli* to Hectorite were detected by the flow cytometer but they were not included in the statistical analysis due to unreasonably low values. As an example of strain #31 is shown in Figure 8: the average percent attached from flow cytometry were 74% lower than the ratios from the settling method.

From Table 2, Hectorite has the smallest particle size, with an average diameter 1 μm . It is much smaller than the size of *E. coli*, 2.5 μm length and cross section with 1 μm as diameter. After attaching to Hectorite particles, the size of *E. coli* would not change greatly. It is difficult to determine the gage limit between “attached” and “unattached” cells (Figure 9). Therefore, *E. coli* “attached” to Hectorite are more likely showing in “unattached” area than attached *E. coli* to other three kinds of clay particles. This is the probable reason for the lower value of attachment ratios in this method and a potential limitation of the flow cytometry method.

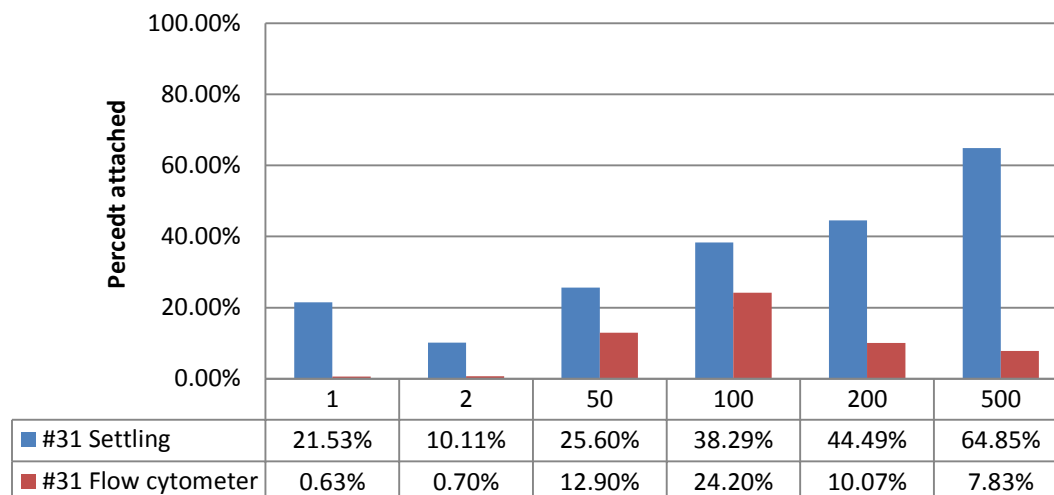


Figure 8. Average percent attached of strain #31 to Hectorite. Each bar represented the average percent attached with one surface area ratio. The attachments tested in the settling method were obviously greater than the attachments tested in flow cytometry.

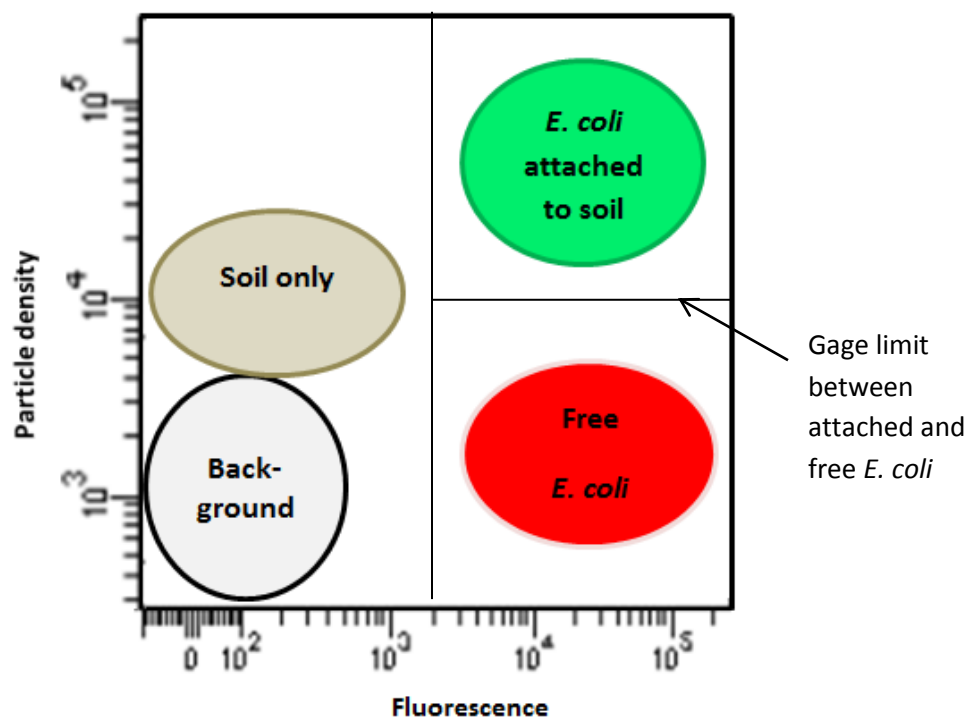


Figure 9. Ideal dot plot from the flow cytometry separation technique.

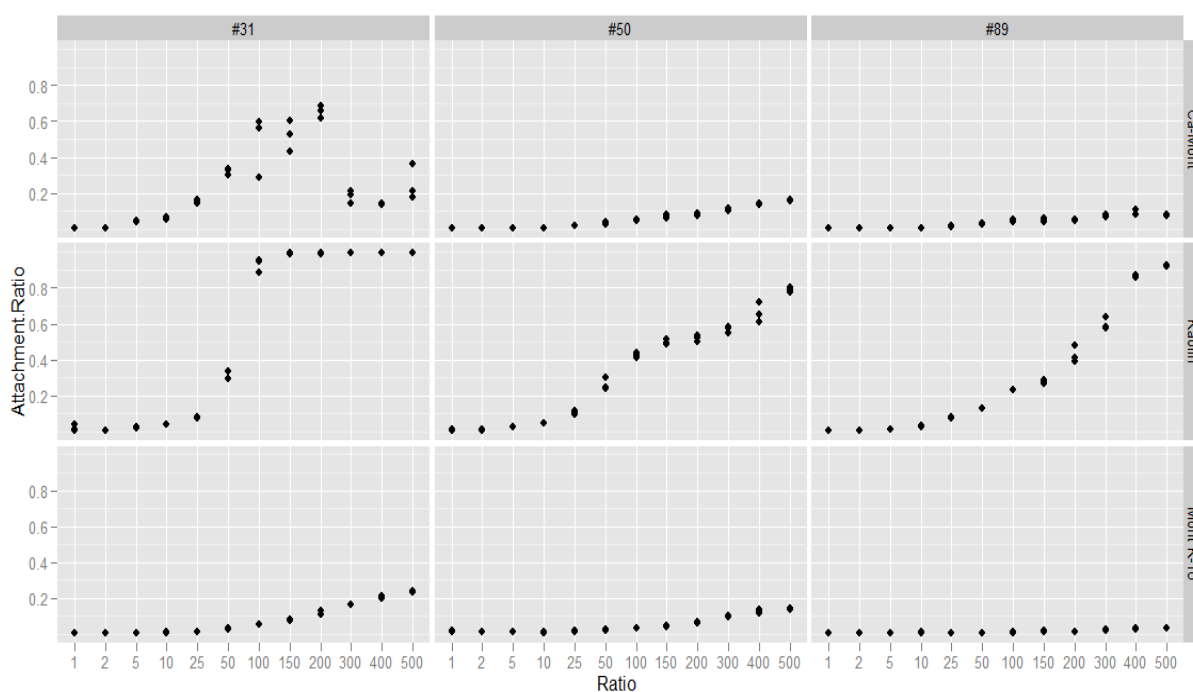


Figure 10. Scatter plots of attachment ratios by from flow cytometry. Each of the plots was made for one “strain+ clay” combination by different surface area ratios. We can observe that *E. coli* showed more likely attaching to Kaolin than attaching to Ca-Montmorillonite and Montmorillonite K-10.

The scatter plots in Figure 10 show that when using the flow cytometry separation technique, Kaolin (averaged 39%) showed the highest attachment fractions to *E. coli*, followed by Ca-Montmorillonite (averaged 11%) and Montmorillonite K-10 (averaged 5%). The pairwise comparison confirmed the observations from the plots and showing that there were significant differences between the attachment ratios to different clay particles (p -value=0). Moreover, Ca-Montmorillonite and Montmorillonite K-10 are belonging to the same phyllosilicate group of minerals- Montmorillonite. These two clay types shared plenty of common characteristics, such as pH and surface charge. The distinct difference is Montmorillonite K-10 has much larger particle size (Table 2). In summary, *E. coli* are more likely attach to small size clay particles, which is consistent with the results obtained from the settling method experiments.

Table 7. Attachment difference between different clays in flow cytometry (p-values are in parentheses). The differences were achieved by subtracting “row” from “column”.

Clay	Kaolin	Ca-Mont	Mont K-10
Kaolin	-	-1.266 (0.0000)	-1.862 (0.0000)
Ca-Mont	1.266 (0.0000)	-	-0.596 (0.0000)
Mont K-10	-1.862 (0.0000)	0.596 (0.0000)	-

4.1.2.2 Impact of particle ratio on attachment

Because testing the attachment via flow cytometry is less time-consuming work i, there were 12 surface area ratios (clay surface area to *E. coli* surface area) tested in the settling method: 1, 2, 5, 10, 25, 50, 100,150, 200, 300, 400, and 500. Surface area ratio 1000 was not included because of the possibility that inlet tubes might be clogged by high concentrations of particles.

Consistent with the results from settling method experiments, the ascending trend of attachment ratios was associated with increased particle ratio (all slopes were greater than 0). The ascending slope was sharper when the clay type was Kaolin (slope =0.02) than when the clay type was Montmorillonite (slope =0.0003). The same conclusion can be drawn from observations from the scatter plots in Figure 11 and 12. There were no obvious differences between the ascending slopes of different strains. The surface area ratio impacts were also compared through pairwise comparisons. The average percent attached between 200(averaged 27%) and 300 (averaged 27%), between 300 (averaged 27%) and 400 (averaged 32%), between 400 (averaged 32%) and 500(averaged 36%) showed no statistically significant differences. The increase from surface area ratio 2 and 5 was greatest (110%) and statistically significant.

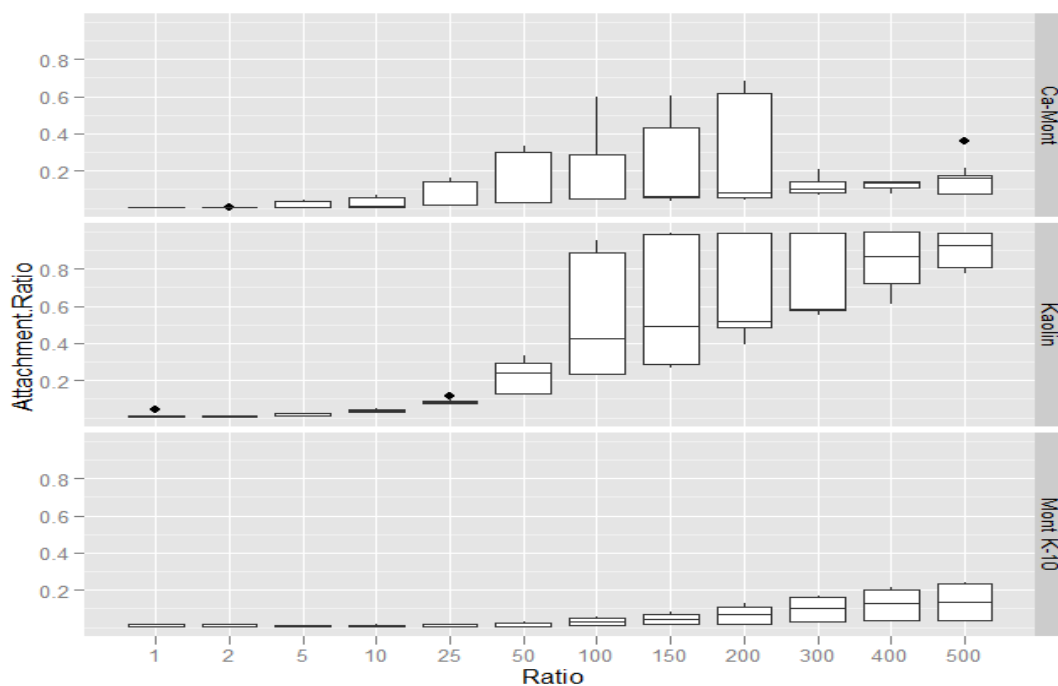


Figure 11. Boxplots of attachment ratios analyzed by clay type from samples collected using flow cytometry separation technique. Each of the plots shows clay type by different surface area ratios. All slopes were positive, which indicated that the ascending trend of attachment ratios was associated with increased particle ratio. And the slopes of Kaolin was greater than the slopes of Ca-Montmorillonite and Montmorillonite K-10.

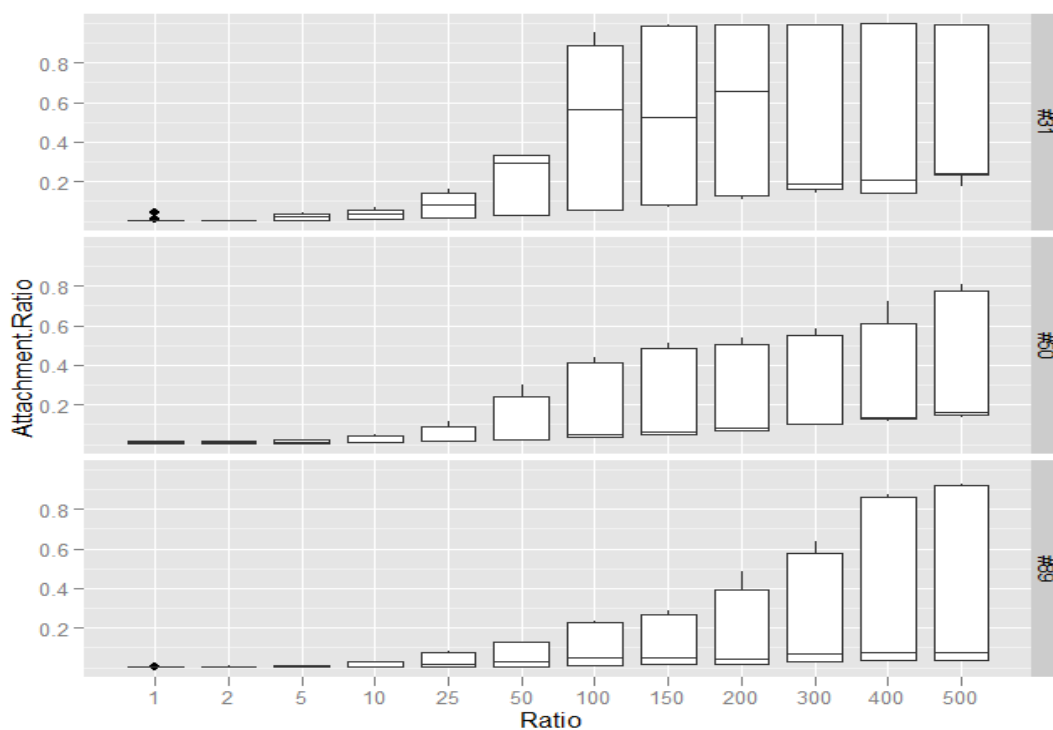


Figure 12. Boxplots of attachment ratios analyzed by strain from samples collected using flow cytometry separation technique. Each of the plots was made for one strain by different surface area ratios. All slopes were greater than 0, which indicated that the ascending trend of attachment ratios was associated with increased particle ratio.

Table 8. Pairwise comparisons of attachment ratios between different particle ratios from flow cytometry (only showing the comparisons without significant differences)

Method	Comparison	Difference	95% Confidence Interval		p-value
			Lower Limit	Upper Limit	
Flow cytometry (natural log transformed)	300-200	0.11876369	-0.049465	0.28699249	0.45683
	400-300	0.15468624	-0.013543	0.32991505	0.10483
	500-400	0.11973391	-0.048495	0.28796272	0.44357

4.1.2.3 Differences in attachment among strains

In flow cytometry experiments, only the attachments of three environmental *E. coli* strains, #31, #50, and #89 were tested. Strain #43888 was not considered in this method due to laboratory safety consideration.

The scatter plots in Figure 13 and Tukey's pairwise comparison in Table 8, showed that #31 had the highest attachment ratios to clay particles while #50 had lower ratios and #89 had the lowest. The results differ from the results obtained from the settling experiments, in which strain #89 had similar attachment ratios to strain #31.

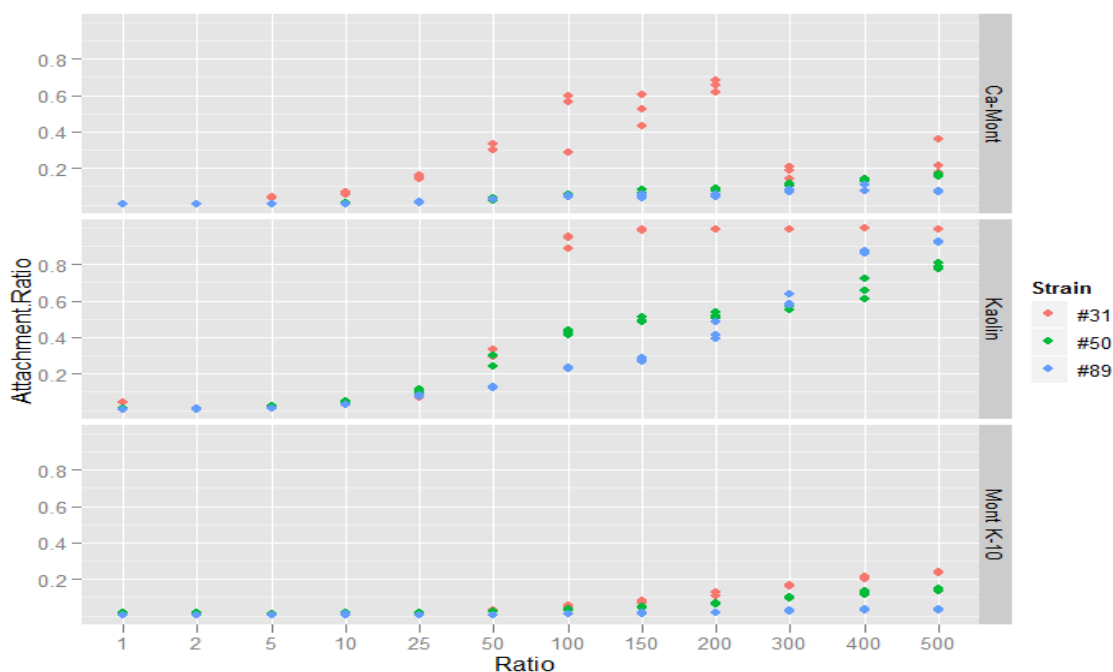


Figure 13. Scatter plots of attachment ratios from the flow cytometry separation technique. Each plot shows the comparison between different surface area ratios and each strain was using one color dots. The attachment fractions of strain #31 had the highest attachment fractions to clay particles while #50 had lower fractions and #89 had the lowest.

Table 9. Attachment difference between different strains in flow cytometry (p-values are in parentheses). The differences were achieved by subtracting “row” from “column”.

Strain	#31	#50	#89
#31	-	-0.503 (0.0000)	-1.161 (0.0000)
#50	0.503 (0.0000)	-	-0.658 (0.0000)
#43888	1.161 (0.0000)	0.658 (0.0000)	-

4.1.3 Method comparisons

In the method comparisons, surface area ratio 1 and 2 was removed to achieve normal distribution and Hectorite were not included in flow cytometry analysis as well as strain #43888. Two methods were compared among the three strains, #31, #50, and #89; three clay types, Kaolin, Ca-Montmorillonite, and Montmorillonite K-10; and six surface area ratios (clay surface area to *E. coli* surface area, 1, 2, 50,100, 200, and 500. The scatter plot of the residuals vs. Fitted values for the natural log attachment ratio differences between flow cytometry and the settling method results is shown in Figure 14 and indicates a normal distribution of data

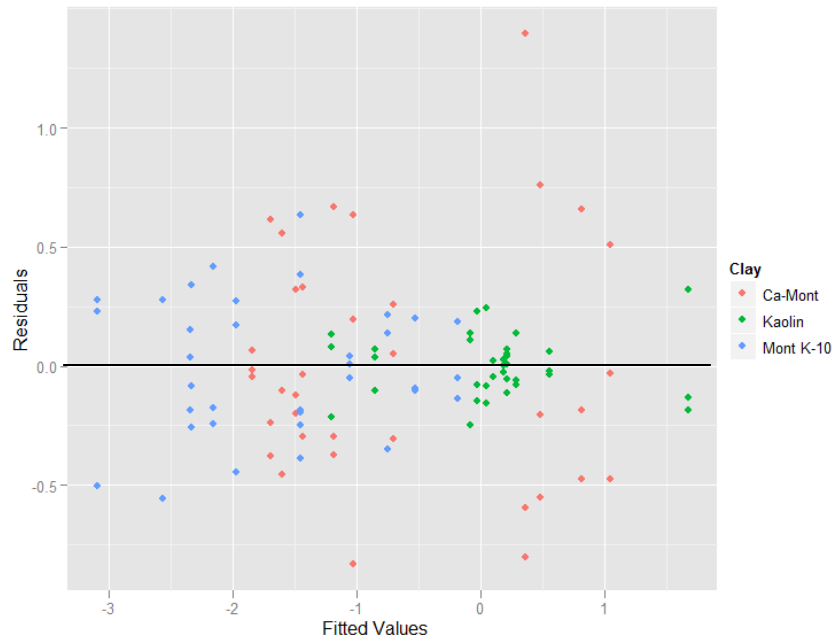


Figure 14. Residuals vs. fitted values for the natural log attachment ratio differences between flow cytometry and the settling method (surface area 1 and 2 removed). The black reference line was set at residuals=0 which indicates that after surface area 1 and 2 removed, the distribution of attachment ratio was almost normal.

From the scatter plot shown in Figure 15, 73 out of 108 (67.6%) natural log attachment ratio differences between flow cytometry and the settling method were below 0. We can conclude that generally the attachment ratios achieved from flow cytometer analysis had smaller values than the ratios from the settling method. However, there were some exceptions. The boxplots analysis by clay type (Figure 16A) showed that when the clay type is Kaolin, the attachment ratios among the two methods were similar. The same observation occurred for strain #50 (Figure 16B) and for surface area ratios 200 and 500 (Figure 16C).

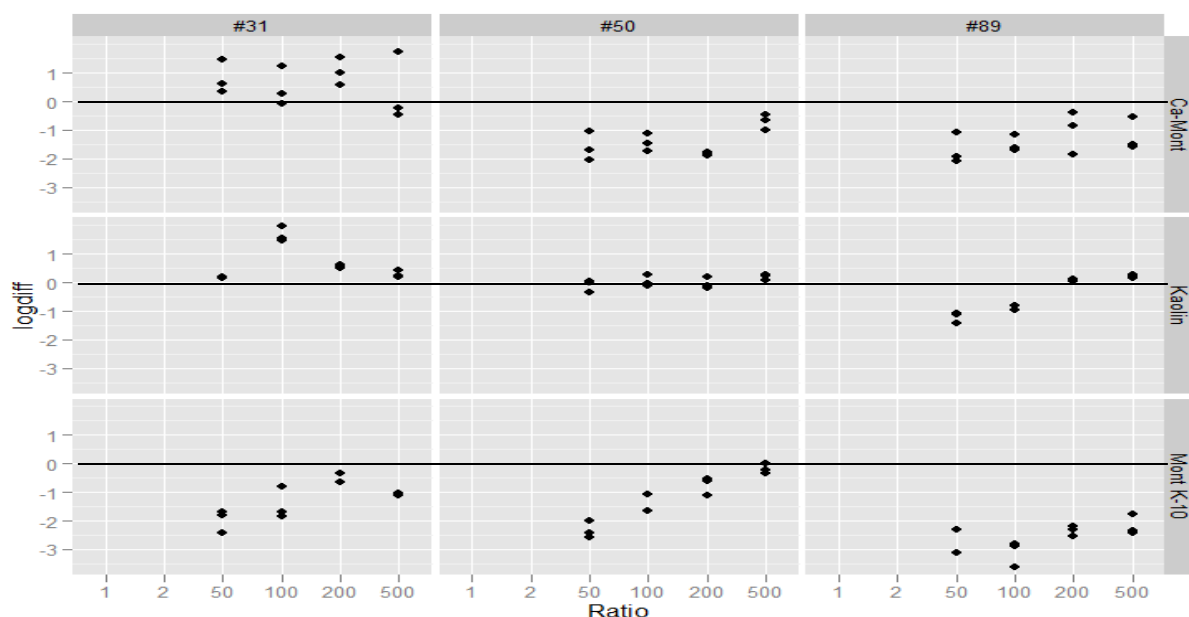


Figure 15. Scatter plot of the natural log attachment ratio differences between flow cytometry and the settling method. Each plot shows one “strain+ clay” combination by different surface area ratios and one blank reference line was set at log difference =0 on each of the plots. Majority of the dots were below the reference lines, which indicated that majority attachment ratios from flow cytometry were lower than the corresponding ratios from the settling method.

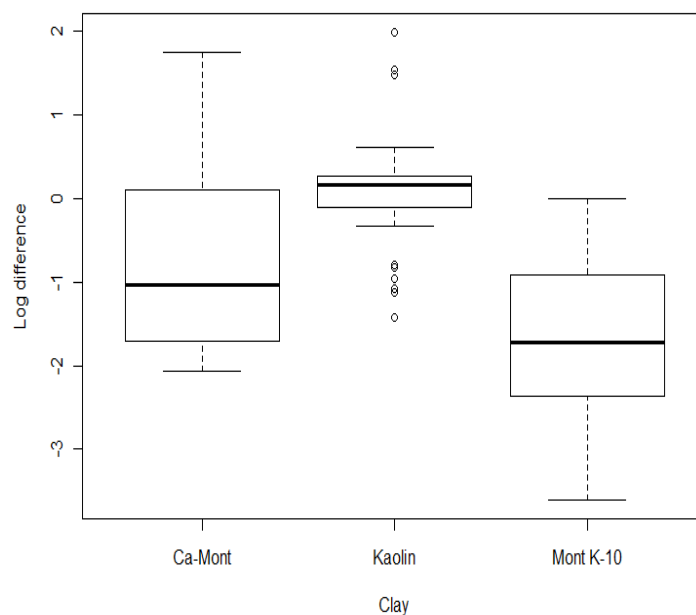


Figure 16A. Boxplots of natural log attachment ratio differences between flow cytometry and the settling method by clay type. The medians in boxplots of Ca-Montmorillonite and Montmorillonite K-10 were below 0 while median of Kaolin was a little above 0. It showed when the clay type is Kaolin, the attachment ratios got from two methods were similar

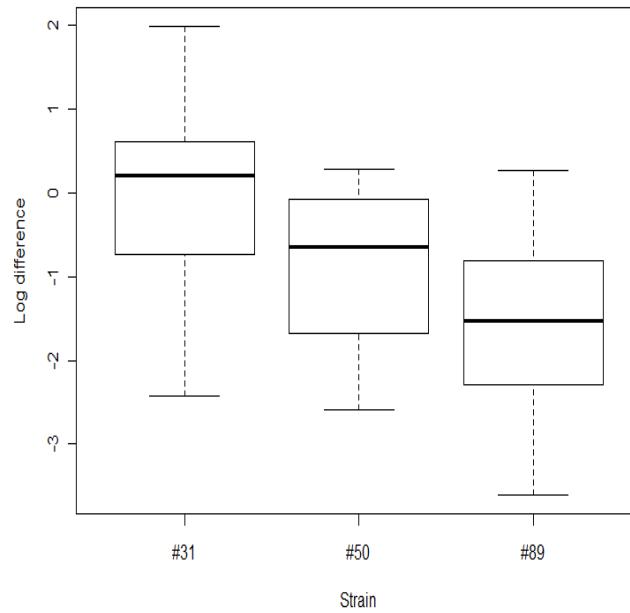


Figure16B. Boxplots of natural log attachment ratio differences between flow cytometry and the settling method by strain. The medians in boxplots of #50 and #89 were below 0 while median of #31 was a little above 0. For strain #31, the attachment ratios from the two methods were similar.

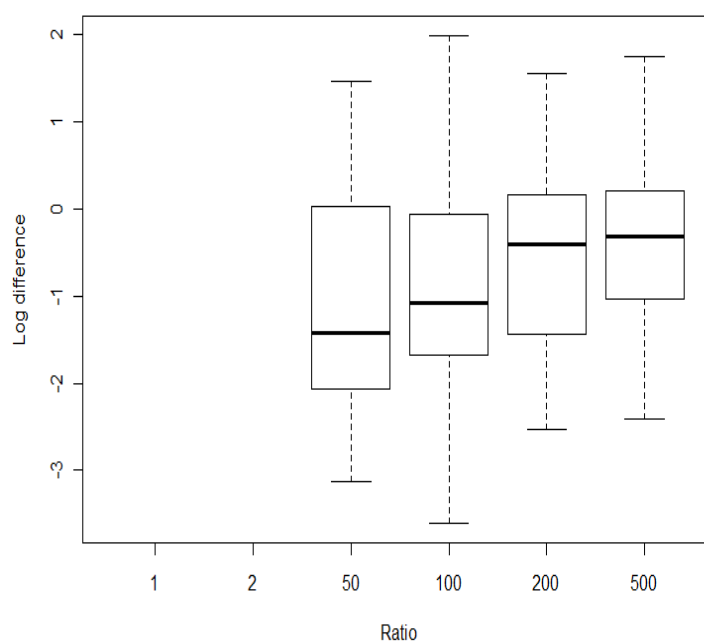


Figure16C. Boxplots of natural log attachment ratio differences between flow cytometry and the settling method by surface area ratio. As the surface area ratio increased from 50 to 500, the median-log difference value increased and approached to zero, which indicated that the attachment ratio difference between using two methods became less significant at higher ratios.

The results from one sample t-tests were consistent with observations in the plots above. When the clay type was Kaolin, the p-value was 0.4421, greater than 0.05. And the p-value was 0.8745 when the strain was #31. According to these, no statistically significant differences between two methods are observed when the clay type is Kaolin or the strain is #31. Each variable and interaction was tested in the one sample t-test. Under most conditions, the t values were negative, which indicated that the expected attachment ratio achieved using flow cytometry was smaller than the ratio from the settling method. The averaged percent attached with three strains, 3 clay particles, and 6 percent attached from the settling method was 27% while from the flow cytometry method, it was 19%. The tested ratios using the settling method were 44% higher than using flow cytometry on average. However, there were still some situations in which percent attached obtained from the flow cytometer were greater than from the settling method: clay type was Kaolin ($t=0.7774$, $p\text{-value}=0.4421$), strain #31 ($t=0.1591$, $p\text{-value}=0.8745$), or clay type was Ca-Montmorillonite with strain #50 ($t=3.183$, $p\text{-value}=0.008715$). For different surface area ratio (clay particle surface area to *E.*

coli surface area), 200 ($t=-2.5583$, $p=0.01669$) and 500 ($t=-2.6477$, $p=0.01359$) had similar distribution, which indicated with an increase in the surface area ratio, the difference between using the flow cytometry and the settling method became less significant.

4.2 Discussion

4.2.1 Impacts of clay type on bacteria attachment

From Chapter 4.1, we concluded that among the four clay particles used in this study, *E. coli* was more likely to attach to Hectorite and Kaolin than to Ca-Montmorillonite or Montmorillonite K-10. Sediment bacterial abundance can be influenced by several variables of soils including sediment size, sediment organic content (Schallenberg and Kalff, 1993) and surface charge (Pachepsky et al., 2006).

In urban storm water runoff, fecal indicator bacteria were adsorbed predominantly to fine clay particles ($<2 \mu\text{m}$) (Muirhead et al., 2006). The author concluded that the reason is that bacteria were an important component of flocs, which can support the transport fine particles in river systems. In 2006, Pachepsky et al., conclude that the content of clay particle $<2 \mu\text{m}$ is the leading factor affecting bacteria attachment to soil. Our results were consistent with their findings. Kaolin, with average diameter $1 \mu\text{m}$, and Hectorite, with average diameter $1.25 \mu\text{m}$, are more likely attaching to *E. coli* compared to Ca-Montmorillonite or Montmorillonite K-10, which both have larger particle size. This observation can likely be explained by the surface area: volume ratio:

$$\frac{\text{Surface area}}{\text{volume}} = \frac{4\pi R^2}{\frac{4}{3}\pi R^3} = \frac{3}{R}$$

where R is the sediment particle radius.

From the above equation, smaller particles would have a larger surface area: volume ratio. Thus, within the same sediment volume (or weight, because pure sediments share similar density), the smaller particle would have more opportunities to attach to bacteria. In this project, within the same surface area ratio (clay particles: *E. coli*), all the samples tested had the same clay particle surface area. But as shown in Table 2, Kaolin and Hectorite have smaller surface area (in m^2/g) than Ca-Montmorillonite and Montmorillonite K-10, which

means Kaolin and Hectorite would have more weight and more particles within the same surface area. Larger amount of particle can also increase bacteria attachment to particles.

Organic content variability can also explain some of the differences between the attachment to Kaolin or Hectorite and to Ca-Montmorillonite or Montmorillonite K-10. Bacteria are more likely to attach to high organic content particles (Nicholson et al., 2005) as their nutrient sources. It was shown previously that Kaolin contains 0.066% organic content a dry weight (Bundy, 2011), Hectorite and Montmorillonite contain <0.05% organic content (Jaynes and Vance, 1999). Highest bacterial attachment to Kaolin may have likely been influenced by the higher organic content of this clay. However, the manufacturers did not provide the organic matter information, therefore tests for clay organic matter content is recommended for further study.

E. coli and clay minerals have a low net negative surface charge over a wide range of pH values (Ohman et al., 1981; Unc and Goss, 2004; Pachepsky et al., 2006). Thus, charge-based attachment from *E. coli* to clay particles is likely to be hindered. A combination of electrostatics combined with hydrophobic effects can overcome the natural repulsion of bacteria and particles which express the similar charges at surfaces (Mills, 2003). Therefore, surface charge is not considered to play an important role in the *E. coli* attachments to clay particles in this study.

As mentioned in Chapter 3, the clay particles are not spherical. So clay shape can be another factor which may impact the bacterial attachment. The shape of clay particles can be tested by scanning electron microscope.

4.2.2 Impacts from particle ratios on bacteria attachment

Generally, the ascending trend of percent attached was associated with increased particle ratios. Since all the clay particles and *E. coli* are in 1-10 μm size range, the particles' movement in water can be explained by Brownian motion. As the particle number increased, the chances for clay particles and *E. coli* meeting with each other would definitely increase. Therefore, the attachment would correspondingly increase.

However, there was one exception. In the settling method, the average percent attached to Montmorillonite K-10 for surface area ratio 500 was 33% while for surface area

ratio 1000 was 24%. The difference might be due to soil aggregation under the high concentration of clay particles. Soil aggregation can be caused by microorganisms, which can excrete substances that act as glue and bind soil particles together or by electrostatic forces from soil particles.

We also observed one interesting phenomenon. Histograms of strain attachment to Kaolin always had the different patterns with histograms of attachment to Hectorite, Ca-Montmorillonite and Montmorillonite K-10. Figure 17-A and 17-B show an example with *E. coli* strain #31. In the histograms, three samples with different particle ratios in the same “strain + clay” combination were overlaid in one figure. Red, blue, and green curves are representing particle ratios 2, 100, and 500, respectively. From Figure 17A, we can observe that the percent attached of strain #31 to Montmorillonite K-10 increased when the particle ratio increased from 2 to 500, but the three curves shared one peak. However, in Figure 17B, in which showed the attachment of strain #31 to Kaolin, the peaks of particle ratio 100 and 500 curves were different from the peak of particle ratio 2 curve: the peak shifted to the right when the particle ratio increased from 2 to 500. The peak shifting indicated that sizes of *E. coli* increased sharply after attaching to Kaolin. When considering the small size of Kaolin particles, it is possible that several clay particles attached to one *E. coli* at the same time. Moreover, Kaolin has the surface area of $11.2 \text{ m}^2/\text{g}$, which is the smallest among surface areas of four clays (Table 2). Thus, within the same particle ratio, the Kaolin suspension had the highest clay particle number, which is consistent with the hypothesis above.

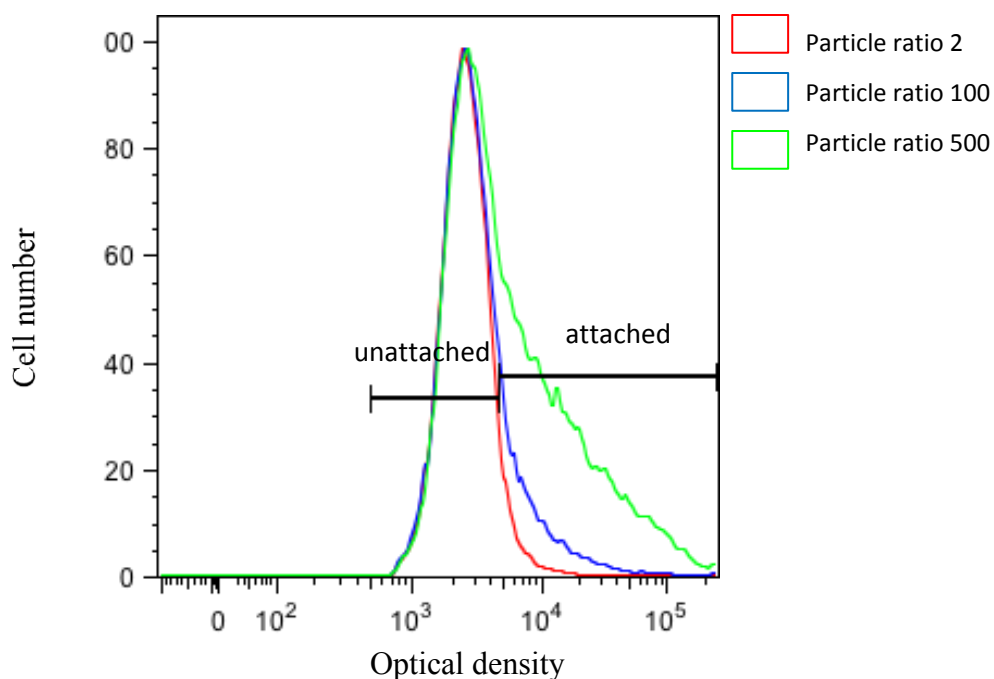


Figure 17A. Histogram of *E. coli* strain #31 attachment to Montmorillonite K-10 over three different particle ratio.

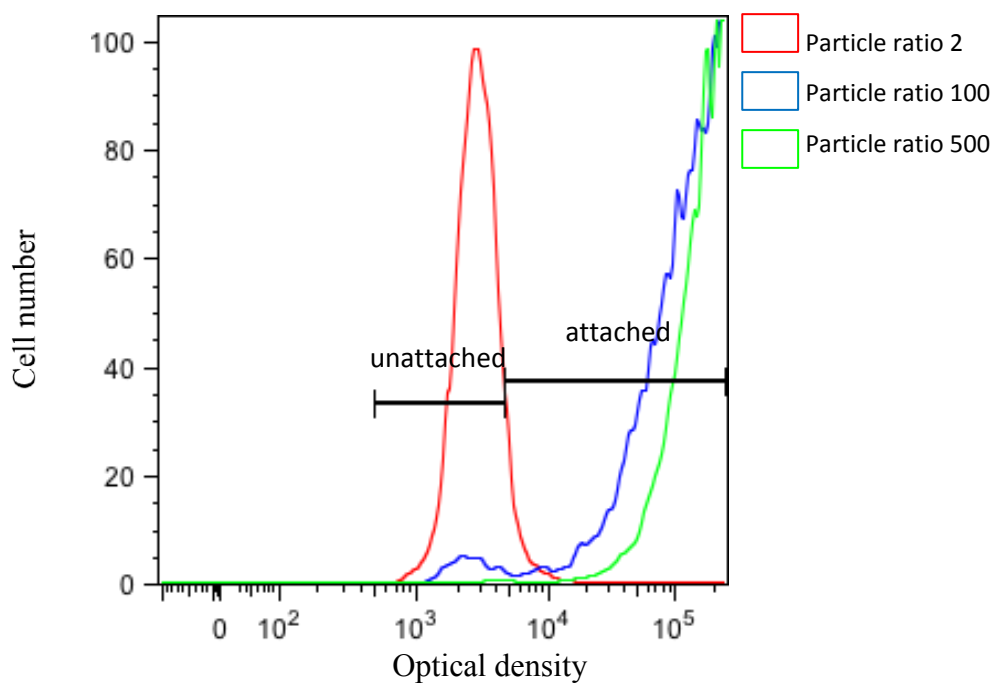


Figure 17B. Histogram of *E. coli* strain #31 attachment to Kaolin over three different particle ratio.

4.2.3 Impacts of bacterial cell properties on attachment to particles

Different strains also showed different attachments to clay particles. We used three environmental strains and one pathogenic strain to evaluate the attachment efficiency in this study. The environmental isolates were collected from swine waste from five swine facilities in Iowa in 2008 and 2009. Two hundred and three isolates were obtained from the samples which had been analyzed by membrane filtration, EPA Method 1603, on modified mTEC agar (USEPA, 2002) and preserved in 25% glycerol stocks at -80°C for further investigation. Three strains were selected from these 203 isolates. Selected strains, #31, #50, and #89 showed the highest attachment fractions (>99%) to quartz particles (Liu et al., 2011) in previous study. ATCCTM #43888, which is a genetically modified version of *E. coli* O157:H7 from human feces, which does not produce either Shiga-like toxin I or II and does not possess the genes for these toxins. This strain was selected to compare attachment behavior of a pathogen to those environmental strains.

Previous research has indicated that significant genetic variability exists among strains of *E. coli* from different host species (Carson et al., 2001) and even from the same host species (Kudva et al., 1997; Galland et al., 2001; Vali et al., 2004; Bolster et al., 2009). If the genetic variability results in differences in surface characteristics that impact attachment, different strains of *E. coli* may exhibit difference attachment to clay particles in water. However, previous researchers have obtained mixed results of impacts on attachment from genes. The underlying genetic basis for bacteria attachment remains unidentified (Liu et al., 2011). Therefore, bacterial cell properties, including electrophoretic mobility, cell size and shape, hydrophobicity, and surface charge density (Bolster et al., 2009) need to be tested in future studies and should be analyzed in combination with the attachment fractions obtained from this study .

Electrophoresis is caused by the presence of a charged interface between the particle and surrounding fluid. Electrophoretic mobility can influence bacteria attachment to negatively charged particles (Vanloosdrecht et al., 1987) and its values can be measured by zeta potential analyzer. Cell size is important in bacteria attachment to particles, but the effect of changing cell size on attachment highly depends on experimental conditions

(Harvey and Garabedian, 1991). Cell shape is measured by the ratio of cell width to cell length. More spherical cells are more likely to attach to particles and transport (Weiss et al., 1995). Bacterial hydrophobicity is an overall parameter for the measurement of bacterial attachment to soil particles and high hydrophobicity values are always associated with high attachment to mineral particles (Stenstrom, 1989). Bacteria surface charge has been characterized by electrostatics interaction (Dickson and Koohmaraie, 1989) and electrostatics combined with hydrophobic effects can overcome the natural repulsion of bacteria and particles which express the similar charges at surfaces (Mills, 2003).

All strains had consistent attachment when comparing the two methods except for strain #89, which exhibited the lowest attachment when tested using the flow cytometry method, but had highest attachment when tested using the settling method. There are two possible reasons: *E. coli* growth or die-off during long period operations impacted the attachment ratios of #89; the *E. coli* attachment was impacted by gene expression.

The first hypothesis to interpret this inconsistency was that *E. coli* strain #89 cells were more likely to grow or die during the settling times (60 min for Montmorillonite K-10, 150 min for Ca-Montmorillonite, 390 min for Hectorite, and 1080 min after centrifugation at 300 rpm for 5 min for Kaolinite). Three one sample t-tests were conducted to determine the differences between the attachment ratios determined using the two methods for strain #89, for each clay. The group “#89 with Kaolin” showed the smallest difference ($t=-2.3531$, $p\text{-value}=0.03828$), followed by “#89 with Ca-Montmorillonite” ($t=-8.5097$, $p\text{-value}=3.614\times 10^{-6}$) and “#89 with Montmorillonite” ($t=-17.97$, $p\text{-value}=1.679\times 10^{-9}$). As presented in Chapter 3, the settling time for Kaolin was longest (1080 min). If *E. coli* strain #89 cells were growing or dying during the settling period, the impact would have been greatest for the particle with the longest operation time, and therefore, attachment ratios of Kaolin should receive the most impacts. Obviously, the t-tests’ results were discrepant with the first hypothesis.

In 2011, Ping Liu et al.’s study found strain #31 and #50 have no known attachment factors while #89 has factor EcpA. EcpA, abbreviation for *E. coli* common pilus, is composed by the subunit protein of *yagZ* gene (Rendon et al., 2007). EcpA was found to

mediate attachment of various *E. coli* to host cells (Blackburn, 2010) and is one of the attachment factors found in *E. coli*. However, EcpA was shown to be not significantly related to attachment to quartz (Liu et al., 2011). Therefore, the second hypothesis was that *E. coli* attachment might receive impacts from EcpA and EcpA expression. This hypothesis needs to be confirmed through further studies.

4.2.4 Advantages and limitations of flow cytometry

Generally speaking, the greatest advantage of flow cytometry is the rapidity in which large numbers of cells can be analyzed (Macey, 2007). In this study, using flow cytometry can shorten the experimental time from up to 1 day to about 1 hour. Moreover, the expenses for using two methods were similar (Table 10).

Table 10. The estimated expense for major cost of 100 samples in two methods.

The settling method		
	Reference unit expense	Estimated expense
Petri dishes	\$142/600 dishes	\$24
0.45 μ m Filters	\$244/600 filters	\$40
Medium	\$225/454g for 7500 plates	\$3
Disposable glass tubes	\$65/1000	\$9
Disposable centrifuge tubes	\$100/500	\$13
Labor fee	\$20/hr	\$200
Total		\$289
Flow cytometry method		
	Reference unit expense	Estimated expense
SYTO 11	\$190/250 μ l	\$170
250 μ l test tubes	\$60/100 tubes	\$6
Labor fee for preparation samples	\$20/hr	\$40
Machine rent and analysis labor fee	\$53/50-60 samples	\$100
Total		\$316

Another advantage of flow cytometry compared to the settling method is its ability to detect the viable but nonculturable (VBNC) portion of the total cell population. From the

comparisons between percent attached using the two methods, the attachments obtained from the settling method were always higher than the attachments from flow cytometry. The attachment difference between the two methods is possibly due the VBNC portion of cells. Culturing bacteria on medium is limited in its ability to recover metabolically active, intact cells that have been exposed to environmental stresses (Oliver, 1993; Khan et al., 2010). The settling method using culturing cells on medium agar to enumerate the number in the sample. Therefore, culturing cells on medium agar is possibly underestimating the cell count since under an appropriate condition, VBNC cells can be resuscitated and become culturable again (Barer et al., 1993). For instance, a combination of several amino acid, including methionine, glutamine, threonine, serine and asparagine, was suggested to be used for *E. coli* resuscitation (Pinto et al., 2011). From the perspective of VBNC cells, the percent attached achieved from the settling method might be less reliable.

Flow cytometry also has some disadvantages. It is difficult to discriminate between live and dead cells when only using one stain. In this study, SYTO 11 was used as a DNA-fluorescent stain in flow cytometry method and each event was counted by one fluorescence DNA unit. The total *E. coli* amounts were overestimated because dead cells with DNA could also produce the fluorescence. And dead cells undoubtedly had lower properties of attachment to soil particles than live cell. Therefore, using flow cytometry likely underestimated the attachments of *E. coli* to clay particles. This is another possible reason for the lower attachment fractions obtained from the flow cytometry method. This problem can be addressed using a double-staining technique. Live cells have intact membranes and are impermeable to dyes such as propidium iodide, which is a cell-impermeant stain that only crosses compromised or damaged cell membrane. Another stain, such as Thiazole orange or SYTO 11, is a cell-permeant dye and can enter all cells. Thus, a combination of these two dyes provides a rapid and reliable method for discriminating live and dead bacteria (BD, 2002).

Another limitation of flow cytometry in this study is difficulties associated with gage limit determination. Gage limit between free *E. coli* and *E. coli*, as shown in Figure 9, is determined by particle size difference. When detecting *E. coli* attachment to Hectorite in this study, for example, determination of gage limit between free *E. coli* and attached *E. coli* was

difficult due to the small particle size of Hectorite. Hectorite has an average diameter 1 μm , which is much smaller than the size of *E. coli*, 2.5 μm length and cross section with 1 μm as diameter. After attaching to Hectorite particles, the size of *E. coli* would not change greatly. Inaccurate gage limit can definitely result in incorrect attachments from flow cytometry.

Flow cytometry also has limitations if used for on environmental applications. First, environmental water samples usually have low bacteria concentrations while 10^3 to 10^7 CFU ml^{-1} was recommended as the *E. coli* concentration used in the flow cytometer (Hussein et al., 2002). Second, for water samples which contain several kinds of bacteria, flow cytometry cannot separate different strains using one stain. Recognizing different strains may be achieved by multiple-staining techniques, but only if the types and properties of the microorganisms are well-known.

On the whole, flow cytometry is a new technique to partition between unattached and attached bacteria, but further improvements are still need in this method.

CHAPTER 5 CONCLUSIONS

5.1 General discussion and conclusions

Two methods, settling (or centrifugation followed by settling) were compared to partition between freely suspended *E. coli* and *E. coli* attached to clay particles. The overall goal of the study was to develop a practical and accurate method to distinguish and quantify between *E. coli* attached to clay particles and *E. coli* freely suspended in solution.

The first objective of this research study as stated in Chapter 1.2 was to develop standard procedures for each appropriate method to partition between unattached and attached *E. coli*. Several candidate methods were identified through a review of past research on bacteria attached and were summarized in Chapter 2.3. The methods selected as most promising for this study were settling (or centrifugation followed by settling). The settling method used density differences (or density difference and centrifugal force) to separate unattached and attached *E. coli*. The dispersion treatment combined the chemical surfactant Tween-85 and hand shaker. Flow cytometry used the particle size differences and DNA fluorescence to separate unattached and attached *E. coli*. SYTO 11 was selected as the DNA-staining fluorescent dye.

The second objective listed in Chapter 1.2 was to determine factors which can impact bacterial attachment to clay particles, and this was achieved through the testing of bacterial attachments to clay particles under numerous designed conditions by both methods. In this section, the study demonstrated that:

- *E. coli* are more likely to attach to clay particles with smaller sizes.
- The increase of percent attached was associated with increased particle ratios. For small sized clay particles, such as Kaolin, several particles can attach to one *E. coli* at the same time when the clay concentration is high.
- Different strains of *E. coli* have different attaching ability to clay particles, even for strains which were from the same host species. A series of cell surface characteristics for four strains used in this study, such as cell size and shape, and surface charge, need to be determined in future researches.

The third research objective was to compare flow cytometry and standard settling/centrifugation separation methods to partition between *E. coli* attached to clay particles and *E. coli* freely suspended in solution. After compared to settling method:

- Flow cytometry is a rapid technique in which large numbers of cells can be analyzed which settling method is time-consuming and labor intensive.
- Flow cytometry can detect the viable but nonculturable (VBNC) portion of cells while settling method cannot and therefore the settling method could potentially underestimate the bacteria count.
- Flow cytometry overestimated the total bacteria number and underestimate the attachment fractions in this study because flow cytometry cannot discriminate between live and dead cells when only using one stain.
- There are still some hindrances for us to apply flow cytometry on environmental water samples. The hindrances include low environmental bacterial concentration and strain diversity in environmental water samples.

5.2 Implications and recommendation for future research

There is clearly a need for more information on bacteria attachment to soil particles to assist water quality modeling efforts. The partitioning methods discussed in this study were successful in distinguishing and quantifying clay-adsorbed and freely suspended *E. coli* and could be used in future experiments examining different aspects of bacteria-sediment interactions. However, there are still some drawbacks in these two methods. Before a standard partitioning method can be established, more research must be conducted. Here are some suggestions for further study:

- Bacterial surface characteristics, including electrophoretic mobility, cell size and shape, hydrophobicity, extracellular protein, extracellular sugar, and surface charge density, need to be measured and to be analyzed combining with the attachment fractions obtained from this study .
- In flow cytometry, live/dead cell need to be tested. It can help with revising the attachment fractions obtained from flow cytometry.

- Die-off was not considered in this study. Quantification of the relative rates of attached and unattached *E. coli* die-off is necessary to develop partitioning method and assist water quality modeling.
- Studies need to be conducted for exploring the attachment of actual waterborne pathogens since current pathogen indicators and standards are not always accurate and sensitive.

REFERENCES

- Aakra, A., M. Hesselsoe, and L. R. Bakken. 2000. Surface attachment of ammonia-oxidizing bacteria in soil. *Microbial Ecology*. 39 (3): 222-235.
- Alhadidi, A., A. J. B. Kemperman, J. C. Schippers, M. Wessling, and W. G. J. van der Meer. 2011. The influence of membrane properties on the Silt Density Index. *Journal of Membrane Science*. 384 (1-2): 205-218.
- Amalfitano, S., and S. Fazi. 2008. Recovery and quantification of bacterial cells associated with streambed sediments. *Journal of Microbiological Methods*. 75 (2): 237-243.
- APHA. 1999. Standard methods for the examination of water and wastewater. A. P. H. Association.
- Bai, S., and W. S. Lung. 2005. Modeling sediment impact on the transport of fecal bacteria. *Water Research*. 39 (20): 5232-5240.
- Barer, M. R., L. T. Gribbon, C.R.Harwood, and C.E.Nwoguh. 1993. The viable but non-culturable hypothesis and medical bacteriology. *Reviews in Medical Microbiology* 4: 183-191.
- BD. 2000. Introduction to Flow Cytometry: A Learning Guide.
- BD. 2002. Bacteria detection and live/dead discrimination by flow cytometry.
- Bitton, G., Y. Henis, and N. Lahav. 1972. Effect of several clay-minerals and humic acid on survival of *Klebsiella-aerogenes* exposed to ultraviolet-irradiation *Applied Microbiology*. 23 (5): 870-&.
- Blackburn, D. 2010. The production of the *E. coli* common plus by enterotoxigenic *Escherichia coli* and *Klebsiella pneumoniae*. Master of Science: University of Florida.
- Bolster, C. H., B. Z. Haznedaroglu, and S. L. Walker. 2009. Diversity in Cell Properties and Transport Behavior among 12 Different Environmental *Escherichia coli* Isolates. *Journal of Environmental Quality*. 38 (2): 465-472.

- Brown, M., and C. Wittwer. 2000. Flow cytometry: Principles and clinical applications in hematology. *Clinical Chemistry*. 46 (8B): 1221-1229.
- Buesing, N., and M. O. Gessner. 2003. Incorporation of radiolabeled leucine into protein to estimate bacterial production in plant litter, sediment, epiphytic biofilms, and water samples. *Microbial Ecology*. 45 (3): 291-301.
- Bundy, W. M. 2011. Patent application title: Kaolin processing. Tesuque, NM,US.
- Cabral, J. P. S. 2010. Water Microbiology. Bacterial Pathogens and Water. *International Journal of Environmental Research and Public Health*. 7 (10): 3657-3703.
- Caracciolo, A. B., P. Grenni, C. Cupo, and S. Rossetti. 2005. In situ analysis of native microbial communities in complex samples with high particulate loads. *Fems Microbiology Letters*. 253 (1): 55-58.
- Carson, C. A., B. L. Shear, M. R. Ellersieck, and A. Asfaw. 2001. Identification of fecal *Escherichia coli* from humans and animals by ribotyping. *Applied and Environmental Microbiology*. 67 (4): 1503-1507.
- CDC. 2002. Surveillance for Waterborne-Disease Outbreaks – United States 1999-2000. C. f. D. Control.
- Cerato, A. B., and A. J. Luttenegger. 2002. Determination of surface area of fine-grained soils by the ethylene (EGME) method. *Geotechnical Testing Journal*. 25 (3): 315-321.
- Characklis, G. W., M. J. Dilts, O. D. Simmons, C. A. Likirdopulos, L. A. H. Krometis, and M. D. Sobsey. 2005. Microbial partitioning to settleable particles in stormwater. *Water Research*. 39 (9): 1773-1782.
- Cook, K. L., C. H. Bolster, K. A. Ayers, and D. N. Reynolds. 2011. *Escherichia coli* Diversity in Livestock Manures and Agriculturally Impacted Stream Waters. *Current Microbiology*. 63 (5): 439-449.
- Craig, D. L., H. J. Fallowfield, and N. J. Cromar. 2002. Enumeration of faecal coliforms from recreational coastal sites: evaluation of techniques for the separation of bacteria from sediments. *Journal of Applied Microbiology*. 93 (4): 557-565.

- Craun. 1986. Waterborne Giardiasis in the United States 1965-84.
- Davies, C. M., and H. J. Bavor. 2000. The fate of stormwater-associated bacteria in constructed wetland and water pollution control pond systems. *Applied Microbiology* 89: 349-360.
- Dickson, J. S., and M. Koochmaraie. 1989. Cell Surface Charge Characteristics and Their Relationship to Bacterial Attachment to Meat Surfaces. *Applied and Environmental Microbiology* 55 (4): 832-836.
- Edwards, D. R., B. T. Larson, and T. T. Lim. 2000. Runoff Nutrient and Fecal Coliform Content from Cattle Manure Application to Fescue Plots. *Journal of The American Water Resources Association*. 36 (4).
- Epstein, S. S., and J. Rossel. 1995. Enumeration of sandy sediment bacteria-search for optimal protocol. *Marine Ecology-Progress Series*. 117 (1-3): 289-298.
- Faegri, A., V. L. Torsvik, and J. Goksoyr. 1977. Bacterial and fungal activities in soil-separation of bacteria and fungi by a rapid fractionated centrifugation technique. *Soil Biology & Biochemistry*. 9 (2): 105-112.
- Flint, K. P. 1987. The Long-term Survival of *Escherichia coli* in River Water. *Applied Bacteriology*. 63 (3): 261-270.
- Fontes, D. E., A. L. Mills, G. M. Hornberger, and J. S. Herman. 1991. Physical and chemical factors influencing transport of microorganisms through porous-media. *Applied and Environmental Microbiology*. 57 (9): 2473-2481.
- Foppen, J. W., G. Lutterodt, W. F. M. Roling, and S. Uhlenbrook. 2010. Towards understanding inter-strain attachment variations of *Escherichia coli* during transport in saturated quartz sand. *Water Research*. 44 (4): 1202-1212.
- Fries, J. S., G. W. Characklis, and R. T. Noble. 2006. Attachment of fecal indicator bacteria to particles in the Neuse River Estuary, NC. *Journal of Environmental Engineering*. 132 (10): 1338-1345.

- Gagliardi, J. V., and J. S. Karns. 2000. Leaching of Escherichia coli O157 : H7 in diverse soils under various agricultural management practices. *Applied and Environmental Microbiology*. 66 (3): 877-883.
- Galland, J. C., D. R. Hyatt, S. S. Crupper, and D. W. Acheson. 2001. Prevalence, antibiotic susceptibility, and diversity of Escherichia coli O157 : H7 isolates from a longitudinal study of beef cattle feedlots. *Applied and Environmental Microbiology*. 67 (4): 1619-1627.
- Garcia, M. I., and C. LeBouguenec. 1996. Role of adhesion in pathogenicity of human uropathogenic and diarrhoeogenic Escherichia coli. *Bulletin De L Institut Pasteur*. 94 (3): 201-236.
- Griebler, C., B. Mindl, and D. Slezak. 2001. Combining DAPI and SYBR Green II for the enumeration of total bacterial numbers in aquatic sediments. *International Review of Hydrobiology*. 86 (4-5): 453-465.
- Grimes, D. J. 1975. Release of sediment-bound fecal coliforms by dredging *Applied Microbiology*. 29 (1): 109-111.
- Guber, A. K., D. R. Shelton, and Y. A. Pachepsky. 2005. Transport and retention of manure-borne coliforms in soil. *Vadose Zone Journal*. 4 (3): 828-837.
- Guindulain, T., J. Comas, and J. VivesRego. 1997. Use of nucleic acid dyes SYTO-13, TOTO-1, and YOYO-1 in the study of Escherichia coli and marine prokaryotic populations by flow cytometry. *Applied and Environmental Microbiology*. 63 (11): 4608-4611.
- Halversen, W. V. 1927. The nitrogen metabolism of nitrogen-fixing bacteria. *Iowa State College Jour Sci*. 1 ((4)): 395-410.
- Harvey, R. W., and S. P. Garabedian. 1991. Use of colloid filtration theory in modeling movement of bacteria through a contaminated sandy aquifer *Environmental Science & Technology*. 25 (1): 178-185.

- Henry, L. A. 2004. Partitioning between the Soil-adsorbed and Planktonic Phases of *Escherichia coli*. M.S., Biological Systems Engineering, Blacksburg, VA: Virginia Polytechnic Institute and State University.
- Hipsey, M. R., J. D. Brookes, R. H. Regel, J. P. Antenucci, and M. D. Burch. 2006. In situ evidence for the association of total coliforms and *Escherichia coli* with suspended inorganic particles in an Australian reservoir. *Water Air and Soil Pollution*. 170 (1-4): 191-209.
- Hogan, C. M. 2010. Bacteria.
- Hussein, H. S., B. H. Thran, and D. Redelman. 2002. Detection of *Escherichia coli* O157 : H7 in bovine rumen fluid and feces by flow cytometry. *Food Control*. 13 (6-7): 387-391.
- Invitrogen. 2008. SYTO Green-Fluorescent Nucleic Acid Stains.
- Jaynes, W. F., and G. f. Vance. 1999. Sorption of benzene, toluene, ethylbenzene, and xylene (BTEX) compounds by hectorite clays exchanged with aromatic organic cations. *Clays and Clay Minerals*. 47 (3): 358-365.
- Jeng, H. W. C., A. J. England, and H. B. Bradford. 2005. Indicator organisms associated with stormwater suspended particles and estuarine sediment. *Journal of Environmental Science and Health Part a-Toxic/Hazardous Substances & Environmental Engineering*. 40 (4): 779-791.
- Kalyuzhnaya, M. G., R. Zabinsky, S. Bowerman, D. R. Baker, M. E. Lidstrom, and L. Chistoserdova. 2006. Fluorescence in situ hybridization-flow cytometry-cell sorting-based method for separation and enrichment of type I and type II methanotroph populations. *Applied and Environmental Microbiology*. 72 (6): 4293-4301.
- Khan, M. M. T., B. H. Pyle, and A. K. Camper. 2010. Specific and Rapid Enumeration of Viable but Nonculturable and Viable-Culturable Gram-Negative Bacteria by Using Flow Cytometry. *Applied and Environmental Microbiology*. 76 (15): 5088-5096.

- Kudva, I. T., C. W. Hunt, C. J. Williams, U. M. Nance, and C. J. Hovde. 1997. Evaluation of dietary influences on *Escherichia coli* O157:H7 shedding by sheep. *Applied and Environmental Microbiology*. 63 (10): 3878-3886.
- Kuwae, T., and Y. Hosokawa. 1999. Determination of abundance and biovolume of bacteria in sediments by dual staining with 4',6-diamidino-2-phenylindole and acridine orange: Relationship to dispersion treatment and sediment characteristics. *Applied and Environmental Microbiology*. 65 (8): 3407-3412.
- Lebaron, P., N. Parthuisot, and P. Catala. 1998. Comparison of blue nucleic acid dyes for flow cytometric enumeration of bacteria in aquatic systems. *Applied and Environmental Microbiology*. 64 (5): 1725-1730.
- Leclerc, H., D. A. A. Mossel, S. C. Edberg, and C. B. Struijk. 2001. Advances in the bacteriology of the Coliform Group: Their suitability as markers of microbial water safety. *Annual Review of Microbiology*. 55: 201-234.
- Lindahl, V., and L. R. Bakken. 1995. Evaluation of methods for extraction of bacteria from soil *Fems Microbiology Ecology*. 16 (2): 135-142.
- Liu, P., M. L. Soupir, M. Zwonitzer, B. Huss, and L. Jarboe. 2010. Antibiotic Resistance in Agricultural *E. coli* Isolates is Associated with Attachment to Quartz. *Applied and Environmental Microbiology*. 78 (1).
- Liu, P., M. L. Soupir, M. Zwonitzer, B. Huss, and L. R. Jarboe. 2011. Association of Antibiotic Resistance in Agricultural *Escherichia coli* Isolates with Attachment to Quartz. *Applied and Environmental Microbiology*. 77 (19): 6945-6953.
- Lunau, M., A. Lemke, K. Walther, W. Martens-Habbena, and M. Simon. 2005. An improved method for counting bacteria from sediments and turbid environments by epifluorescence microscopy. *Environmental Microbiology*. 7 (7): 961-968.
- Lutterodt, G., M. Basnet, J. W. A. Foppen, and S. Uhlenbrook. 2009. The effect of surface characteristics on the transport of multiple *Escherichia coli* isolates in large scale columns of quartz sand. *Water Research*. 43 (3): 595-604.

- Macey, M. G. 2007. Flow cytometry: principles and applications, edited by M. G. Macey: Humana Press.
- Marvin, ed. *Flow Cytometry Basic Training- A Look Inside the Box*. Northwestern University.
- Mayr, C., A. Winding, and N. B. Hendriksen. 1999. Community level physiological profile of soil bacteria unaffected by extraction method. *Journal of Microbiological Methods*. 36 (1-2): 29-33.
- Mills, A. L. 2003. Keeping in touch: Microbial life on soil particle surfaces. *Advances in Agronomy*. 78: 1-43.
- Muirhead, R. W., R. P. Collins, and P. J. Bremer. 2005. Erosion and subsequent transport state of *Escherichia coli* from cowpats. *Applied and Environmental Microbiology*. 71 (6): 2875-2879.
- Muirhead, R. W., R. P. Collins, and P. J. Bremer. 2006. Interaction of *Escherichia coli* and soil particles in runoff. *Applied and Environmental Microbiology*. 72 (5): 3406-3411.
- Myers, D. N., D. M. Stoeckel, R. N. Bushon, D. S. Francy, and A. M. G. Brady. 2007. Fecal Indicator Bacteria In *TWRI Book 9*: U.S. Geological Survey
- Newton, J. W., P. W. Wilson, and R. H. Burris. 1953. Direct demonstration of ammonia as an intermediate in nitrogen fixation by *azotobacter*. *Journal of Biological Chemistry*. 204 (1): 445-451.
- NHDES. 2003. Environmental Fact Sheet- Fecal Coliform as an Indicator Organism. New Hampshire Department of Environmental Services.
- Nicholson, F. A., S. J. Groves, and B. J. Chambers. 2005. Pathogen survival during livestock manure storage and following land application. *Bioresource Technology*. 96 (2): 135-143.
- Ohman, L., B. Normann, and O. Stendahl. 1981. Physicochemical surface-properties of *Escherichia coli* strains isolated from different types of urinary-tract infections *Infection and Immunity*. 32 (2): 951-955.

- Oliver, J. D. 1993. *Formation of viable but nonculturable cells*. New York, NY: Plenum Press.
- Pachepsky, Y. A., A. M. Sadeghi, S. A. Bradford, D. R. Shelton, A. K. Guber, and T. Dao. 2006. Transport and fate of manure-borne pathogens: Modeling perspective. *Agricultural Water Management*. 86 (1-2): 81-92.
- Pachepsky, Y. A., O. Yu, J. S. Karns, D. R. Shelton, A. K. Guber, and J. S. van Kessel. 2008. Strain-dependent variations in attachment of E. coli to soil particles of different sizes. *International Agrophysics*. 22 (1): 61-66.
- Payment, A. L. 2011. Pathogens in Water: Value and Limits of Correlation with Microbial Indicators. *Ground Water* 49 (No.1): 4-11.
- Peeva, P. D., A. E. Palupi, and M. Ulbricht. 2011. Ultrafiltration of humic acid solutions through unmodified and surface functionalized low-fouling polyethersulfone membranes - Effects of feed properties, molecular weight cut-off and membrane chemistry on fouling behavior and cleanability. *Separation and Purification Technology*. 81 (2): 124-133.
- Pinto, D., V. Almeida, M. A. Santos, and L. Chambel. 2011. Resuscitation of Escherichia coli VBNC cells depends on a variety of environmental or chemical stimuli. *Applied Microbiology*. 110 (6): 1601-1611.
- Pond, K. 2005. *Water Recreation and Disease* London, Seattle: International Water Association.
- Porter, J., D. Deere, M. Hardman, C. Edwards, and R. Pickup. 1997. Go with the flow - use of flow cytometry in environmental microbiology. *Fems Microbiology Ecology*. 24 (2): 93-101.
- Qualls, R. G., M. P. Flynn, and J. D. Johnson. 1983. The role of suspended particles in ultraviolet disinfection *Journal Water Pollution Control Federation*. 55 (10): 1280-1285.

- Ram, P. V., R.S. 2008. Rapid Culture-Independent Quantitative Detection of Enterotoxigenic *Escherichia coli* in Surface Waters by Real-Time PCR with Molecular Beacon. *Environmental Science & Technology*. 42: 4577-4582.
- Ramchandani, M., A. R. Manges, C. DebRoy, S. P. Smith, J. R. Johnson, and L. W. Riley. 2005. Possible animal origin of human-associated, multidrug-resistant, uropathogenic *Escherichia coli*. *Clinical Infectious Diseases*. 40 (2): 251-257.
- Rendon, M. A., Z. Saldana, A. L. Erdem, V. Monteiro-Neto, A. Vazquez, J. B. Kaper, J. L. Puente, and J. A. Giron. 2007. Commensal and pathogenic *Escherichia coli* use a common pilus adherence factor for epithelial cell colonization. *Proceedings of the National Academy of Sciences of the United States of America*. 104 (25): 10637-10642.
- Reynolds. 2008. What Does *E. coli* in Water Really Mean.
- Reynolds, K. A. 2003. Coliform Bacteria: A Failed Indicator of Water Quality? . *Water Conditioning & Purification* 45.
- Rosen, B. H. 2001. Waterborne Pathogens in Agricultural Watersheds. U. S. D. o. Agriculture and N. R. C. Service.
- Schallenberg, M., and J. Kalff. 1993. The ecology of sediment bacteria in lakes and comparisons with other aquatic ecosystems *Ecology*. 74 (3): 919-934.
- Schillinger, J. E., and J. J. Gannon. 1985. Bacterial adsorption and suspended particles in urban stormwater. *Water Pollution Control Federation*. 57 (5): 384-389.
- Sherer, B. M., J. R. Miner, J. A. Moore, and J. C. Buckhouse. 1992. Indicator Bacterial Survival in Stream Sediments. *Environmental Quality* 21: 591-595.
- Soupir, M. L., and S. Mostaghimi. 2003. Bacteria Release and Transport from Livestock Manure Applied to Pastureland In *ASAE Meeting*. Las Vegas, Nevada, USA.
- Soupir, M. L., S. Mostaghimi, E. R. Yagow, C. Hagedorn, and D. H. Vaughan. 2006. Transport of fecal bacteria from poultry litter and cattle manures applied to pastureland. *Water Air and Soil Pollution*. 169 (1-4): 125-136.

- Soupir, M. L., S. Mostaghimi, and N. G. Love. 2008. Method to partition between attached and unattached *E. coli* in runoff from agricultural lands. *Journal of the American Water Resources Association*. 44 (6): 1591-1599.
- Soupir, M. L., S. Mostaghimi, and T. Dillaha. 2010. Attachment of *Escherichia coli* and Enterococci to Particles in Runoff. *Journal of Environmental Quality*. 39 (3): 1019-1027.
- Soupir, M. L., and S. Mostaghimi. 2011. *Escherichia coli* and Enterococci Attachment to Particles in Runoff from Highly and Sparsely Vegetated Grassland. *Water Air and Soil Pollution*. 216 (1-4): 167-178.
- Stenstrom, T. A. 1989. Bacteria hydrophobicity, and overall parameter for the measurement of adhesion potential to soil particles. *Applied and Environmental Microbiology*. 55 (1): 142-147.
- Todar, K. 2009. *The Microbial World*.
- Todar, K. 2011. *Pathogenic E. coli*
- UllaL, Pisetsky, and Reich. 2009. Use of SYTO 13, a Fluorescent Dye Binding Nucleic Acids, for the Detection of Microparticles in In Vitro System. *International Society for Advancement of Cytometry Cytometry Part A (77A)*: 294-301.
- Unc, A., and M. J. Goss. 2004. Transport of bacteria from manure and protection of water resources. *Applied Soil Ecology*. 25 (1): 1-18.
- UNIEF/WHO. 2009. *Diarrhoea: Why Children are Still Dying and What Can Be Done*.
- USEPA. 1986. *Ambient Water Quality Criteria for Bacteria-1986*. United States Environmental Protection Agency.
- USEPA. 2002. *Method 1603: Escherichia coli (E. coli) in water by membrane filtration using modified membrane-thermotolerant Escherichia coli agar (modified mTEC)*. United States Environmental Protection Agency.
- USEPA. 2004. 40 CFR 141.2. United States Environmental Protection Agency.

- USEPA. 2005. Membrane Filtration Guidance Manual. United States Environmental Protection Agency.
- USEPA. 2006. Voluntary Estuary Monitoring Manual Chapter 17: Bacteria Indicators of Potential Pathogens. United States Environmental Protection Agency.
- USEPA. 2009. National Water Quality Inventory: Report to Congress 2004 Reporting Cycle. EPA 841-R-08-001. United States Environmental Protection Agency.
- USEPA. 2010. *5.1.1 Fecal Bacteria, Monitoring & Assessment*.
<http://water.epa.gov/type/rsl/monitoring/vms511.cfm>. Accessed 02/10, 2012. United States Environmental Protection Agency.
- USEPA. 2011. Revisions to Chapter 61- Iowa Water Quality Standards. United States Environmental Protection Agency.
- Vali, L., K. A. Wisely, M. C. Pearce, E. J. Turner, H. I. Knight, A. W. Smith, and S. G. B. Amyes. 2004. High-level genotypic variation and antibiotic sensitivity among *Escherichia coli* O157 strains isolated from two Scottish beef cattle farms. *Applied and Environmental Microbiology*. 70 (10): 5947-5954.
- Vanloosdrecht, M. C. M., J. Lyklema, W. Norde, G. Schraa, and A. J. B. Zehnder. 1987. Electrophoretic mobility and hydrophobicity as a measure to predict the initial steps of bacteria adhesion. *Applied and Environmental Microbiology*. 53 (8): 1898-1901.
- Veal, D. A., D. Deere, B. Ferrari, J. Piper, and P. V. Attfield. 2000. Fluorescence staining and flow cytometry for monitoring microbial cells. *Journal of Immunological Methods*. 243 (1-2): 191-210.
- Vigil, P. D., A. E. Stapleton, J. R. Johnson, T. M. Hooton, A. P. Hodges, Y. Q. He, and H. L. T. Mobley. 2011. Presence of Putative Repeat-in-Toxin Gene *tosA* in *Escherichia coli* Predicts Successful Colonization of the Urinary Tract. *Microbiology* 2(3): 10.
- Vital, M., D. Stucki, T. Egli, and F. Hammes. 2010. Evaluating the Growth Potential of Pathogenic Bacteria in Water. *Applied and Environmental Microbiology*. 76 (19): 6477-6484.

- Vives-Rego, J., P. Lebaron, and G. Nebe-von Caron. 2000. Current and future applications of flow cytometry in aquatic microbiology. *Fems Microbiology Reviews*. 24 (4): 429-448.
- Weiss, T. H., A. L. Mills, G. M. Hornberger, and J. S. Herman. 1995. Effect of bacteria-cell shape on transport of bacteria in porous media. *Environmental Science & Technology*. 29 (7): 1737-1740.
- WHO. 2004. Burden of Disease and Cost-effectiveness Estimates: Worth Health Organization.
- WHO. 2008. Guidelines for Drinking-water Quality, 3rd edition. 1.
- WSDH. 2010. Coliform Bacteria and Drinking Water. Washington State Department of Health.

APPENDIX A. RESEARCH CONSIDERATIONS

APPENDIX A1. Absorbance values of soil samples at discrete time

Clay Particles	30 min	60 min	90 min	120 min	150 min	180 min	210 min
Hectorite	-	-	-	-	-	-	-
Kaolin	-	-	-	-	-	-	-
Ca-Montmorillonite	-	0.045	0.035	0.027	0.022	0.022	-
Montmorillonite K-10	0.027	0.017	0.017	-	-	-	-
Clay Particles	300 min	390 min	420 min	24 hr	36 hr	48 hr	50 hr
Hectorite	0.027	0.021	0.021	-	-	-	-
Kaolin	-	-	0.258	0.125	0.088	0.022	0.022
Ca-Montmorillonite	-	-	-	-	-	-	-
Montmorillonite K-10	-	-	-	-	-	-	-

APPENDIX A2. Bacteria count changes after centrifugation

Group (Speed+ Time)	Colony Forming Unit (CFU ml ⁻¹)									AVG (CFU ml ⁻¹)	Reduction (%)
Control 1	27	17	19	47	51	54	69	64	50	42.2	-
300rpm+5 min	29	17	-	41	44	-	62	78	-	45.2	-7
400 rpm+3 min	21	14	10	32	30	21	61	56	77	35.8	15.2
Control 2	38	45	44	54	-	-	-	-	-	45.25	-
300 rpm+8 min	38	36	50	29	-	-	-	-	-	38.25	15.5
300 rpm+10 min	35	34	24	43	-	-	-	-	-	34	24.9

APPENDIX A3. Calculations for soil concentrations by surface area

E. coli:

Surface area: $((1.1 \mu\text{m}/2)^2 * 3.14 * 2 \mu\text{m} + (1.5 \mu\text{m}/2)^2 * 3.14 * 6 \mu\text{m})/2 = 6 \mu\text{m}^2 = 6 * 10^{-12} \text{m}^2$

For 10^7ml^{-1} *E. coli*, the surface area $6 * 10^{-12} \text{m}^2 * 10^7 \text{ml}^{-1} = 6 * 10^{-5} \text{m}^2 \text{ml}^{-1}$

Kaolin:

Surface area: $11.2 \text{m}^2 \text{g}^{-1}$

The concentration for $6 * 10^{-5} \text{m}^2 \text{ml}^{-1}$: $5.4 * 10^{-6} \text{g ml}^{-1} = 5.4 * 10^{-3} \text{g L}^{-1}$

→ $6 * 10^{-3} \text{g L}^{-1}$ selected

Hectorite:

Surface area: $63 \text{m}^2 \text{g}^{-1}$

The concentration for $6 * 10^{-5} \text{m}^2 \text{ml}^{-1}$: $9.5 * 10^{-7} \text{g ml}^{-1} = 9.5 * 10^{-4} \text{g L}^{-1}$

→ $1.0 * 10^{-3} \text{g L}^{-1}$ selected

Ca-Montmorillonite

Surface area: $84 \text{m}^2 \text{g}^{-1}$

The concentration for $6 * 10^{-5} \text{m}^2 \text{ml}^{-1}$: $7.1 * 10^{-7} \text{g ml}^{-1} = 7.1 * 10^{-4} \text{g L}^{-1}$

→ $8 * 10^{-4} \text{g L}^{-1}$ selected

Montmorillonite K-10

Surface area: $240 \text{m}^2 \text{g}^{-1}$

The concentration for $6 * 10^{-5} \text{m}^2 \text{ml}^{-1}$: $2.5 * 10^{-7} \text{g ml}^{-1} = 2.5 * 10^{-4} \text{g L}^{-1}$

→ $2.8 * 10^{-4} \text{g L}^{-1}$ selected

APPENDIX B. EXPERIMENTAL DESIGN

APPENDIX B1. Settling samples

Particle Ratio	Clay	Clay concentration (g L ⁻¹)	Concentration of <i>E. coli</i> (CFU ml ⁻¹)	Clay suspension (ml)	10 ⁸ ml ⁻¹ <i>E. coli</i> suspension (ml)	PBS (ml)
1	Kaolin	0.12	0.25*10 ⁷	0.625	1.25	48.13
			0.5*10 ⁷	1.25	2.5	46.25
			1.0*10 ⁷	2.5	5	42.5
	Hectorite	0.05	0.25*10 ⁷	0.25	1.25	48.5
			0.5*10 ⁷	0.5	2.5	47
			1.0*10 ⁷	1	5	44
	Ca-Mont	0.04	0.25*10 ⁷	0.25	1.25	48.5
			0.5*10 ⁷	0.5	2.5	47
			1.0*10 ⁷	1	5	44
	Mont K-10	0.014	0.25*10 ⁷	0.25	1.25	48.5
			0.5*10 ⁷	0.5	2.5	47
			1.0*10 ⁷	1	5	44
2	Kaolin	0.12	0.25*10 ⁷	1.25	1.25	47.5
			0.5*10 ⁷	2.5	2.5	45
			1.0*10 ⁷	5	5	40
	Hectorite	0.05	0.25*10 ⁷	0.5	1.25	48.25
			0.5*10 ⁷	1	2.5	46.5
			1.0*10 ⁷	2	5	43
	Ca-Mont	0.04	0.25*10 ⁷	0.5	1.25	48.25
			0.5*10 ⁷	1	2.5	46.5
			1.0*10 ⁷	2	5	43
	Mont K-10	0.014	0.25*10 ⁷	0.5	1.25	48.25
			0.5*10 ⁷	1	2.5	46.5
			1.0*10 ⁷	2	5	43
50	Kaolin	0.6	0.25*10 ⁷	6.25	1.25	42.5
			0.5*10 ⁷	12.5	2.5	35
			1.0*10 ⁷	25	5	20
	Hectorite	0.25	0.25*10 ⁷	2.5	1.25	46.25
			0.5*10 ⁷	5	2.5	42.5
			1.0*10 ⁷	10	5	35
	Ca-Mont	0.2	0.25*10 ⁷	2.5	1.25	46.25
			0.5*10 ⁷	5	2.5	42.5
			1.0*10 ⁷	10	5	35
	Mont K-10	0.07	0.25*10 ⁷	2.5	1.25	46.25
			0.5*10 ⁷	5	2.5	42.5
			1.0*10 ⁷	10	5	35

Particle Ratio	Clay	Clay concentration (g L ⁻¹)	Concentration of <i>E. coli</i> (CFU ml ⁻¹)	Clay suspension (ml)	10 ⁸ ml ⁻¹ <i>E. coli</i> suspension (ml)	PBS (ml)
100	Kaolin	1.2	0.25*10 ⁷	6.25	1.25	42.5
			0.5*10 ⁷	12.5	2.5	35
			1.0*10 ⁷	25	5	20
	Hectorite	0.25	0.25*10 ⁷	5	1.25	43.75
			0.5*10 ⁷	10	2.5	37.5
			1.0*10 ⁷	20	5	25
	Ca-Mont	0.2	0.25*10 ⁷	5	1.25	43.75
			0.5*10 ⁷	10	2.5	37.5
			1.0*10 ⁷	20	5	25
	Mont K-10	0.07	0.25*10 ⁷	5	1.25	43.75
			0.5*10 ⁷	10	2.5	37.5
			1.0*10 ⁷	20	5	25
200	Kaolin	3.75	0.25*10 ⁷	4	1.25	44.75
			0.5*10 ⁷	8	2.5	39.5
			1.0*10 ⁷	16	5	29
	Hectorite	0.25	0.25*10 ⁷	10	1.25	38.75
			0.5*10 ⁷	20	2.5	27.5
			1.0*10 ⁷	40	5	5
	Ca-Mont	0.2	0.25*10 ⁷	10	1.25	38.75
			0.5*10 ⁷	20	2.5	27.5
			1.0*10 ⁷	40	5	5
	Mont K-10	0.07	0.25*10 ⁷	10	1.25	38.75
			0.5*10 ⁷	20	2.5	27.5
			1.0*10 ⁷	40	5	5
500	Kaolin	3.75	0.25*10 ⁷	10	1.25	38.75
			0.5*10 ⁷	20	2.5	27.5
			1.0*10 ⁷	40	5	5
	Hectorite	0.625	0.25*10 ⁷	10	1.25	38.75
			0.5*10 ⁷	20	2.5	27.5
			1.0*10 ⁷	40	5	5
	Ca-Mont	0.5	0.25*10 ⁷	10	1.25	38.75
			0.5*10 ⁷	20	2.5	27.5
			1.0*10 ⁷	40	5	5
	Mont K-10	0.175	0.25*10 ⁷	10	1.25	38.75
			0.5*10 ⁷	20	2.5	27.5
			1.0*10 ⁷	40	5	5

Ratio	Clay	Clay concentration (g L ⁻¹)	Concentration of <i>E. coli</i> (CFU ml ⁻¹)	Clay suspension (ml)	10 ⁸ ml ⁻¹ <i>E. coli</i> suspension (ml)	PBS (ml)
1000	Kaolin	7.5	0.25*10 ⁷	10	1.25	38.75
			0.5*10 ⁷	20	2.5	27.5
			1.0*10 ⁷	40	5	5
	Hectorite	1.25	0.25*10 ⁷	10	1.25	38.75
			0.5*10 ⁷	20	2.5	27.5
			1.0*10 ⁷	40	5	5
	Ca-Mont	1	0.25*10 ⁷	10	1.25	38.75
			0.5*10 ⁷	20	2.5	27.5
			1.0*10 ⁷	40	5	5
	Mont K-10	0.35	0.25*10 ⁷	10	1.25	38.75
			0.5*10 ⁷	20	2.5	27.5
			1.0*10 ⁷	40	5	5

APPENDIX B2. Flow cytometry samples

(Concentrations of clay suspensions: Montmorillonite K-10 0.175g L⁻¹; Ca-Montmorillonite 0.5g L⁻¹; Hectorite 0.625g L⁻¹; Kaolin 3.75g L⁻¹)

Surface area Ratio	No.	10 ⁸ ml ⁻¹ <i>E. coli</i> suspension (μl)	Clay suspension (μl)	SYTO 11 (μl)	PBS (μl)
Control	1	0	0	0	250
	2	0	0	2	248
	3	25	0	0	225
	4	25	0	2	223
1	5	0	0.4	0	249.6
	6	0	0.4	2	247.6
	7	25	0.4	2	222.6
	8	25	0.4	2	222.6
	9	25	0.4	2	222.6
2	10	0	0.8	0	249.2
	11	0	0.8	2	247.2
	12	25	0.8	2	222.2
	13	25	0.8	2	222.2
	14	25	0.8	2	222.2
5	15	0	2	0	248
	16	0	2	2	246
	17	25	2	2	221
	18	25	2	2	221
	19	25	2	2	221
10	20	0	4	0	246
	21	0	4	2	244
	22	25	4	2	219
	23	25	4	2	219
	24	25	4	2	219
25	25	0	10	0	240
	26	0	10	2	238
	27	25	10	2	213
	28	25	10	2	213
	29	25	10	2	213
50	30	0	20	0	230
	31	0	20	2	228
	32	25	20	2	203
	33	25	20	2	203
	34	25	20	2	203
100	35	0	40	0	210
	36	0	40	2	208

100	37	25	40	2	183
	38	25	40	2	183
	39	25	40	2	183
150	40	0	60	0	190
	41	0	60	2	188
	42	25	60	2	163
	43	25	60	2	163
	44	25	60	2	163
200	45	0	80	0	170
	46	0	80	2	168
	47	25	80	2	143
	48	25	80	2	143
	49	25	80	2	143
300	50	0	120	0	130
	51	0	120	2	128
	52	25	120	2	103
	53	25	120	2	103
	54	25	120	2	103
400	55	0	160	0	90
	56	0	160	2	88
	57	25	160	2	63
	58	25	160	2	63
	59	25	160	2	63
500	60	0	200	0	50
	61	0	200	2	48
	62	25	200	2	23
	63	25	200	2	23
	64	25	200	2	23

APPENDIX C. RAW DATA

APPENDIX C1. Percent attached of strain #31 in the settling method

Particle Ratio	Clay	Sample No.	<i>E. coli</i> Concentration (CFU ml ⁻¹)	Percent attached
1	Hectorite	1	0.25*10 ⁷	16.38%
1	Hectorite	2	0.5*10 ⁷	26.74%
1	Hectorite	3	1*10 ⁷	27.93%
1	Hectorite	4	0.25*10 ⁷	2.94%
1	Hectorite	5	0.5*10 ⁷	10.34%
1	Hectorite	6	1*10 ⁷	6.43%
1	Hectorite	7	0.25*10 ⁷	41.77%
1	Hectorite	8	0.5*10 ⁷	48.27%
1	Hectorite	9	1*10 ⁷	12.94%
1	Kaolin	1	0.25*10 ⁷	29.55%
1	Kaolin	2	0.5*10 ⁷	26.00%
1	Kaolin	3	1*10 ⁷	0.00%
1	Kaolin	4	0.25*10 ⁷	16.67%
1	Kaolin	5	0.5*10 ⁷	0.00%
1	Kaolin	6	1*10 ⁷	13.61%
1	Kaolin	7	0.25*10 ⁷	0.00%
1	Kaolin	8	0.5*10 ⁷	16.36%
1	Kaolin	9	1*10 ⁷	0.00%
1	Ca-Mont	1	0.25*10 ⁷	3.11%
1	Ca-Mont	2	0.5*10 ⁷	4.57%
1	Ca-Mont	3	1*10 ⁷	11.41%
1	Ca-Mont	4	0.25*10 ⁷	4.97%
1	Ca-Mont	5	0.5*10 ⁷	7.98%
1	Ca-Mont	6	1*10 ⁷	10.33%
1	Ca-Mont	7	0.25*10 ⁷	4.95%
1	Ca-Mont	8	0.5*10 ⁷	10.96%
1	Ca-Mont	9	1*10 ⁷	17.97%
1	Mont K-10	1	0.25*10 ⁷	5.88%
1	Mont K-10	2	0.5*10 ⁷	11.21%
1	Mont K-10	3	1*10 ⁷	18.07%
1	Mont K-10	4	0.25*10 ⁷	2.07%
1	Mont K-10	5	0.5*10 ⁷	29.55%
1	Mont K-10	6	1*10 ⁷	0.00%
1	Mont K-10	7	0.25*10 ⁷	4.35%
1	Mont K-10	8	0.5*10 ⁷	0.00%
1	Mont K-10	9	1*10 ⁷	0.00%

Particle Ratio	Clay	Sample No.	<i>E. coli</i> Concentration (CFU ml ⁻¹)	Percent attached
2	Hectorite	1	0.25*10 ⁷	0.00%
2	Hectorite	2	0.5*10 ⁷	10.07%
2	Hectorite	3	1*10 ⁷	16.14%
2	Hectorite	4	0.25*10 ⁷	0.00%
2	Hectorite	5	0.5*10 ⁷	19.23%
2	Hectorite	6	1*10 ⁷	10.53%
2	Hectorite	7	0.25*10 ⁷	21.05%
2	Hectorite	8	0.5*10 ⁷	0.00%
2	Hectorite	9	1*10 ⁷	13.98%
2	Kaolin	1	0.25*10 ⁷	7.59%
2	Kaolin	2	0.5*10 ⁷	17.76%
2	Kaolin	3	1*10 ⁷	5.33%
2	Kaolin	4	0.25*10 ⁷	13.60%
2	Kaolin	5	0.5*10 ⁷	21.25%
2	Kaolin	6	1*10 ⁷	3.81%
2	Kaolin	7	0.25*10 ⁷	33.33%
2	Kaolin	8	0.5*10 ⁷	40.37%
2	Kaolin	9	1*10 ⁷	0.00%
2	Ca-Mont	1	0.25*10 ⁷	34.45%
2	Ca-Mont	2	0.5*10 ⁷	36.23%
2	Ca-Mont	3	1*10 ⁷	16.52%
2	Ca-Mont	4	0.25*10 ⁷	25.68%
2	Ca-Mont	5	0.5*10 ⁷	26.72%
2	Ca-Mont	6	1*10 ⁷	37.23%
2	Ca-Mont	7	0.25*10 ⁷	6.59%
2	Ca-Mont	8	0.5*10 ⁷	30.67%
2	Ca-Mont	9	1*10 ⁷	4.31%
2	Mont K-10	1	0.25*10 ⁷	53.04%
2	Mont K-10	2	0.5*10 ⁷	0.00%
2	Mont K-10	3	1*10 ⁷	16.78%
2	Mont K-10	4	0.25*10 ⁷	5.13%
2	Mont K-10	5	0.5*10 ⁷	24.64%
2	Mont K-10	6	1*10 ⁷	24.44%
2	Mont K-10	7	0.25*10 ⁷	0.00%
2	Mont K-10	8	0.5*10 ⁷	0.00%
2	Mont K-10	9	1*10 ⁷	25.73%

Particle Ratio	Clay	Sample No.	<i>E. coli</i> Concentration (CFU ml ⁻¹)	Percent attached
50	Hectorite	1	0.25*10 ⁷	20.00%
50	Hectorite	2	0.5*10 ⁷	35.71%
50	Hectorite	3	1*10 ⁷	17.93%
50	Hectorite	4	0.25*10 ⁷	14.63%
50	Hectorite	5	0.5*10 ⁷	46.99%
50	Hectorite	6	1*10 ⁷	20.00%
50	Hectorite	7	0.25*10 ⁷	14.55%
50	Hectorite	8	0.5*10 ⁷	36.73%
50	Hectorite	9	1*10 ⁷	23.91%
50	Kaolin	1	0.25*10 ⁷	20.00%
50	Kaolin	2	0.5*10 ⁷	35.71%
50	Kaolin	3	1*10 ⁷	17.93%
50	Kaolin	4	0.25*10 ⁷	14.63%
50	Kaolin	5	0.5*10 ⁷	46.99%
50	Kaolin	6	1*10 ⁷	20.00%
50	Kaolin	7	0.25*10 ⁷	14.55%
50	Kaolin	8	0.5*10 ⁷	36.73%
50	Kaolin	9	1*10 ⁷	23.91%
50	Ca-Mont	1	0.25*10 ⁷	25.37%
50	Ca-Mont	2	0.5*10 ⁷	0.00%
50	Ca-Mont	3	1*10 ⁷	27.75%
50	Ca-Mont	4	0.25*10 ⁷	0.00%
50	Ca-Mont	5	0.5*10 ⁷	20.69%
50	Ca-Mont	6	1*10 ⁷	0.00%
50	Ca-Mont	7	0.25*10 ⁷	22.12%
50	Ca-Mont	8	0.5*10 ⁷	27.84%
50	Ca-Mont	9	1*10 ⁷	21.54%
50	Mont K-10	1	0.25*10 ⁷	10.89%
50	Mont K-10	2	0.5*10 ⁷	21.59%
50	Mont K-10	3	1*10 ⁷	12.02%
50	Mont K-10	4	0.25*10 ⁷	0.00%
50	Mont K-10	5	0.5*10 ⁷	36.61%
50	Mont K-10	6	1*10 ⁷	21.83%
50	Mont K-10	7	0.25*10 ⁷	50.00%
50	Mont K-10	8	0.5*10 ⁷	11.11%
50	Mont K-10	9	1*10 ⁷	30.41%

Particle Ratio	Clay	Sample No.	<i>E. coli</i> Concentration (CFU ml ⁻¹)	Percent attached
100	Hectorite	1	0.25*10 ⁷	26.55%
100	Hectorite	2	0.5*10 ⁷	28.70%
100	Hectorite	3	1*10 ⁷	53.45%
100	Hectorite	4	0.25*10 ⁷	17.14%
100	Hectorite	5	0.5*10 ⁷	46.17%
100	Hectorite	6	1*10 ⁷	49.78%
100	Hectorite	7	0.25*10 ⁷	39.73%
100	Hectorite	8	0.5*10 ⁷	40.25%
100	Hectorite	9	1*10 ⁷	42.86%
100	Kaolin	1	0.25*10 ⁷	4.76%
100	Kaolin	2	0.5*10 ⁷	8.17%
100	Kaolin	3	1*10 ⁷	23.49%
100	Kaolin	4	0.25*10 ⁷	26.63%
100	Kaolin	5	0.5*10 ⁷	17.22%
100	Kaolin	6	1*10 ⁷	17.30%
100	Kaolin	7	0.25*10 ⁷	17.99%
100	Kaolin	8	0.5*10 ⁷	29.18%
100	Kaolin	9	1*10 ⁷	17.60%
100	Ca-Mont	1	0.25*10 ⁷	0.00%
100	Ca-Mont	2	0.5*10 ⁷	44.58%
100	Ca-Mont	3	1*10 ⁷	7.06%
100	Ca-Mont	4	0.25*10 ⁷	55.56%
100	Ca-Mont	5	0.5*10 ⁷	29.41%
100	Ca-Mont	6	1*10 ⁷	43.07%
100	Ca-Mont	7	0.25*10 ⁷	23.53%
100	Ca-Mont	8	0.5*10 ⁷	33.33%
100	Ca-Mont	9	1*10 ⁷	34.88%
100	Mont K-10	1	0.25*10 ⁷	6.67%
100	Mont K-10	2	0.5*10 ⁷	12.77%
100	Mont K-10	3	1*10 ⁷	18.67%
100	Mont K-10	4	0.25*10 ⁷	0.00%
100	Mont K-10	5	0.5*10 ⁷	36.36%
100	Mont K-10	6	1*10 ⁷	52.69%
100	Mont K-10	7	0.25*10 ⁷	15.79%
100	Mont K-10	8	0.5*10 ⁷	37.84%
100	Mont K-10	9	1*10 ⁷	46.75%

Particle Ratio	Clay	Sample No.	<i>E. coli</i> Concentration (CFU ml ⁻¹)	Percent attached
200	Hectorite	1	0.25*10 ⁷	49.55%
200	Hectorite	2	0.5*10 ⁷	22.35%
200	Hectorite	3	1*10 ⁷	57.86%
200	Hectorite	4	0.25*10 ⁷	35.78%
200	Hectorite	5	0.5*10 ⁷	66.50%
200	Hectorite	6	1*10 ⁷	55.32%
200	Hectorite	7	0.25*10 ⁷	31.03%
200	Hectorite	8	0.5*10 ⁷	52.49%
200	Hectorite	9	1*10 ⁷	29.57%
200	Kaolin	1	0.25*10 ⁷	58.33%
200	Kaolin	2	0.5*10 ⁷	36.23%
200	Kaolin	3	1*10 ⁷	67.12%
200	Kaolin	4	0.25*10 ⁷	58.14%
200	Kaolin	5	0.5*10 ⁷	61.19%
200	Kaolin	6	1*10 ⁷	54.78%
200	Kaolin	7	0.25*10 ⁷	43.59%
200	Kaolin	8	0.5*10 ⁷	77.78%
200	Kaolin	9	1*10 ⁷	56.14%
200	Ca-Mont	1	0.25*10 ⁷	0.00%
200	Ca-Mont	2	0.5*10 ⁷	36.73%
200	Ca-Mont	3	1*10 ⁷	6.72%
200	Ca-Mont	4	0.25*10 ⁷	39.53%
200	Ca-Mont	5	0.5*10 ⁷	22.11%
200	Ca-Mont	6	1*10 ⁷	43.04%
200	Ca-Mont	7	0.25*10 ⁷	24.59%
200	Ca-Mont	8	0.5*10 ⁷	37.35%
200	Ca-Mont	9	1*10 ⁷	9.55%
200	Mont K-10	1	0.25*10 ⁷	16.33%
200	Mont K-10	2	0.5*10 ⁷	8.55%
200	Mont K-10	3	1*10 ⁷	19.90%
200	Mont K-10	4	0.25*10 ⁷	21.00%
200	Mont K-10	5	0.5*10 ⁷	30.07%
200	Mont K-10	6	1*10 ⁷	20.86%
200	Mont K-10	7	0.25*10 ⁷	28.57%
200	Mont K-10	8	0.5*10 ⁷	9.59%
200	Mont K-10	9	1*10 ⁷	25.25%

Particle Ratio	Clay	Sample No.	<i>E. coli</i> Concentration (CFU ml ⁻¹)	Percent attached
500	Hectorite	1	0.25*10 ⁷	52.87%
500	Hectorite	2	0.5*10 ⁷	72.97%
500	Hectorite	3	1*10 ⁷	68.54%
500	Hectorite	4	0.25*10 ⁷	59.72%
500	Hectorite	5	0.5*10 ⁷	76.95%
500	Hectorite	6	1*10 ⁷	54.21%
500	Hectorite	7	0.25*10 ⁷	75.95%
500	Hectorite	8	0.5*10 ⁷	69.16%
500	Hectorite	9	1*10 ⁷	53.23%
500	Kaolin	1	0.25*10 ⁷	63.08%
500	Kaolin	2	0.5*10 ⁷	91.67%
500	Kaolin	3	1*10 ⁷	89.23%
500	Kaolin	4	0.25*10 ⁷	73.68%
500	Kaolin	5	0.5*10 ⁷	77.33%
500	Kaolin	6	1*10 ⁷	88.84%
500	Kaolin	7	0.25*10 ⁷	42.22%
500	Kaolin	8	0.5*10 ⁷	71.74%
500	Kaolin	9	1*10 ⁷	82.20%
500	Ca-Mont	1	0.25*10 ⁷	1.45%
500	Ca-Mont	2	0.5*10 ⁷	0.00%
500	Ca-Mont	3	1*10 ⁷	17.24%
500	Ca-Mont	4	0.25*10 ⁷	47.95%
500	Ca-Mont	5	0.5*10 ⁷	11.69%
500	Ca-Mont	6	1*10 ⁷	21.45%
500	Ca-Mont	7	0.25*10 ⁷	9.86%
500	Ca-Mont	8	0.5*10 ⁷	40.96%
500	Ca-Mont	9	1*10 ⁷	31.37%
500	Mont K-10	1	0.25*10 ⁷	77.65%
500	Mont K-10	2	0.5*10 ⁷	50.41%
500	Mont K-10	3	1*10 ⁷	79.55%
500	Mont K-10	4	0.25*10 ⁷	75.63%
500	Mont K-10	5	0.5*10 ⁷	62.83%
500	Mont K-10	6	1*10 ⁷	81.27%
500	Mont K-10	7	0.25*10 ⁷	59.34%
500	Mont K-10	8	0.5*10 ⁷	60.00%
500	Mont K-10	9	1*10 ⁷	74.44%

Particle Ratio	Clay	Sample No.	<i>E. coli</i> Concentration (CFU ml ⁻¹)	Percent attached
1000	Hectorite	1	0.25*10 ⁷	80.33%
1000	Hectorite	2	0.5*10 ⁷	100.00%
1000	Hectorite	3	1*10 ⁷	43.96%
1000	Hectorite	4	0.25*10 ⁷	75.76%
1000	Hectorite	5	0.5*10 ⁷	91.03%
1000	Hectorite	6	1*10 ⁷	94.07%
1000	Hectorite	7	0.25*10 ⁷	78.57%
1000	Hectorite	8	0.5*10 ⁷	91.38%
1000	Hectorite	9	1*10 ⁷	93.20%
1000	Kaolin	1	0.25*10 ⁷	68.09%
1000	Kaolin	2	0.5*10 ⁷	88.71%
1000	Kaolin	3	1*10 ⁷	95.15%
1000	Kaolin	4	0.25*10 ⁷	89.47%
1000	Kaolin	5	0.5*10 ⁷	88.79%
1000	Kaolin	6	1*10 ⁷	96.61%
1000	Kaolin	7	0.25*10 ⁷	84.00%
1000	Kaolin	8	0.5*10 ⁷	94.59%
1000	Kaolin	9	1*10 ⁷	92.93%
1000	Ca-Mont	1	0.25*10 ⁷	22.54%
1000	Ca-Mont	2	0.5*10 ⁷	30.23%
1000	Ca-Mont	3	1*10 ⁷	52.94%
1000	Ca-Mont	4	0.25*10 ⁷	15.92%
1000	Ca-Mont	5	0.5*10 ⁷	7.63%
1000	Ca-Mont	6	1*10 ⁷	46.97%
1000	Ca-Mont	7	0.25*10 ⁷	15.11%
1000	Ca-Mont	8	0.5*10 ⁷	32.69%
1000	Ca-Mont	9	1*10 ⁷	38.79%
1000	Mont K-10	1	0.25*10 ⁷	17.50%
1000	Mont K-10	2	0.5*10 ⁷	16.86%
1000	Mont K-10	3	1*10 ⁷	55.04%
1000	Mont K-10	4	0.25*10 ⁷	0.00%
1000	Mont K-10	5	0.5*10 ⁷	43.07%
1000	Mont K-10	6	1*10 ⁷	51.25%
1000	Mont K-10	7	0.25*10 ⁷	9.30%
1000	Mont K-10	8	0.5*10 ⁷	65.20%
1000	Mont K-10	9	1*10 ⁷	62.16%

APPENDIX C2. Percent attached of strain #50 in the settling method

Particle Ratio	Clay	Sample No.	<i>E. coli</i> Concentration (CFU ml ⁻¹)	Percent attached
1	Hectorite	1	0.25*10 ⁷	0.00%
1	Hectorite	2	0.5*10 ⁷	17.44%
1	Hectorite	3	1*10 ⁷	33.33%
1	Hectorite	4	0.25*10 ⁷	1.05%
1	Hectorite	5	0.5*10 ⁷	0.00%
1	Hectorite	6	1*10 ⁷	-
1	Hectorite	7	0.25*10 ⁷	19.72%
1	Hectorite	8	0.5*10 ⁷	22.99%
1	Hectorite	9	1*10 ⁷	16.19%
1	Kaolin	1	0.25*10 ⁷	19.69%
1	Kaolin	2	0.5*10 ⁷	7.62%
1	Kaolin	3	1*10 ⁷	25.34%
1	Kaolin	4	0.25*10 ⁷	15.83%
1	Kaolin	5	0.5*10 ⁷	0.00%
1	Kaolin	6	1*10 ⁷	0.00%
1	Kaolin	7	0.25*10 ⁷	32.10%
1	Kaolin	8	0.5*10 ⁷	17.62%
1	Kaolin	9	1*10 ⁷	0.00%
1	Ca-Mont	1	0.25*10 ⁷	4.41%
1	Ca-Mont	2	0.5*10 ⁷	1.17%
1	Ca-Mont	3	1*10 ⁷	3.67%
1	Ca-Mont	4	0.25*10 ⁷	8.11%
1	Ca-Mont	5	0.5*10 ⁷	0.00%
1	Ca-Mont	6	1*10 ⁷	0.44%
1	Ca-Mont	7	0.25*10 ⁷	13.89%
1	Ca-Mont	8	0.5*10 ⁷	3.49%
1	Ca-Mont	9	1*10 ⁷	6.50%
1	Mont K-10	1	0.25*10 ⁷	0.00%
1	Mont K-10	2	0.5*10 ⁷	0.00%
1	Mont K-10	3	1*10 ⁷	0.00%
1	Mont K-10	4	0.25*10 ⁷	29.52%
1	Mont K-10	5	0.5*10 ⁷	10.98%
1	Mont K-10	6	1*10 ⁷	22.70%
1	Mont K-10	7	0.25*10 ⁷	21.74%
1	Mont K-10	8	0.5*10 ⁷	0.00%
1	Mont K-10	9	1*10 ⁷	7.39%

Particle Ratio	Clay	Sample No.	<i>E. coli</i> Concentration (CFU ml ⁻¹)	Percent attached
2	Hectorite	1	0.25*10 ⁷	39.69%
2	Hectorite	2	0.5*10 ⁷	0.00%
2	Hectorite	3	1*10 ⁷	6.14%
2	Hectorite	4	0.25*10 ⁷	0.00%
2	Hectorite	5	0.5*10 ⁷	0.00%
2	Hectorite	6	1*10 ⁷	9.04%
2	Hectorite	7	0.25*10 ⁷	19.28%
2	Hectorite	8	0.5*10 ⁷	0.60%
2	Hectorite	9	1*10 ⁷	6.16%
2	Kaolin	1	0.25*10 ⁷	10.34%
2	Kaolin	2	0.5*10 ⁷	28.89%
2	Kaolin	3	1*10 ⁷	7.93%
2	Kaolin	4	0.25*10 ⁷	10.26%
2	Kaolin	5	0.5*10 ⁷	5.97%
2	Kaolin	6	1*10 ⁷	34.00%
2	Kaolin	7	0.25*10 ⁷	32.71%
2	Kaolin	8	0.5*10 ⁷	0.00%
2	Kaolin	9	1*10 ⁷	43.61%
2	Ca-Mont	1	0.25*10 ⁷	23.64%
2	Ca-Mont	2	0.5*10 ⁷	10.58%
2	Ca-Mont	3	1*10 ⁷	9.07%
2	Ca-Mont	4	0.25*10 ⁷	0.00%
2	Ca-Mont	5	0.5*10 ⁷	3.48%
2	Ca-Mont	6	1*10 ⁷	18.44%
2	Ca-Mont	7	0.25*10 ⁷	0.00%
2	Ca-Mont	8	0.5*10 ⁷	0.00%
2	Ca-Mont	9	1*10 ⁷	0.00%
2	Mont K-10	1	0.25*10 ⁷	19.63%
2	Mont K-10	2	0.5*10 ⁷	4.86%
2	Mont K-10	3	1*10 ⁷	25.59%
2	Mont K-10	4	0.25*10 ⁷	39.46%
2	Mont K-10	5	0.5*10 ⁷	0.00%
2	Mont K-10	6	1*10 ⁷	11.89%
2	Mont K-10	7	0.25*10 ⁷	0.00%
2	Mont K-10	8	0.5*10 ⁷	15.38%
2	Mont K-10	9	1*10 ⁷	0.00%

Particle Ratio	Clay	Sample No.	<i>E. coli</i> Concentration (CFU ml ⁻¹)	Percent attached
50	Hectorite	1	0.25*10 ⁷	36.72%
50	Hectorite	2	0.5*10 ⁷	15.30%
50	Hectorite	3	1*10 ⁷	38.73%
50	Hectorite	4	0.25*10 ⁷	20.31%
50	Hectorite	5	0.5*10 ⁷	43.41%
50	Hectorite	6	1*10 ⁷	8.01%
50	Hectorite	7	0.25*10 ⁷	29.37%
50	Hectorite	8	0.5*10 ⁷	42.96%
50	Hectorite	9	1*10 ⁷	12.04%
50	Kaolin	1	0.25*10 ⁷	
50	Kaolin	2	0.5*10 ⁷	36.65%
50	Kaolin	3	1*10 ⁷	31.02%
50	Kaolin	4	0.25*10 ⁷	26.88%
50	Kaolin	5	0.5*10 ⁷	24.29%
50	Kaolin	6	1*10 ⁷	18.32%
50	Kaolin	7	0.25*10 ⁷	22.95%
50	Kaolin	8	0.5*10 ⁷	43.28%
50	Kaolin	9	1*10 ⁷	21.71%
50	Ca-Mont	1	0.25*10 ⁷	0.00%
50	Ca-Mont	2	0.5*10 ⁷	26.06%
50	Ca-Mont	3	1*10 ⁷	15.26%
50	Ca-Mont	4	0.25*10 ⁷	20.00%
50	Ca-Mont	5	0.5*10 ⁷	11.25%
50	Ca-Mont	6	1*10 ⁷	32.43%
50	Ca-Mont	7	0.25*10 ⁷	7.38%
50	Ca-Mont	8	0.5*10 ⁷	12.47%
50	Ca-Mont	9	1*10 ⁷	13.45%
50	Mont K-10	1	0.25*10 ⁷	15.32%
50	Mont K-10	2	0.5*10 ⁷	12.90%
50	Mont K-10	3	1*10 ⁷	20.26%
50	Mont K-10	4	0.25*10 ⁷	28.65%
50	Mont K-10	5	0.5*10 ⁷	26.69%
50	Mont K-10	6	1*10 ⁷	18.92%
50	Mont K-10	7	0.25*10 ⁷	39.74%
50	Mont K-10	8	0.5*10 ⁷	9.83%
50	Mont K-10	9	1*10 ⁷	46.47%

Particle Ratio	Clay	Sample No.	<i>E. coli</i> Concentration (CFU ml ⁻¹)	Percent attached
100	Hectorite	1	0.25*10 ⁷	23.46%
100	Hectorite	2	0.5*10 ⁷	35.91%
100	Hectorite	3	1*10 ⁷	24.65%
100	Hectorite	4	0.25*10 ⁷	0.00%
100	Hectorite	5	0.5*10 ⁷	13.01%
100	Hectorite	6	1*10 ⁷	0.00%
100	Hectorite	7	0.25*10 ⁷	15.48%
100	Hectorite	8	0.5*10 ⁷	21.08%
100	Hectorite	9	1*10 ⁷	25.00%
100	Kaolin	1	0.25*10 ⁷	39.39%
100	Kaolin	2	0.5*10 ⁷	46.76%
100	Kaolin	3	1*10 ⁷	-
100	Kaolin	4	0.25*10 ⁷	33.33%
100	Kaolin	5	0.5*10 ⁷	59.73%
100	Kaolin	6	1*10 ⁷	49.44%
100	Kaolin	7	0.25*10 ⁷	21.74%
100	Kaolin	8	0.5*10 ⁷	44.00%
100	Kaolin	9	1*10 ⁷	-
100	Ca-Mont	1	0.25*10 ⁷	5.88%
100	Ca-Mont	2	0.5*10 ⁷	0.00%
100	Ca-Mont	3	1*10 ⁷	45.16%
100	Ca-Mont	4	0.25*10 ⁷	32.31%
100	Ca-Mont	5	0.5*10 ⁷	34.58%
100	Ca-Mont	6	1*10 ⁷	0.00%
100	Ca-Mont	7	0.25*10 ⁷	37.04%
100	Ca-Mont	8	0.5*10 ⁷	4.95%
100	Ca-Mont	9	1*10 ⁷	38.16%
100	Mont K-10	1	0.25*10 ⁷	33.61%
100	Mont K-10	2	0.5*10 ⁷	8.77%
100	Mont K-10	3	1*10 ⁷	9.13%
100	Mont K-10	4	0.25*10 ⁷	20.81%
100	Mont K-10	5	0.5*10 ⁷	6.19%
100	Mont K-10	6	1*10 ⁷	22.44%
100	Mont K-10	7	0.25*10 ⁷	8.20%
100	Mont K-10	8	0.5*10 ⁷	7.94%
100	Mont K-10	9	1*10 ⁷	14.56%

Particle Ratio	Clay	Sample No.	<i>E. coli</i> Concentration (CFU ml ⁻¹)	Percent attached
200	Hectorite	1	0.25*10 ⁷	62.71%
200	Hectorite	2	0.5*10 ⁷	63.27%
200	Hectorite	3	1*10 ⁷	56.18%
200	Hectorite	4	0.25*10 ⁷	14.69%
200	Hectorite	5	0.5*10 ⁷	29.57%
200	Hectorite	6	1*10 ⁷	46.04%
200	Hectorite	7	0.25*10 ⁷	6.15%
200	Hectorite	8	0.5*10 ⁷	36.51%
200	Hectorite	9	1*10 ⁷	57.11%
200	Kaolin	1	0.25*10 ⁷	64.71%
200	Kaolin	2	0.5*10 ⁷	66.67%
200	Kaolin	3	1*10 ⁷	48.84%
200	Kaolin	4	0.25*10 ⁷	76.92%
200	Kaolin	5	0.5*10 ⁷	26.32%
200	Kaolin	6	1*10 ⁷	70.00%
200	Kaolin	7	0.25*10 ⁷	19.67%
200	Kaolin	8	0.5*10 ⁷	48.22%
200	Kaolin	9	1*10 ⁷	63.57%
200	Ca-Mont	1	0.25*10 ⁷	20.69%
200	Ca-Mont	2	0.5*10 ⁷	63.91%
200	Ca-Mont	3	1*10 ⁷	71.14%
200	Ca-Mont	4	0.25*10 ⁷	36.00%
200	Ca-Mont	5	0.5*10 ⁷	54.20%
200	Ca-Mont	6	1*10 ⁷	78.01%
200	Ca-Mont	7	0.25*10 ⁷	21.74%
200	Ca-Mont	8	0.5*10 ⁷	57.47%
200	Ca-Mont	9	1*10 ⁷	64.44%
200	Mont K-10	1	0.25*10 ⁷	17.95%
200	Mont K-10	2	0.5*10 ⁷	40.83%
200	Mont K-10	3	1*10 ⁷	4.41%
200	Mont K-10	4	0.25*10 ⁷	0.00%
200	Mont K-10	5	0.5*10 ⁷	30.23%
200	Mont K-10	6	1*10 ⁷	4.76%
200	Mont K-10	7	0.25*10 ⁷	0.00%
200	Mont K-10	8	0.5*10 ⁷	3.36%
200	Mont K-10	9	1*10 ⁷	31.15%

Particle Ratio	Clay	Sample No.	<i>E. coli</i> Concentration (CFU ml ⁻¹)	Percent attached
500	Hectorite	1	0.25*10 ⁷	0.00%
500	Hectorite	2	0.5*10 ⁷	0.00%
500	Hectorite	3	1*10 ⁷	8.96%
500	Hectorite	4	0.25*10 ⁷	4.08%
500	Hectorite	5	0.5*10 ⁷	0.00%
500	Hectorite	6	1*10 ⁷	17.55%
500	Hectorite	7	0.25*10 ⁷	8.80%
500	Hectorite	8	0.5*10 ⁷	4.27%
500	Hectorite	9	1*10 ⁷	26.55%
500	Kaolin	1	0.25*10 ⁷	62.57%
500	Kaolin	2	0.5*10 ⁷	52.24%
500	Kaolin	3	1*10 ⁷	68.21%
500	Kaolin	4	0.25*10 ⁷	53.45%
500	Kaolin	5	0.5*10 ⁷	67.09%
500	Kaolin	6	1*10 ⁷	
500	Kaolin	7	0.25*10 ⁷	71.76%
500	Kaolin	8	0.5*10 ⁷	71.56%
500	Kaolin	9	1*10 ⁷	
500	Ca-Mont	1	0.25*10 ⁷	39.36%
500	Ca-Mont	2	0.5*10 ⁷	11.43%
500	Ca-Mont	3	1*10 ⁷	27.66%
500	Ca-Mont	4	0.25*10 ⁷	34.15%
500	Ca-Mont	5	0.5*10 ⁷	56.98%
500	Ca-Mont	6	1*10 ⁷	45.16%
500	Ca-Mont	7	0.25*10 ⁷	20.70%
500	Ca-Mont	8	0.5*10 ⁷	48.48%
500	Ca-Mont	9	1*10 ⁷	19.76%
500	Mont K-10	1	0.25*10 ⁷	0.00%
500	Mont K-10	2	0.5*10 ⁷	23.67%
500	Mont K-10	3	1*10 ⁷	17.38%
500	Mont K-10	4	0.25*10 ⁷	13.46%
500	Mont K-10	5	0.5*10 ⁷	17.46%
500	Mont K-10	6	1*10 ⁷	29.89%
500	Mont K-10	7	0.25*10 ⁷	0.00%
500	Mont K-10	8	0.5*10 ⁷	28.70%
500	Mont K-10	9	1*10 ⁷	22.44%

Particle Ratio	Clay	Sample No.	<i>E. coli</i> Concentration (CFU ml ⁻¹)	Percent attached
1000	Hectorite	1	0.25*10 ⁷	88.37%
1000	Hectorite	2	0.5*10 ⁷	93.97%
1000	Hectorite	3	1*10 ⁷	96.20%
1000	Hectorite	4	0.25*10 ⁷	83.25%
1000	Hectorite	5	0.5*10 ⁷	85.92%
1000	Hectorite	6	1*10 ⁷	98.18%
1000	Hectorite	7	0.25*10 ⁷	75.37%
1000	Hectorite	8	0.5*10 ⁷	95.68%
1000	Hectorite	9	1*10 ⁷	94.37%
1000	Kaolin	1	0.25*10 ⁷	89.04%
1000	Kaolin	2	0.5*10 ⁷	82.35%
1000	Kaolin	3	1*10 ⁷	84.62%
1000	Kaolin	4	0.25*10 ⁷	86.13%
1000	Kaolin	5	0.5*10 ⁷	93.52%
1000	Kaolin	6	1*10 ⁷	81.93%
1000	Kaolin	7	0.25*10 ⁷	94.24%
1000	Kaolin	8	0.5*10 ⁷	88.63%
1000	Kaolin	9	1*10 ⁷	88.86%
1000	Ca-Mont	1	0.25*10 ⁷	81.82%
1000	Ca-Mont	2	0.5*10 ⁷	72.86%
1000	Ca-Mont	3	1*10 ⁷	60.00%
1000	Ca-Mont	4	0.25*10 ⁷	53.33%
1000	Ca-Mont	5	0.5*10 ⁷	86.67%
1000	Ca-Mont	6	1*10 ⁷	30.32%
1000	Ca-Mont	7	0.25*10 ⁷	50.52%
1000	Ca-Mont	8	0.5*10 ⁷	76.47%
1000	Ca-Mont	9	1*10 ⁷	66.73%
1000	Mont K-10	1	0.25*10 ⁷	39.60%
1000	Mont K-10	2	0.5*10 ⁷	17.12%
1000	Mont K-10	3	1*10 ⁷	13.84%
1000	Mont K-10	4	0.25*10 ⁷	26.86%
1000	Mont K-10	5	0.5*10 ⁷	30.46%
1000	Mont K-10	6	1*10 ⁷	15.72%
1000	Mont K-10	7	0.25*10 ⁷	20.21%
1000	Mont K-10	8	0.5*10 ⁷	13.94%
1000	Mont K-10	9	1*10 ⁷	0.73%

APPENDIX C3. Percent attached of strain #89 in the settling method

Particle Ratio	Clay	Sample No.	<i>E. coli</i> Concentration (CFU ml ⁻¹)	Percent attached
1	Hectorite	1	0.25*10 ⁷	0.00%
1	Hectorite	2	0.5*10 ⁷	13.89%
1	Hectorite	3	1*10 ⁷	11.74%
1	Hectorite	4	0.25*10 ⁷	24.21%
1	Hectorite	5	0.5*10 ⁷	7.83%
1	Hectorite	6	1*10 ⁷	18.40%
1	Hectorite	7	0.25*10 ⁷	62.50%
1	Hectorite	8	0.5*10 ⁷	25.49%
1	Hectorite	9	1*10 ⁷	17.47%
1	Kaolin	1	0.25*10 ⁷	2.60%
1	Kaolin	2	0.5*10 ⁷	11.36%
1	Kaolin	3	1*10 ⁷	11.37%
1	Kaolin	4	0.25*10 ⁷	10.24%
1	Kaolin	5	0.5*10 ⁷	59.18%
1	Kaolin	6	1*10 ⁷	0.00%
1	Kaolin	7	0.25*10 ⁷	28.13%
1	Kaolin	8	0.5*10 ⁷	10.20%
1	Kaolin	9	1*10 ⁷	17.93%
1	Ca-Mont	1	0.25*10 ⁷	9.33%
1	Ca-Mont	2	0.5*10 ⁷	16.92%
1	Ca-Mont	3	1*10 ⁷	30.88%
1	Ca-Mont	4	0.25*10 ⁷	37.50%
1	Ca-Mont	5	0.5*10 ⁷	21.57%
1	Ca-Mont	6	1*10 ⁷	22.83%
1	Ca-Mont	7	0.25*10 ⁷	18.37%
1	Ca-Mont	8	0.5*10 ⁷	25.64%
1	Ca-Mont	9	1*10 ⁷	19.65%
1	Mont K-10	1	0.25*10 ⁷	14.29%
1	Mont K-10	2	0.5*10 ⁷	47.89%
1	Mont K-10	3	1*10 ⁷	24.17%
1	Mont K-10	4	0.25*10 ⁷	34.02%
1	Mont K-10	5	0.5*10 ⁷	0.00%
1	Mont K-10	6	1*10 ⁷	2.59%
1	Mont K-10	7	0.25*10 ⁷	20.45%
1	Mont K-10	8	0.5*10 ⁷	18.87%
1	Mont K-10	9	1*10 ⁷	36.12%

Particle Ratio	Clay	Sample No.	<i>E. coli</i> Concentration (CFU ml ⁻¹)	Percent attached
2	Hectorite	1	0.25*10 ⁷	26.32%
2	Hectorite	2	0.5*10 ⁷	10.34%
2	Hectorite	3	1*10 ⁷	1.74%
2	Hectorite	4	0.25*10 ⁷	0.00%
2	Hectorite	5	0.5*10 ⁷	0.00%
2	Hectorite	6	1*10 ⁷	7.17%
2	Hectorite	7	0.25*10 ⁷	43.59%
2	Hectorite	8	0.5*10 ⁷	16.55%
2	Hectorite	9	1*10 ⁷	1.49%
2	Kaolin	1	0.25*10 ⁷	7.22%
2	Kaolin	2	0.5*10 ⁷	12.70%
2	Kaolin	3	1*10 ⁷	21.85%
2	Kaolin	4	0.25*10 ⁷	0.00%
2	Kaolin	5	0.5*10 ⁷	0.00%
2	Kaolin	6	1*10 ⁷	0.81%
2	Kaolin	7	0.25*10 ⁷	39.62%
2	Kaolin	8	0.5*10 ⁷	28.36%
2	Kaolin	9	1*10 ⁷	16.72%
2	Ca-Mont	1	0.25*10 ⁷	24.39%
2	Ca-Mont	2	0.5*10 ⁷	25.15%
2	Ca-Mont	3	1*10 ⁷	33.07%
2	Ca-Mont	4	0.25*10 ⁷	3.90%
2	Ca-Mont	5	0.5*10 ⁷	23.66%
2	Ca-Mont	6	1*10 ⁷	35.75%
2	Ca-Mont	7	0.25*10 ⁷	10.81%
2	Ca-Mont	8	0.5*10 ⁷	18.41%
2	Ca-Mont	9	1*10 ⁷	16.98%
2	Mont K-10	1	0.25*10 ⁷	5.56%
2	Mont K-10	2	0.5*10 ⁷	31.40%
2	Mont K-10	3	1*10 ⁷	29.72%
2	Mont K-10	4	0.25*10 ⁷	21.74%
2	Mont K-10	5	0.5*10 ⁷	36.28%
2	Mont K-10	6	1*10 ⁷	0.00%
2	Mont K-10	7	0.25*10 ⁷	0.00%
2	Mont K-10	8	0.5*10 ⁷	37.50%
2	Mont K-10	9	1*10 ⁷	25.14%

Particle Ratio	Clay	Sample No.	<i>E. coli</i> Concentration (CFU ml ⁻¹)	Percent attached
50	Hectorite	1	0.25*10 ⁷	28.21%
50	Hectorite	2	0.5*10 ⁷	50.94%
50	Hectorite	3	1*10 ⁷	36.77%
50	Hectorite	4	0.25*10 ⁷	0.00%
50	Hectorite	5	0.5*10 ⁷	36.07%
50	Hectorite	6	1*10 ⁷	59.63%
50	Hectorite	7	0.25*10 ⁷	43.75%
50	Hectorite	8	0.5*10 ⁷	14.55%
50	Hectorite	9	1*10 ⁷	22.46%
50	Kaolin	1	0.25*10 ⁷	39.78%
50	Kaolin	2	0.5*10 ⁷	34.44%
50	Kaolin	3	1*10 ⁷	43.08%
50	Kaolin	4	0.25*10 ⁷	43.64%
50	Kaolin	5	0.5*10 ⁷	42.44%
50	Kaolin	6	1*10 ⁷	28.63%
50	Kaolin	7	0.25*10 ⁷	60.53%
50	Kaolin	8	0.5*10 ⁷	62.65%
50	Kaolin	9	1*10 ⁷	32.90%
50	Ca-Mont	1	0.25*10 ⁷	16.36%
50	Ca-Mont	2	0.5*10 ⁷	23.53%
50	Ca-Mont	3	1*10 ⁷	26.65%
50	Ca-Mont	4	0.25*10 ⁷	0.00%
50	Ca-Mont	5	0.5*10 ⁷	17.83%
50	Ca-Mont	6	1*10 ⁷	9.54%
50	Ca-Mont	7	0.25*10 ⁷	26.32%
50	Ca-Mont	8	0.5*10 ⁷	0.00%
50	Ca-Mont	9	1*10 ⁷	33.73%
50	Mont K-10	1	0.25*10 ⁷	28.21%
50	Mont K-10	2	0.5*10 ⁷	0.00%
50	Mont K-10	3	1*10 ⁷	12.78%
50	Mont K-10	4	0.25*10 ⁷	0.00%
50	Mont K-10	5	0.5*10 ⁷	11.25%
50	Mont K-10	6	1*10 ⁷	3.60%
50	Mont K-10	7	0.25*10 ⁷	0.00%
50	Mont K-10	8	0.5*10 ⁷	0.00%
50	Mont K-10	9	1*10 ⁷	14.89%

Particle Ratio	Clay	Sample No.	<i>E. coli</i> Concentration (CFU ml ⁻¹)	Percent attached
100	Hectorite	1	0.25*10 ⁷	20.00%
100	Hectorite	2	0.5*10 ⁷	45.16%
100	Hectorite	3	1*10 ⁷	35.27%
100	Hectorite	4	0.25*10 ⁷	57.89%
100	Hectorite	5	0.5*10 ⁷	61.29%
100	Hectorite	6	1*10 ⁷	
100	Hectorite	7	0.25*10 ⁷	45.83%
100	Hectorite	8	0.5*10 ⁷	52.86%
100	Hectorite	9	1*10 ⁷	68.55%
100	Kaolin	1	0.25*10 ⁷	55.22%
100	Kaolin	2	0.5*10 ⁷	65.93%
100	Kaolin	3	1*10 ⁷	58.33%
100	Kaolin	4	0.25*10 ⁷	59.04%
100	Kaolin	5	0.5*10 ⁷	35.26%
100	Kaolin	6	1*10 ⁷	64.15%
100	Kaolin	7	0.25*10 ⁷	32.17%
100	Kaolin	8	0.5*10 ⁷	72.13%
100	Kaolin	9	1*10 ⁷	48.15%
100	Ca-Mont	1	0.25*10 ⁷	32.77%
100	Ca-Mont	2	0.5*10 ⁷	21.85%
100	Ca-Mont	3	1*10 ⁷	25.40%
100	Ca-Mont	4	0.25*10 ⁷	19.63%
100	Ca-Mont	5	0.5*10 ⁷	24.44%
100	Ca-Mont	6	1*10 ⁷	17.81%
100	Ca-Mont	7	0.25*10 ⁷	14.04%
100	Ca-Mont	8	0.5*10 ⁷	20.16%
100	Ca-Mont	9	1*10 ⁷	17.20%
100	Mont K-10	1	0.25*10 ⁷	19.51%
100	Mont K-10	2	0.5*10 ⁷	10.89%
100	Mont K-10	3	1*10 ⁷	22.45%
100	Mont K-10	4	0.25*10 ⁷	30.56%
100	Mont K-10	5	0.5*10 ⁷	31.43%
100	Mont K-10	6	1*10 ⁷	37.10%
100	Mont K-10	7	0.25*10 ⁷	10.34%
100	Mont K-10	8	0.5*10 ⁷	19.79%
100	Mont K-10	9	1*10 ⁷	25.26%

Particle Ratio	Clay	Sample No.	<i>E. coli</i> Concentration (CFU ml ⁻¹)	Percent attached
200	Hectorite	1	0.25*10 ⁷	0.00%
200	Hectorite	2	0.5*10 ⁷	50.72%
200	Hectorite	3	1*10 ⁷	61.34%
200	Hectorite	4	0.25*10 ⁷	60.10%
200	Hectorite	5	0.5*10 ⁷	20.90%
200	Hectorite	6	1*10 ⁷	0.00%
200	Hectorite	7	0.25*10 ⁷	17.91%
200	Hectorite	8	0.5*10 ⁷	53.68%
200	Hectorite	9	1*10 ⁷	86.25%
200	Kaolin	1	0.25*10 ⁷	32.31%
200	Kaolin	2	0.5*10 ⁷	36.32%
200	Kaolin	3	1*10 ⁷	34.97%
200	Kaolin	4	0.25*10 ⁷	28.28%
200	Kaolin	5	0.5*10 ⁷	44.83%
200	Kaolin	6	1*10 ⁷	43.58%
200	Kaolin	7	0.25*10 ⁷	37.93%
200	Kaolin	8	0.5*10 ⁷	65.81%
200	Kaolin	9	1*10 ⁷	24.04%
200	Ca-Mont	1	0.25*10 ⁷	31.75%
200	Ca-Mont	2	0.5*10 ⁷	0.00%
200	Ca-Mont	3	1*10 ⁷	0.00%
200	Ca-Mont	4	0.25*10 ⁷	46.27%
200	Ca-Mont	5	0.5*10 ⁷	12.64%
200	Ca-Mont	6	1*10 ⁷	29.78%
200	Ca-Mont	7	0.25*10 ⁷	0.00%
200	Ca-Mont	8	0.5*10 ⁷	0.00%
200	Ca-Mont	9	1*10 ⁷	25.00%
200	Mont K-10	1	0.25*10 ⁷	0.00%
200	Mont K-10	2	0.5*10 ⁷	25.71%
200	Mont K-10	3	1*10 ⁷	22.43%
200	Mont K-10	4	0.25*10 ⁷	28.77%
200	Mont K-10	5	0.5*10 ⁷	0.00%
200	Mont K-10	6	1*10 ⁷	14.20%
200	Mont K-10	7	0.25*10 ⁷	13.85%
200	Mont K-10	8	0.5*10 ⁷	26.95%
200	Mont K-10	9	1*10 ⁷	15.57%

Particle Ratio	Clay	Sample No.	<i>E. coli</i> Concentration (CFU ml ⁻¹)	Percent attached
500	Hectorite	1	0.25*10 ⁷	71.29%
500	Hectorite	2	0.5*10 ⁷	74.03%
500	Hectorite	3	1*10 ⁷	89.64%
500	Hectorite	4	0.25*10 ⁷	87.12%
500	Hectorite	5	0.5*10 ⁷	85.00%
500	Hectorite	6	1*10 ⁷	97.20%
500	Hectorite	7	0.25*10 ⁷	83.87%
500	Hectorite	8	0.5*10 ⁷	84.62%
500	Hectorite	9	1*10 ⁷	92.66%
500	Kaolin	1	0.25*10 ⁷	75.76%
500	Kaolin	2	0.5*10 ⁷	64.79%
500	Kaolin	3	1*10 ⁷	82.72%
500	Kaolin	4	0.25*10 ⁷	73.68%
500	Kaolin	5	0.5*10 ⁷	71.22%
500	Kaolin	6	1*10 ⁷	68.66%
500	Kaolin	7	0.25*10 ⁷	73.58%
500	Kaolin	8	0.5*10 ⁷	84.71%
500	Kaolin	9	1*10 ⁷	77.63%
500	Ca-Mont	1	0.25*10 ⁷	35.95%
500	Ca-Mont	2	0.5*10 ⁷	47.42%
500	Ca-Mont	3	1*10 ⁷	14.86%
500	Ca-Mont	4	0.25*10 ⁷	67.01%
500	Ca-Mont	5	0.5*10 ⁷	31.64%
500	Ca-Mont	6	1*10 ⁷	13.45%
500	Ca-Mont	7	0.25*10 ⁷	0.00%
500	Ca-Mont	8	0.5*10 ⁷	0.00%
500	Ca-Mont	9	1*10 ⁷	35.40%
500	Mont K-10	1	0.25*10 ⁷	24.56%
500	Mont K-10	2	0.5*10 ⁷	36.61%
500	Mont K-10	3	1*10 ⁷	47.49%
500	Mont K-10	4	0.25*10 ⁷	50.36%
500	Mont K-10	5	0.5*10 ⁷	42.54%
500	Mont K-10	6	1*10 ⁷	13.48%
500	Mont K-10	7	0.25*10 ⁷	41.73%
500	Mont K-10	8	0.5*10 ⁷	0.00%
500	Mont K-10	9	1*10 ⁷	21.96%

Particle Ratio	Clay	Sample No.	<i>E. coli</i> Concentration (CFU ml ⁻¹)	Percent attached
1000	Hectorite	1	0.25*10 ⁷	64.77%
1000	Hectorite	2	0.5*10 ⁷	91.30%
1000	Hectorite	3	1*10 ⁷	92.33%
1000	Hectorite	4	0.25*10 ⁷	71.43%
1000	Hectorite	5	0.5*10 ⁷	91.60%
1000	Hectorite	6	1*10 ⁷	90.48%
1000	Hectorite	7	0.25*10 ⁷	87.30%
1000	Hectorite	8	0.5*10 ⁷	94.85%
1000	Hectorite	9	1*10 ⁷	97.03%
1000	Kaolin	1	0.25*10 ⁷	77.05%
1000	Kaolin	2	0.5*10 ⁷	89.16%
1000	Kaolin	3	1*10 ⁷	90.61%
1000	Kaolin	4	0.25*10 ⁷	91.67%
1000	Kaolin	5	0.5*10 ⁷	88.96%
1000	Kaolin	6	1*10 ⁷	95.79%
1000	Kaolin	7	0.25*10 ⁷	76.47%
1000	Kaolin	8	0.5*10 ⁷	90.53%
1000	Kaolin	9	1*10 ⁷	87.50%
1000	Ca-Mont	1	0.25*10 ⁷	18.64%
1000	Ca-Mont	2	0.5*10 ⁷	26.76%
1000	Ca-Mont	3	1*10 ⁷	48.26%
1000	Ca-Mont	4	0.25*10 ⁷	8.33%
1000	Ca-Mont	5	0.5*10 ⁷	13.70%
1000	Ca-Mont	6	1*10 ⁷	31.75%
1000	Ca-Mont	7	0.25*10 ⁷	20.69%
1000	Ca-Mont	8	0.5*10 ⁷	26.51%
1000	Ca-Mont	9	1*10 ⁷	35.14%
1000	Mont K-10	1	0.25*10 ⁷	26.58%
1000	Mont K-10	2	0.5*10 ⁷	27.20%
1000	Mont K-10	3	1*10 ⁷	16.33%
1000	Mont K-10	4	0.25*10 ⁷	5.75%
1000	Mont K-10	5	0.5*10 ⁷	11.22%
1000	Mont K-10	6	1*10 ⁷	15.17%
1000	Mont K-10	7	0.25*10 ⁷	8.33%
1000	Mont K-10	8	0.5*10 ⁷	10.23%
1000	Mont K-10	9	1*10 ⁷	19.62%

APPENDIX C4. Percent attached of strain #43888 in the settling method

Particle Ratio	Clay	Sample No.	<i>E. coli</i> Concentration (CFU ml ⁻¹)	Percent attached
1	Hectorite	1	0.25*10 ⁷	3.28%
1	Hectorite	2	0.5*10 ⁷	27.65%
1	Hectorite	3	1*10 ⁷	27.62%
1	Hectorite	4	0.25*10 ⁷	28.38%
1	Hectorite	5	0.5*10 ⁷	5.15%
1	Hectorite	6	1*10 ⁷	29.10%
1	Hectorite	7	0.25*10 ⁷	14.67%
1	Hectorite	8	0.5*10 ⁷	23.19%
1	Hectorite	9	1*10 ⁷	33.56%
1	Kaolin	1	0.25*10 ⁷	0.00%
1	Kaolin	2	0.5*10 ⁷	21.89%
1	Kaolin	3	1*10 ⁷	36.86%
1	Kaolin	4	0.25*10 ⁷	0.00%
1	Kaolin	5	0.5*10 ⁷	8.48%
1	Kaolin	6	1*10 ⁷	9.69%
1	Kaolin	7	0.25*10 ⁷	0.00%
1	Kaolin	8	0.5*10 ⁷	3.07%
1	Kaolin	9	1*10 ⁷	28.35%
1	Ca-Mont	1	0.25*10 ⁷	0.00%
1	Ca-Mont	2	0.5*10 ⁷	24.76%
1	Ca-Mont	3	1*10 ⁷	37.25%
1	Ca-Mont	4	0.25*10 ⁷	87.34%
1	Ca-Mont	5	0.5*10 ⁷	30.44%
1	Ca-Mont	6	1*10 ⁷	25.08%
1	Ca-Mont	7	0.25*10 ⁷	35.00%
1	Ca-Mont	8	0.5*10 ⁷	21.51%
1	Ca-Mont	9	1*10 ⁷	15.90%
1	Mont K-10	1	0.25*10 ⁷	26.00%
1	Mont K-10	2	0.5*10 ⁷	58.79%
1	Mont K-10	3	1*10 ⁷	24.23%
1	Mont K-10	4	0.25*10 ⁷	24.00%
1	Mont K-10	5	0.5*10 ⁷	18.18%
1	Mont K-10	6	1*10 ⁷	34.33%
1	Mont K-10	7	0.25*10 ⁷	
1	Mont K-10	8	0.5*10 ⁷	29.95%
1	Mont K-10	9	1*10 ⁷	15.60%

Particle Ratio	Clay	Sample No.	<i>E. coli</i> Concentration (CFU ml ⁻¹)	Percent attached
2	Hectorite	1	0.25*10 ⁷	0.00%
2	Hectorite	2	0.5*10 ⁷	75.76%
2	Hectorite	3	1*10 ⁷	40.44%
2	Hectorite	4	0.25*10 ⁷	45.45%
2	Hectorite	5	0.5*10 ⁷	55.22%
2	Hectorite	6	1*10 ⁷	63.00%
2	Hectorite	7	0.25*10 ⁷	88.24%
2	Hectorite	8	0.5*10 ⁷	14.29%
2	Hectorite	9	1*10 ⁷	39.52%
2	Kaolin	1	0.25*10 ⁷	21.74%
2	Kaolin	2	0.5*10 ⁷	14.84%
2	Kaolin	3	1*10 ⁷	26.97%
2	Kaolin	4	0.25*10 ⁷	0.00%
2	Kaolin	5	0.5*10 ⁷	51.52%
2	Kaolin	6	1*10 ⁷	35.18%
2	Kaolin	7	0.25*10 ⁷	66.67%
2	Kaolin	8	0.5*10 ⁷	24.41%
2	Kaolin	9	1*10 ⁷	0.00%
2	Ca-Mont	1	0.25*10 ⁷	0.00%
2	Ca-Mont	2	0.5*10 ⁷	16.67%
2	Ca-Mont	3	1*10 ⁷	2.86%
2	Ca-Mont	4	0.25*10 ⁷	0.00%
2	Ca-Mont	5	0.5*10 ⁷	18.52%
2	Ca-Mont	6	1*10 ⁷	0.00%
2	Ca-Mont	7	0.25*10 ⁷	33.33%
2	Ca-Mont	8	0.5*10 ⁷	0.00%
2	Ca-Mont	9	1*10 ⁷	36.36%
2	Mont K-10	1	0.25*10 ⁷	17.76%
2	Mont K-10	2	0.5*10 ⁷	20.63%
2	Mont K-10	3	1*10 ⁷	15.73%
2	Mont K-10	4	0.25*10 ⁷	29.90%
2	Mont K-10	5	0.5*10 ⁷	4.17%
2	Mont K-10	6	1*10 ⁷	8.06%
2	Mont K-10	7	0.25*10 ⁷	1.23%
2	Mont K-10	8	0.5*10 ⁷	9.80%
2	Mont K-10	9	1*10 ⁷	21.39%

Particle Ratio	Clay	Sample No.	<i>E. coli</i> Concentration (CFU ml ⁻¹)	Percent attached
50	Hectorite	1	0.25*10 ⁷	50.00%
50	Hectorite	2	0.5*10 ⁷	26.83%
50	Hectorite	3	1*10 ⁷	39.27%
50	Hectorite	4	0.25*10 ⁷	75.34%
50	Hectorite	5	0.5*10 ⁷	46.10%
50	Hectorite	6	1*10 ⁷	43.46%
50	Hectorite	7	0.25*10 ⁷	33.33%
50	Hectorite	8	0.5*10 ⁷	29.03%
50	Hectorite	9	1*10 ⁷	36.51%
50	Kaolin	1	0.25*10 ⁷	33.33%
50	Kaolin	2	0.5*10 ⁷	16.67%
50	Kaolin	3	1*10 ⁷	73.33%
50	Kaolin	4	0.25*10 ⁷	0.00%
50	Kaolin	5	0.5*10 ⁷	41.18%
50	Kaolin	6	1*10 ⁷	0.00%
50	Kaolin	7	0.25*10 ⁷	63.64%
50	Kaolin	8	0.5*10 ⁷	0.00%
50	Kaolin	9	1*10 ⁷	70.00%
50	Ca-Mont	1	0.25*10 ⁷	0.00%
50	Ca-Mont	2	0.5*10 ⁷	13.04%
50	Ca-Mont	3	1*10 ⁷	34.00%
50	Ca-Mont	4	0.25*10 ⁷	0.00%
50	Ca-Mont	5	0.5*10 ⁷	30.91%
50	Ca-Mont	6	1*10 ⁷	29.69%
50	Ca-Mont	7	0.25*10 ⁷	4.76%
50	Ca-Mont	8	0.5*10 ⁷	30.91%
50	Ca-Mont	9	1*10 ⁷	39.62%
50	Mont K-10	1	0.25*10 ⁷	20.00%
50	Mont K-10	2	0.5*10 ⁷	0.00%
50	Mont K-10	3	1*10 ⁷	0.00%
50	Mont K-10	4	0.25*10 ⁷	0.00%
50	Mont K-10	5	0.5*10 ⁷	0.00%
50	Mont K-10	6	1*10 ⁷	21.43%
50	Mont K-10	7	0.25*10 ⁷	11.11%
50	Mont K-10	8	0.5*10 ⁷	0.00%
50	Mont K-10	9	1*10 ⁷	14.29%

Particle Ratio	Clay	Sample No.	<i>E. coli</i> Concentration (CFU ml ⁻¹)	Percent attached
100	Hectorite	1	0.25*10 ⁷	0.00%
100	Hectorite	2	0.5*10 ⁷	19.61%
100	Hectorite	3	1*10 ⁷	37.97%
100	Hectorite	4	0.25*10 ⁷	100.00%
100	Hectorite	5	0.5*10 ⁷	24.80%
100	Hectorite	6	1*10 ⁷	29.23%
100	Hectorite	7	0.25*10 ⁷	88.89%
100	Hectorite	8	0.5*10 ⁷	17.72%
100	Hectorite	9	1*10 ⁷	17.28%
100	Kaolin	1	0.25*10 ⁷	41.82%
100	Kaolin	2	0.5*10 ⁷	29.45%
100	Kaolin	3	1*10 ⁷	0.00%
100	Kaolin	4	0.25*10 ⁷	22.42%
100	Kaolin	5	0.5*10 ⁷	22.78%
100	Kaolin	6	1*10 ⁷	5.38%
100	Kaolin	7	0.25*10 ⁷	21.84%
100	Kaolin	8	0.5*10 ⁷	8.16%
100	Kaolin	9	1*10 ⁷	37.85%
100	Ca-Mont	1	0.25*10 ⁷	0.00%
100	Ca-Mont	2	0.5*10 ⁷	50.00%
100	Ca-Mont	3	1*10 ⁷	61.70%
100	Ca-Mont	4	0.25*10 ⁷	0.00%
100	Ca-Mont	5	0.5*10 ⁷	88.24%
100	Ca-Mont	6	1*10 ⁷	55.56%
100	Ca-Mont	7	0.25*10 ⁷	100.00%
100	Ca-Mont	8	0.5*10 ⁷	62.50%
100	Ca-Mont	9	1*10 ⁷	58.62%
100	Mont K-10	1	0.25*10 ⁷	35.59%
100	Mont K-10	2	0.5*10 ⁷	19.84%
100	Mont K-10	3	1*10 ⁷	0.00%
100	Mont K-10	4	0.25*10 ⁷	22.33%
100	Mont K-10	5	0.5*10 ⁷	13.48%
100	Mont K-10	6	1*10 ⁷	16.51%
100	Mont K-10	7	0.25*10 ⁷	0.00%
100	Mont K-10	8	0.5*10 ⁷	17.95%
100	Mont K-10	9	1*10 ⁷	6.89%

Particle Ratio	Clay	Sample No.	<i>E. coli</i> Concentration (CFU ml ⁻¹)	Percent attached
200	Hectorite	1	0.25*10 ⁷	50.00%
200	Hectorite	2	0.5*10 ⁷	49.02%
200	Hectorite	3	1*10 ⁷	68.63%
200	Hectorite	4	0.25*10 ⁷	25.00%
200	Hectorite	5	0.5*10 ⁷	60.78%
200	Hectorite	6	1*10 ⁷	62.86%
200	Hectorite	7	0.25*10 ⁷	36.00%
200	Hectorite	8	0.5*10 ⁷	57.38%
200	Hectorite	9	1*10 ⁷	56.10%
200	Kaolin	1	0.25*10 ⁷	58.68%
200	Kaolin	2	0.5*10 ⁷	47.45%
200	Kaolin	3	1*10 ⁷	0.00%
200	Kaolin	4	0.25*10 ⁷	38.33%
200	Kaolin	5	0.5*10 ⁷	40.08%
200	Kaolin	6	1*10 ⁷	27.49%
200	Kaolin	7	0.25*10 ⁷	34.92%
200	Kaolin	8	0.5*10 ⁷	49.54%
200	Kaolin	9	1*10 ⁷	22.29%
200	Ca-Mont	1	0.25*10 ⁷	0.00%
200	Ca-Mont	2	0.5*10 ⁷	0.00%
200	Ca-Mont	3	1*10 ⁷	8.33%
200	Ca-Mont	4	0.25*10 ⁷	0.00%
200	Ca-Mont	5	0.5*10 ⁷	25.00%
200	Ca-Mont	6	1*10 ⁷	17.65%
200	Ca-Mont	7	0.25*10 ⁷	100.00%
200	Ca-Mont	8	0.5*10 ⁷	25.00%
200	Ca-Mont	9	1*10 ⁷	37.50%
200	Mont K-10	1	0.25*10 ⁷	33.33%
200	Mont K-10	2	0.5*10 ⁷	20.00%
200	Mont K-10	3	1*10 ⁷	40.05%
200	Mont K-10	4	0.25*10 ⁷	0.00%
200	Mont K-10	5	0.5*10 ⁷	0.00%
200	Mont K-10	6	1*10 ⁷	30.93%
200	Mont K-10	7	0.25*10 ⁷	66.67%
200	Mont K-10	8	0.5*10 ⁷	27.27%
200	Mont K-10	9	1*10 ⁷	25.93%

Particle Ratio	Clay	Sample No.	<i>E. coli</i> Concentration (CFU ml ⁻¹)	Percent attached
500	Hectorite	1	0.25*10 ⁷	0.00%
500	Hectorite	2	0.5*10 ⁷	100.00%
500	Hectorite	3	1*10 ⁷	100.00%
500	Hectorite	4	0.25*10 ⁷	0.00%
500	Hectorite	5	0.5*10 ⁷	100.00%
500	Hectorite	6	1*10 ⁷	27.27%
500	Hectorite	7	0.25*10 ⁷	71.43%
500	Hectorite	8	0.5*10 ⁷	100.00%
500	Hectorite	9	1*10 ⁷	0.00%
500	Kaolin	1	0.25*10 ⁷	84.91%
500	Kaolin	2	0.5*10 ⁷	77.78%
500	Kaolin	3	1*10 ⁷	80.30%
500	Kaolin	4	0.25*10 ⁷	68.60%
500	Kaolin	5	0.5*10 ⁷	92.00%
500	Kaolin	6	1*10 ⁷	66.67%
500	Kaolin	7	0.25*10 ⁷	87.01%
500	Kaolin	8	0.5*10 ⁷	75.00%
500	Kaolin	9	1*10 ⁷	86.18%
500	Ca-Mont	1	0.25*10 ⁷	27.78%
500	Ca-Mont	2	0.5*10 ⁷	28.51%
500	Ca-Mont	3	1*10 ⁷	15.56%
500	Ca-Mont	4	0.25*10 ⁷	16.92%
500	Ca-Mont	5	0.5*10 ⁷	17.71%
500	Ca-Mont	6	1*10 ⁷	14.72%
500	Ca-Mont	7	0.25*10 ⁷	12.33%
500	Ca-Mont	8	0.5*10 ⁷	52.83%
500	Ca-Mont	9	1*10 ⁷	31.79%
500	Mont K-10	1	0.25*10 ⁷	41.41%
500	Mont K-10	2	0.5*10 ⁷	10.14%
500	Mont K-10	3	1*10 ⁷	18.02%
500	Mont K-10	4	0.25*10 ⁷	15.49%
500	Mont K-10	5	0.5*10 ⁷	28.89%
500	Mont K-10	6	1*10 ⁷	11.89%
500	Mont K-10	7	0.25*10 ⁷	0.00%
500	Mont K-10	8	0.5*10 ⁷	13.70%
500	Mont K-10	9	1*10 ⁷	3.73%

Particle Ratio	Clay	Sample No.	<i>E. coli</i> Concentration (CFU ml ⁻¹)	Percent attached
1000	Hectorite	1	0.25*10 ⁷	91.84%
1000	Hectorite	2	0.5*10 ⁷	97.44%
1000	Hectorite	3	1*10 ⁷	84.76%
1000	Hectorite	4	0.25*10 ⁷	96.15%
1000	Hectorite	5	0.5*10 ⁷	98.11%
1000	Hectorite	6	1*10 ⁷	91.87%
1000	Hectorite	7	0.25*10 ⁷	95.74%
1000	Hectorite	8	0.5*10 ⁷	92.59%
1000	Hectorite	9	1*10 ⁷	88.89%
1000	Kaolin	1	0.25*10 ⁷	60.00%
1000	Kaolin	2	0.5*10 ⁷	60.00%
1000	Kaolin	3	1*10 ⁷	52.14%
1000	Kaolin	4	0.25*10 ⁷	41.67%
1000	Kaolin	5	0.5*10 ⁷	47.27%
1000	Kaolin	6	1*10 ⁷	73.46%
1000	Kaolin	7	0.25*10 ⁷	56.76%
1000	Kaolin	8	0.5*10 ⁷	48.57%
1000	Kaolin	9	1*10 ⁷	50.98%
1000	Ca-Mont	1	0.25*10 ⁷	72.73%
1000	Ca-Mont	2	0.5*10 ⁷	71.83%
1000	Ca-Mont	3	1*10 ⁷	71.74%
1000	Ca-Mont	4	0.25*10 ⁷	58.73%
1000	Ca-Mont	5	0.5*10 ⁷	32.26%
1000	Ca-Mont	6	1*10 ⁷	51.15%
1000	Ca-Mont	7	0.25*10 ⁷	41.67%
1000	Ca-Mont	8	0.5*10 ⁷	75.00%
1000	Ca-Mont	9	1*10 ⁷	71.31%
1000	Mont K-10	1	0.25*10 ⁷	11.32%
1000	Mont K-10	2	0.5*10 ⁷	38.35%
1000	Mont K-10	3	1*10 ⁷	19.17%
1000	Mont K-10	4	0.25*10 ⁷	40.87%
1000	Mont K-10	5	0.5*10 ⁷	20.34%
1000	Mont K-10	6	1*10 ⁷	32.59%
1000	Mont K-10	7	0.25*10 ⁷	15.70%
1000	Mont K-10	8	0.5*10 ⁷	40.23%
1000	Mont K-10	9	1*10 ⁷	19.42%

APPENDIX C5. Percent attached of strain #31 in flow cytometry

Particle Ratio	Clay	Sample No.	Percent attached	Particle Ratio	Clay	Sample No.	Percent attached
1	Hectorite	1	0.60%	1	Kaolin	1	4.20%
1	Hectorite	2	0.60%	1	Kaolin	2	0.50%
1	Hectorite	3	0.60%	1	Kaolin	3	1.10%
2	Hectorite	1	0.80%	2	Kaolin	1	0.40%
2	Hectorite	2	0.60%	2	Kaolin	2	0.30%
2	Hectorite	3	0.70%	2	Kaolin	3	0.30%
5	Hectorite	1	1.10%	5	Kaolin	1	2.40%
5	Hectorite	2	1.00%	5	Kaolin	2	2.10%
5	Hectorite	3	2.00%	5	Kaolin	3	1.80%
10	Hectorite	1	1.70%	10	Kaolin	1	4.10%
10	Hectorite	2	2.30%	10	Kaolin	2	4.00%
10	Hectorite	3	1.90%	10	Kaolin	3	3.70%
25	Hectorite	1	4.70%	25	Kaolin	1	8.40%
25	Hectorite	2	4.80%	25	Kaolin	2	7.20%
25	Hectorite	3	5.00%	25	Kaolin	3	8.30%
50	Hectorite	1	12.80%	50	Kaolin	1	29.50%
50	Hectorite	2	13.30%	50	Kaolin	2	33.50%
50	Hectorite	3	12.60%	50	Kaolin	3	29.30%
100	Hectorite	1	23.40%	100	Kaolin	1	88.70%
100	Hectorite	2	27.00%	100	Kaolin	2	94.80%
100	Hectorite	3	22.20%	100	Kaolin	3	95.20%
150	Hectorite	1	12.60%	150	Kaolin	1	98.60%
150	Hectorite	2	10.30%	150	Kaolin	2	99.30%
150	Hectorite	3	11.20%	150	Kaolin	3	99.20%
200	Hectorite	1	9.30%	200	Kaolin	1	99.60%
200	Hectorite	2	9.00%	200	Kaolin	2	99.00%
200	Hectorite	3	11.90%	200	Kaolin	3	99.40%
300	Hectorite	1	8.60%	300	Kaolin	1	99.40%
300	Hectorite	2	3.30%	300	Kaolin	2	99.50%
300	Hectorite	3	8.90%	300	Kaolin	3	99.60%
400	Hectorite	1	6.30%	400	Kaolin	1	99.80%
400	Hectorite	2	4.70%	400	Kaolin	2	99.80%
400	Hectorite	3	7.60%	400	Kaolin	3	99.80%
500	Hectorite	1	5.30%	500	Kaolin	1	99.40%
500	Hectorite	2	8.60%	500	Kaolin	2	99.60%
500	Hectorite	3	9.60%	500	Kaolin	3	99.50%

Particle Ratio	Clay	Sample No.	Percent attached	Particle Ratio	Clay	Sample No.	Percent attached
1	Ca-Mont	1	0.70%	1	Mont K-10	1	0.50%
1	Ca-Mont	2	0.70%	1	Mont K-10	2	0.40%
1	Ca-Mont	3	0.70%	1	Mont K-10	3	0.50%
2	Ca-Mont	1	0.30%	2	Mont K-10	1	0.30%
2	Ca-Mont	2	0.50%	2	Mont K-10	2	0.50%
2	Ca-Mont	3	0.20%	2	Mont K-10	3	0.50%
5	Ca-Mont	1	3.90%	5	Mont K-10	1	0.60%
5	Ca-Mont	2	4.40%	5	Mont K-10	2	0.60%
5	Ca-Mont	3	3.60%	5	Mont K-10	3	0.60%
10	Ca-Mont	1	5.60%	10	Mont K-10	1	0.40%
10	Ca-Mont	2	6.20%	10	Mont K-10	2	1.00%
10	Ca-Mont	3	6.70%	10	Mont K-10	3	0.50%
25	Ca-Mont	1	15.80%	25	Mont K-10	1	1.50%
25	Ca-Mont	2	14.50%	25	Mont K-10	2	1.30%
25	Ca-Mont	3	16.50%	25	Mont K-10	3	1.40%
50	Ca-Mont	1	33.10%	50	Mont K-10	1	2.70%
50	Ca-Mont	2	30.00%	50	Mont K-10	2	3.20%
50	Ca-Mont	3	33.40%	50	Mont K-10	3	2.70%
100	Ca-Mont	1	59.50%	100	Mont K-10	1	5.60%
100	Ca-Mont	2	56.20%	100	Mont K-10	2	5.40%
100	Ca-Mont	3	28.50%	100	Mont K-10	3	5.30%
150	Ca-Mont	1	43.40%	150	Mont K-10	1	7.20%
150	Ca-Mont	2	52.40%	150	Mont K-10	2	7.80%
150	Ca-Mont	3	60.40%	150	Mont K-10	3	8.20%
200	Ca-Mont	1	68.60%	200	Mont K-10	1	10.70%
200	Ca-Mont	2	61.60%	200	Mont K-10	2	12.80%
200	Ca-Mont	3	65.60%	200	Mont K-10	3	11.20%
300	Ca-Mont	1	21.10%	300	Mont K-10	1	16.50%
300	Ca-Mont	2	14.40%	300	Mont K-10	2	16.70%
300	Ca-Mont	3	19.20%	300	Mont K-10	3	16.40%
400	Ca-Mont	1	14.10%	400	Mont K-10	1	20.00%
400	Ca-Mont	2	13.50%	400	Mont K-10	2	21.30%
400	Ca-Mont	3	14.40%	400	Mont K-10	3	20.70%
500	Ca-Mont	1	36.10%	500	Mont K-10	1	24.10%
500	Ca-Mont	2	21.40%	500	Mont K-10	2	24.10%
500	Ca-Mont	3	17.60%	500	Mont K-10	3	23.30%

APPENDIX C6. Percent attached of strain #50 in flow cytometry

Particle Ratio	Clay	Sample No.	Percent attached	Particle Ratio	Clay	Sample No.	Percent attached
1	Hectorite	1	1.30%	1	Kaolin	1	1.10%
1	Hectorite	2	1.50%	1	Kaolin	2	0.90%
1	Hectorite	3	1.30%	1	Kaolin	3	0.70%
2	Hectorite	1	1.60%	2	Kaolin	1	1.20%
2	Hectorite	2	1.70%	2	Kaolin	2	1.10%
2	Hectorite	3	2.00%	2	Kaolin	3	0.80%
5	Hectorite	1	2.40%	5	Kaolin	1	2.50%
5	Hectorite	2	2.40%	5	Kaolin	2	2.40%
5	Hectorite	3	2.20%	5	Kaolin	3	2.30%
10	Hectorite	1	4.30%	10	Kaolin	1	4.50%
10	Hectorite	2	4.00%	10	Kaolin	2	4.90%
10	Hectorite	3	4.20%	10	Kaolin	3	4.70%
25	Hectorite	1	7.00%	25	Kaolin	1	11.60%
25	Hectorite	2	7.70%	25	Kaolin	2	10.30%
25	Hectorite	3	7.70%	25	Kaolin	3	9.20%
50	Hectorite	1	16.80%	50	Kaolin	1	24.20%
50	Hectorite	2	15.90%	50	Kaolin	2	24.30%
50	Hectorite	3	12.10%	50	Kaolin	3	29.90%
100	Hectorite	1	10.50%	100	Kaolin	1	41.30%
100	Hectorite	2	16.40%	100	Kaolin	2	42.40%
100	Hectorite	3	15.50%	100	Kaolin	3	43.80%
150	Hectorite	1	18.30%	150	Kaolin	1	51.10%
150	Hectorite	2	14.40%	150	Kaolin	2	49.30%
150	Hectorite	3	13.00%	150	Kaolin	3	48.40%
200	Hectorite	1	14.20%	200	Kaolin	1	50.30%
200	Hectorite	2	16.70%	200	Kaolin	2	51.80%
200	Hectorite	3	13.20%	200	Kaolin	3	53.50%
300	Hectorite	1	26.00%	300	Kaolin	1	55.20%
300	Hectorite	2	27.70%	300	Kaolin	2	58.20%
300	Hectorite	3	25.40%	300	Kaolin	3	57.30%
400	Hectorite	1	31.20%	400	Kaolin	1	72.00%
400	Hectorite	2	21.90%	400	Kaolin	2	65.40%
400	Hectorite	3	43.10%	400	Kaolin	3	60.90%
500	Hectorite	1	38.20%	500	Kaolin	1	80.60%
500	Hectorite	2	26.60%	500	Kaolin	2	77.50%
500	Hectorite	3	25.40%	500	Kaolin	3	78.80%

Particle Ratio	Clay	Sample No.	Percent attached	Particle Ratio	Clay	Sample No.	Percent attached
1	Ca-Mont	1	0.40%	1	Mont K-10	1	2.00%
1	Ca-Mont	2	0.50%	1	Mont K-10	2	1.50%
1	Ca-Mont	3	0.30%	1	Mont K-10	3	1.50%
2	Ca-Mont	1	0.20%	2	Mont K-10	1	1.50%
2	Ca-Mont	2	0.40%	2	Mont K-10	2	1.60%
2	Ca-Mont	3	0.30%	2	Mont K-10	3	1.60%
5	Ca-Mont	1	0.50%	5	Mont K-10	1	1.30%
5	Ca-Mont	2	0.40%	5	Mont K-10	2	1.30%
5	Ca-Mont	3	0.40%	5	Mont K-10	3	1.30%
10	Ca-Mont	1	0.80%	10	Mont K-10	1	1.40%
10	Ca-Mont	2	0.80%	10	Mont K-10	2	1.30%
10	Ca-Mont	3	0.80%	10	Mont K-10	3	0.90%
25	Ca-Mont	1	1.80%	25	Mont K-10	1	1.70%
25	Ca-Mont	2	1.70%	25	Mont K-10	2	1.50%
25	Ca-Mont	3	1.70%	25	Mont K-10	3	1.50%
50	Ca-Mont	1	2.50%	50	Mont K-10	1	2.20%
50	Ca-Mont	2	2.70%	50	Mont K-10	2	2.20%
50	Ca-Mont	3	3.90%	50	Mont K-10	3	2.40%
100	Ca-Mont	1	5.60%	100	Mont K-10	1	3.30%
100	Ca-Mont	2	5.10%	100	Mont K-10	2	3.20%
100	Ca-Mont	3	4.70%	100	Mont K-10	3	3.50%
150	Ca-Mont	1	8.00%	150	Mont K-10	1	4.20%
150	Ca-Mont	2	6.10%	150	Mont K-10	2	4.50%
150	Ca-Mont	3	6.50%	150	Mont K-10	3	4.70%
200	Ca-Mont	1	8.70%	200	Mont K-10	1	7.00%
200	Ca-Mont	2	8.40%	200	Mont K-10	2	6.30%
200	Ca-Mont	3	7.40%	200	Mont K-10	3	6.70%
300	Ca-Mont	1	10.50%	300	Mont K-10	1	10.30%
300	Ca-Mont	2	11.30%	300	Mont K-10	2	9.60%
300	Ca-Mont	3	10.00%	300	Mont K-10	3	10.00%
400	Ca-Mont	1	13.80%	400	Mont K-10	1	13.60%
400	Ca-Mont	2	13.20%	400	Mont K-10	2	12.70%
400	Ca-Mont	3	14.10%	400	Mont K-10	3	11.90%
500	Ca-Mont	1	16.60%	500	Mont K-10	1	13.70%
500	Ca-Mont	2	16.40%	500	Mont K-10	2	14.70%
500	Ca-Mont	3	15.30%	500	Mont K-10	3	13.50%

APPENDIX C7. Percent attached of strain #89 in flow cytometry

Particle Ratio	Clay	Sample No.	Percent attached	Particle Ratio	Clay	Sample No.	Percent attached
1	Hectorite	1	0.20%	1	Kaolin	1	0.30%
1	Hectorite	2	0.20%	1	Kaolin	2	0.60%
1	Hectorite	3	0.30%	1	Kaolin	3	0.30%
2	Hectorite	1	0.20%	2	Kaolin	1	0.70%
2	Hectorite	2	0.20%	2	Kaolin	2	0.60%
2	Hectorite	3	0.30%	2	Kaolin	3	0.80%
5	Hectorite	1	0.40%	5	Kaolin	1	1.30%
5	Hectorite	2	0.40%	5	Kaolin	2	1.30%
5	Hectorite	3	0.30%	5	Kaolin	3	1.10%
10	Hectorite	1	0.80%	10	Kaolin	1	2.90%
10	Hectorite	2	1.00%	10	Kaolin	2	3.20%
10	Hectorite	3	1.00%	10	Kaolin	3	2.80%
25	Hectorite	1	2.40%	25	Kaolin	1	8.20%
25	Hectorite	2	1.30%	25	Kaolin	2	7.90%
25	Hectorite	3	1.80%	25	Kaolin	3	7.70%
50	Hectorite	1	3.70%	50	Kaolin	1	12.70%
50	Hectorite	2	2.80%	50	Kaolin	2	13.10%
50	Hectorite	3	3.10%	50	Kaolin	3	12.60%
100	Hectorite	1	8.50%	100	Kaolin	1	22.90%
100	Hectorite	2	8.10%	100	Kaolin	2	23.20%
100	Hectorite	3	7.30%	100	Kaolin	3	23.10%
150	Hectorite	1	8.70%	150	Kaolin	1	26.80%
150	Hectorite	2	9.40%	150	Kaolin	2	28.10%
150	Hectorite	3	11.20%	150	Kaolin	3	28.70%
200	Hectorite	1	8.70%	200	Kaolin	1	39.10%
200	Hectorite	2	9.70%	200	Kaolin	2	41.20%
200	Hectorite	3	9.30%	200	Kaolin	3	48.30%
300	Hectorite	1	10.90%	300	Kaolin	1	57.90%
300	Hectorite	2	9.80%	300	Kaolin	2	63.70%
300	Hectorite	3	10.40%	300	Kaolin	3	58.40%
400	Hectorite	1	22.20%	400	Kaolin	1	87.00%
400	Hectorite	2	22.20%	400	Kaolin	2	86.10%
400	Hectorite	3	15.90%	400	Kaolin	3	87.30%
500	Hectorite	1	27.40%	500	Kaolin	1	92.70%
500	Hectorite	2	28.20%	500	Kaolin	2	92.60%
500	Hectorite	3	27.30%	500	Kaolin	3	92.30%

Particle Ratio	Clay	Sample No.	Percent attached	Particle Ratio	Clay	Sample No.	Percent attached
1	Ca-Mont	1	0.30%	1	Mont K-10	1	0.40%
1	Ca-Mont	2	0.30%	1	Mont K-10	2	0.30%
1	Ca-Mont	3	0.30%	1	Mont K-10	3	0.30%
2	Ca-Mont	1	0.30%	2	Mont K-10	1	0.40%
2	Ca-Mont	2	0.30%	2	Mont K-10	2	0.40%
2	Ca-Mont	3	0.30%	2	Mont K-10	3	0.30%
5	Ca-Mont	1	0.50%	5	Mont K-10	1	0.40%
5	Ca-Mont	2	0.40%	5	Mont K-10	2	0.30%
5	Ca-Mont	3	0.50%	5	Mont K-10	3	0.30%
10	Ca-Mont	1	0.60%	10	Mont K-10	1	0.40%
10	Ca-Mont	2	0.60%	10	Mont K-10	2	1.10%
10	Ca-Mont	3	0.30%	10	Mont K-10	3	0.50%
25	Ca-Mont	1	1.40%	25	Mont K-10	1	0.40%
25	Ca-Mont	2	1.40%	25	Mont K-10	2	0.30%
25	Ca-Mont	3	1.60%	25	Mont K-10	3	0.30%
50	Ca-Mont	1	2.80%	50	Mont K-10	1	0.60%
50	Ca-Mont	2	3.10%	50	Mont K-10	2	0.50%
50	Ca-Mont	3	2.90%	50	Mont K-10	3	0.50%
100	Ca-Mont	1	4.90%	100	Mont K-10	1	1.00%
100	Ca-Mont	2	4.10%	100	Mont K-10	2	0.90%
100	Ca-Mont	3	5.30%	100	Mont K-10	3	1.10%
150	Ca-Mont	1	3.60%	150	Mont K-10	1	1.80%
150	Ca-Mont	2	5.70%	150	Mont K-10	2	1.20%
150	Ca-Mont	3	5.20%	150	Mont K-10	3	1.20%
200	Ca-Mont	1	4.60%	200	Mont K-10	1	1.60%
200	Ca-Mont	2	4.60%	200	Mont K-10	2	1.60%
200	Ca-Mont	3	5.60%	200	Mont K-10	3	1.50%
300	Ca-Mont	1	8.00%	300	Mont K-10	1	2.30%
300	Ca-Mont	2	7.00%	300	Mont K-10	2	2.80%
300	Ca-Mont	3	6.90%	300	Mont K-10	3	2.70%
400	Ca-Mont	1	10.90%	400	Mont K-10	1	3.40%
400	Ca-Mont	2	7.70%	400	Mont K-10	2	3.40%
400	Ca-Mont	3	7.90%	400	Mont K-10	3	2.90%
500	Ca-Mont	1	7.40%	500	Mont K-10	1	3.50%
500	Ca-Mont	2	7.80%	500	Mont K-10	2	3.20%
500	Ca-Mont	3	7.00%	500	Mont K-10	3	3.70%

APPENDIX D. FLOW CYTOMETRY RESULT ANALYSIS FIGURES

Appendix D1. Strain #31

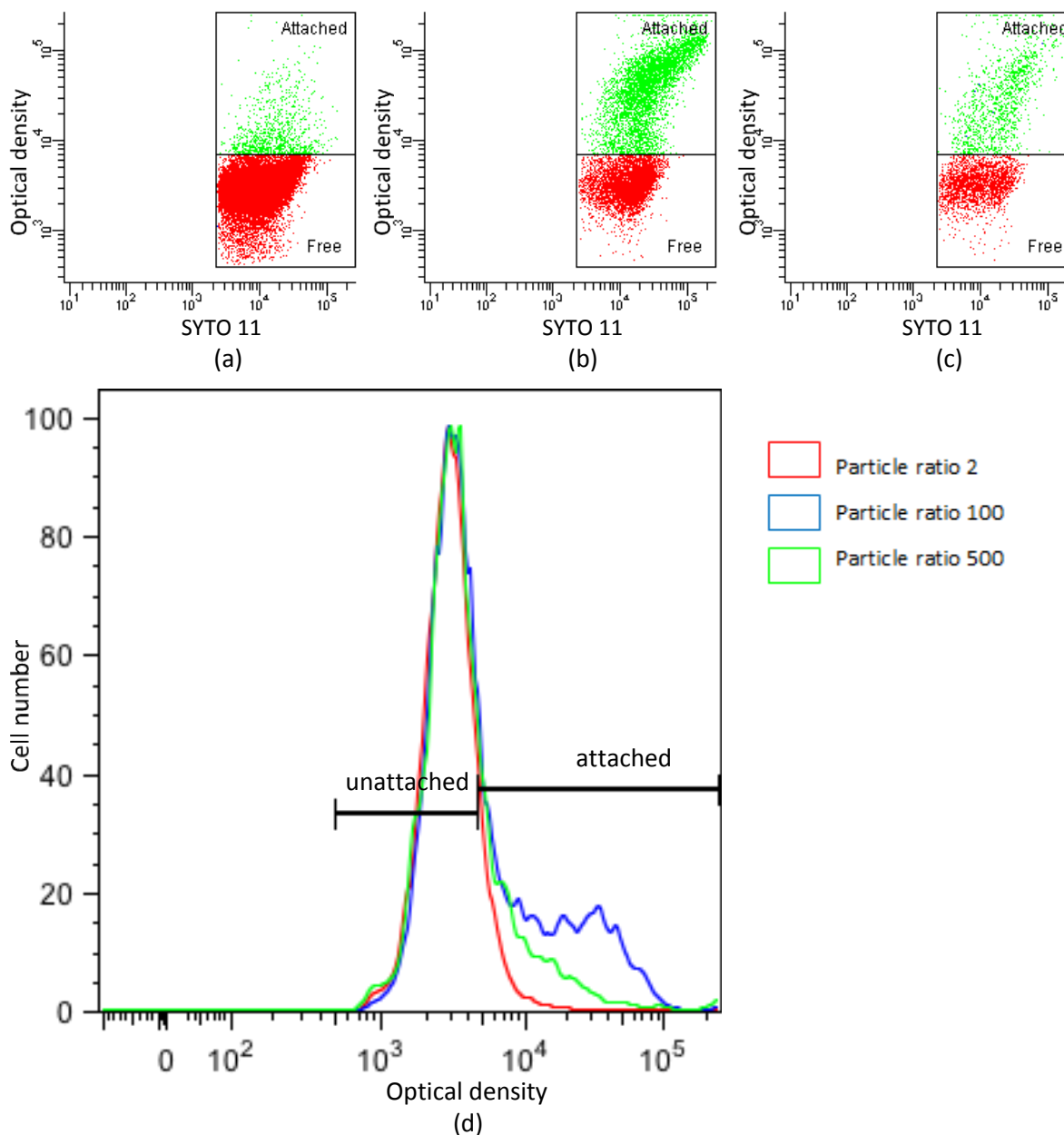


Figure D1-1. Strain #31 with Hectorite. (a) is the dot plot of particle ratio 2, (b) is of particle ratio 100 and (c) is of particle ratio 500. In (a), (b), and (c), each green dot shows one attached event while red dots show unattached events. (d) is the histogram with red, blue and green curve for particle ratio 2, 100 and 500, respectively. Gage limits were set and labeled.

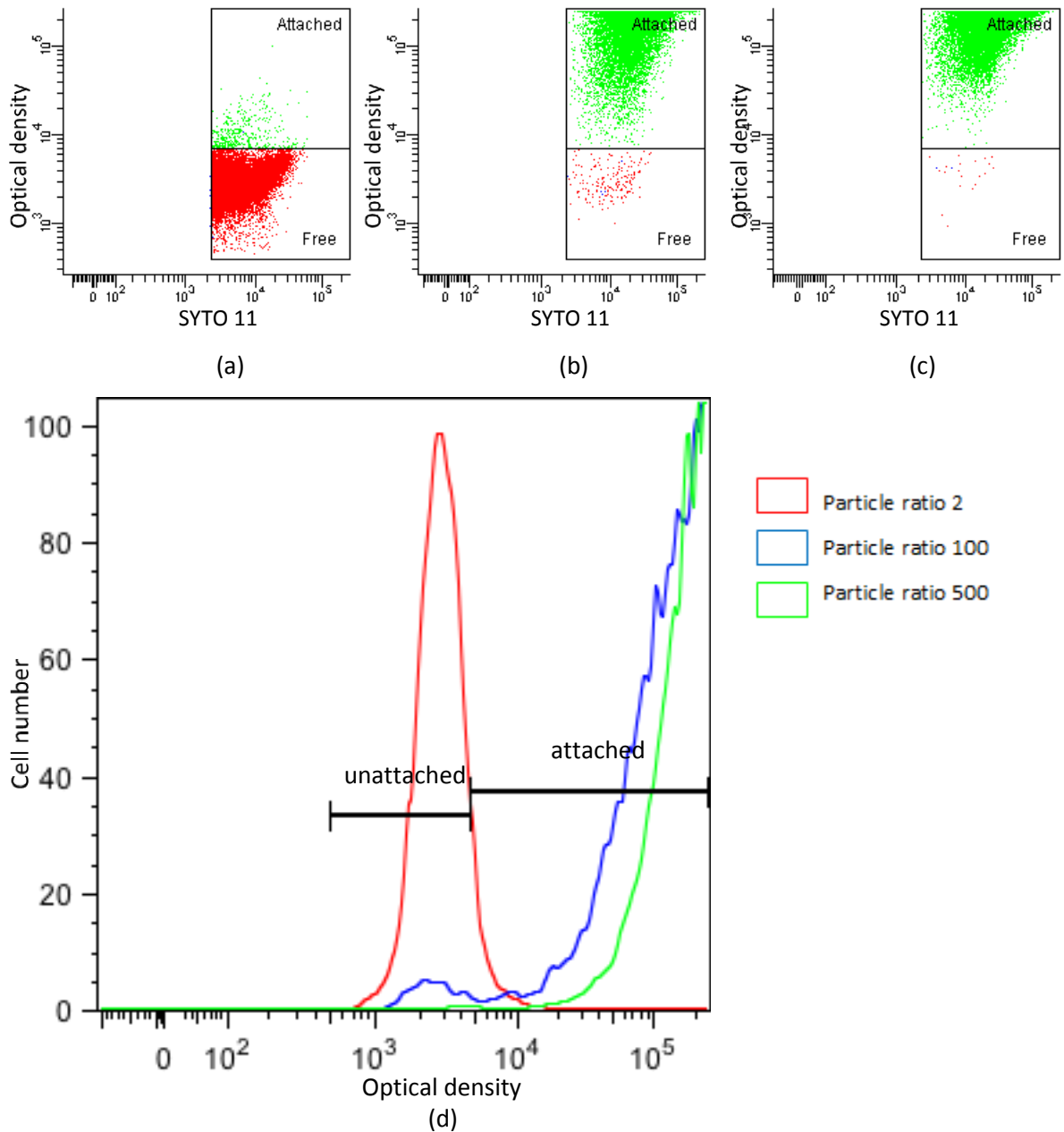


Figure D1-2. Strain #31 with Kaolin. (a) is the dot plot of particle ratio 2, (b) is of particle ratio 100 and (c) is of particle ratio 500. In (a), (b), and (c), each green dot shows one attached event while red dots show unattached events. (d) is the histogram with red, blue and green curve for particle ratio 2, 100 and 500, respectively. Gage limits were set and labeled.

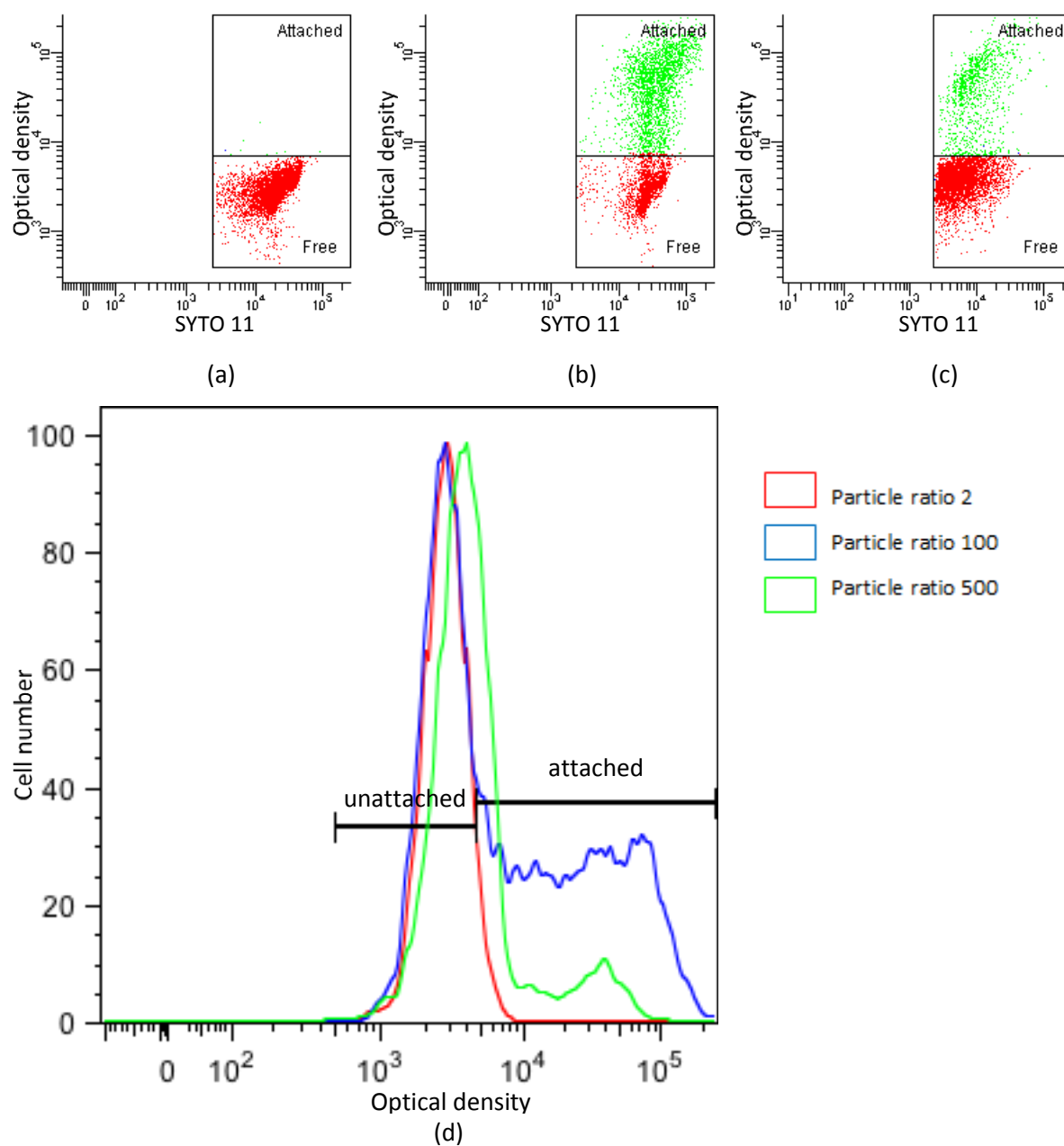


Figure D1-3. Strain #31 with Ca-Montmorillonite. (a) is the dot plot of particle ratio 2, (b) is of particle ratio 100 and (c) is of particle ratio 500. In (a), (b), and (c), each green dot shows one attached event while red dots show unattached events. (d) is the histogram with red, blue and green curve for particle ratio 2, 100 and 500, respectively. Gate limits were set and labeled.

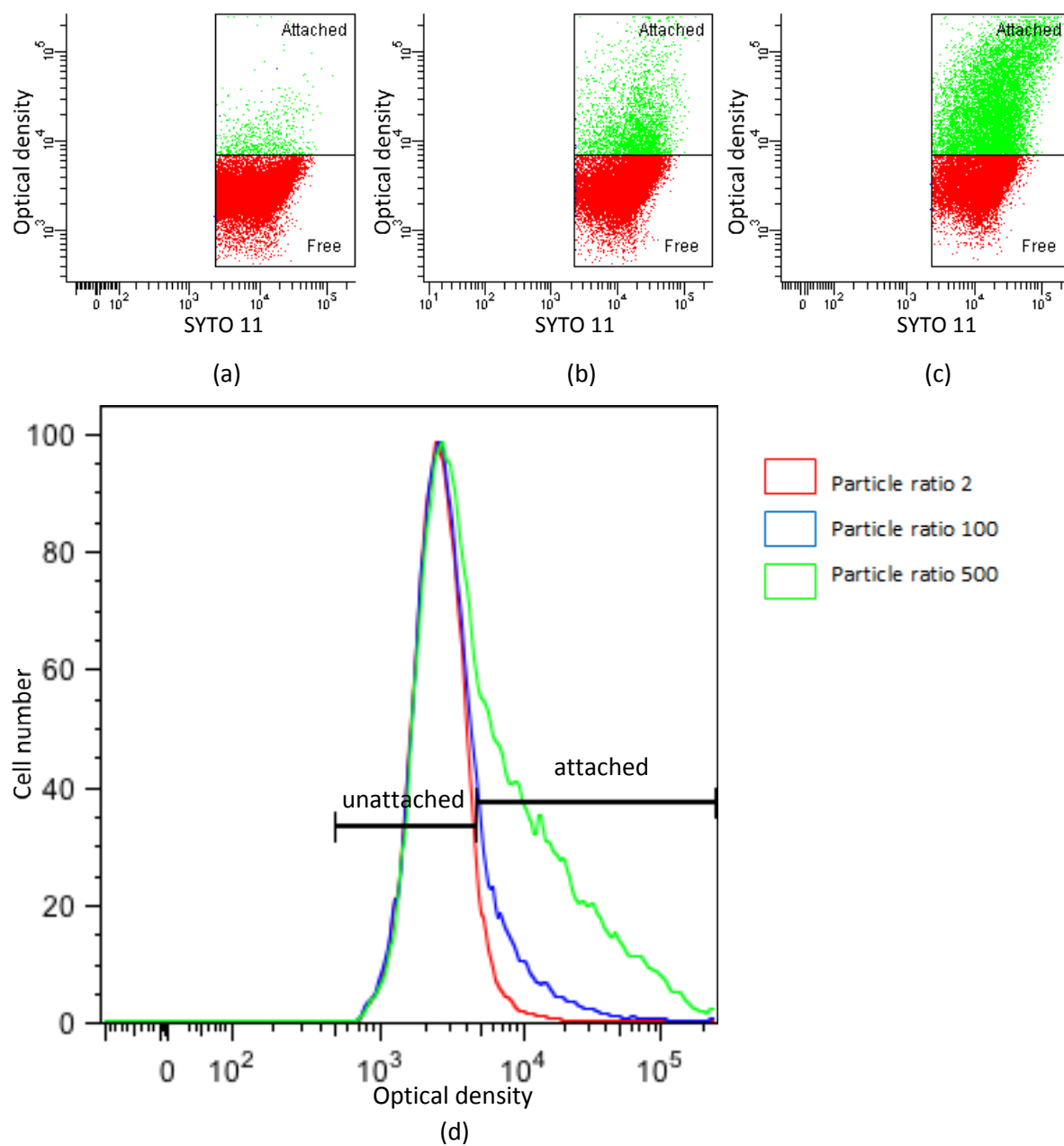


Figure D1-3. Strain #31 with Montmorillonite K-10. (a) is the dot plot of particle ratio 2, (b) is of partilce ratio 100 and (c) is of particle ratio 500. In (a), (b), and (c), each green dot shows one attached event while red dots show unattached events. (d) is the histogram with red, blue and green curve for particle ratio 2, 100 and 500, respectively. Gage limits were set and labeled.

Appendix D2. Strain #50

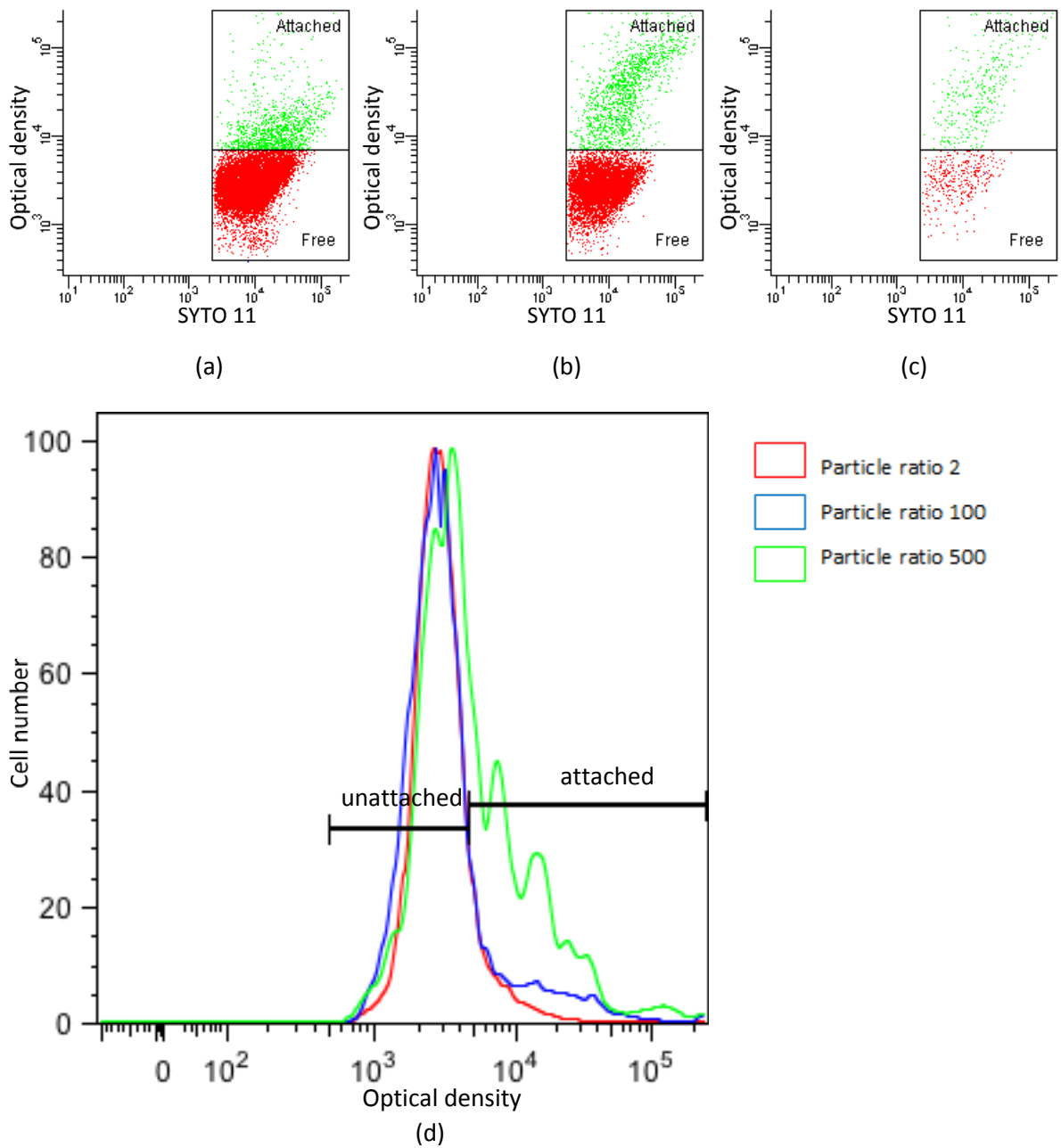


Figure D2-1. Strain #50 with Hectorite. (a) is the dot plot of particle ratio 2, (b) is of particle ratio 100 and (c) is of particle ratio 500. In (a), (b), and (c), each green dot shows one attached event while red dots show unattached events. (d) is the histogram with red, blue and green curve for particle ratio 2, 100 and 500, respectively. Gage limits were set and labeled.

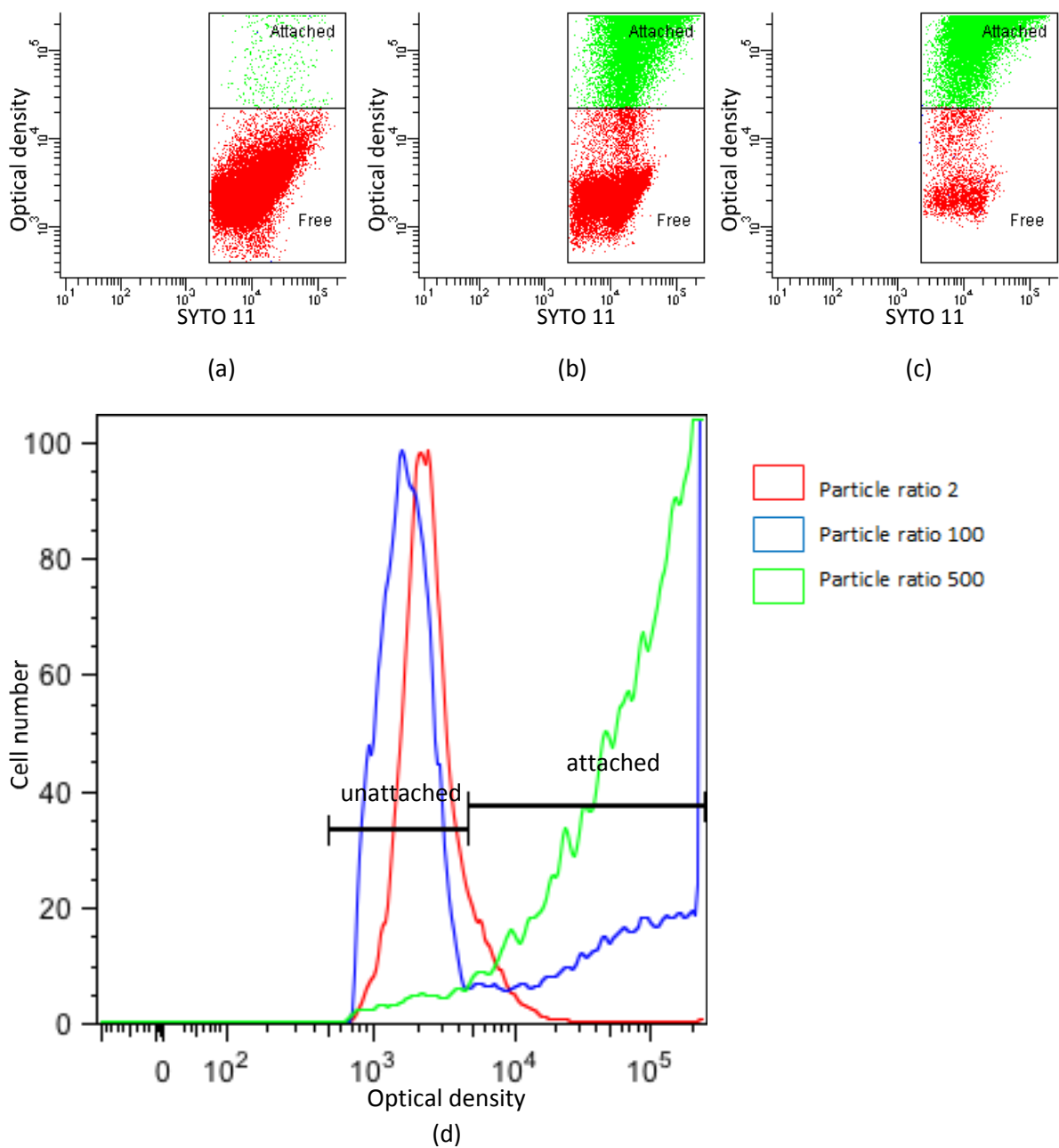


Figure D2-2. Strain #50 with Kaolin. (a) is the dot plot of particle ratio 2, (b) is of particle ratio 100 and (c) is of particle ratio 500. In (a), (b), and (c), each green dot shows one attached event while red dots show unattached events. (d) is the histogram with red, blue and green curve for particle ratio 2, 100 and 500, respectively. Gage limits were set and labeled.

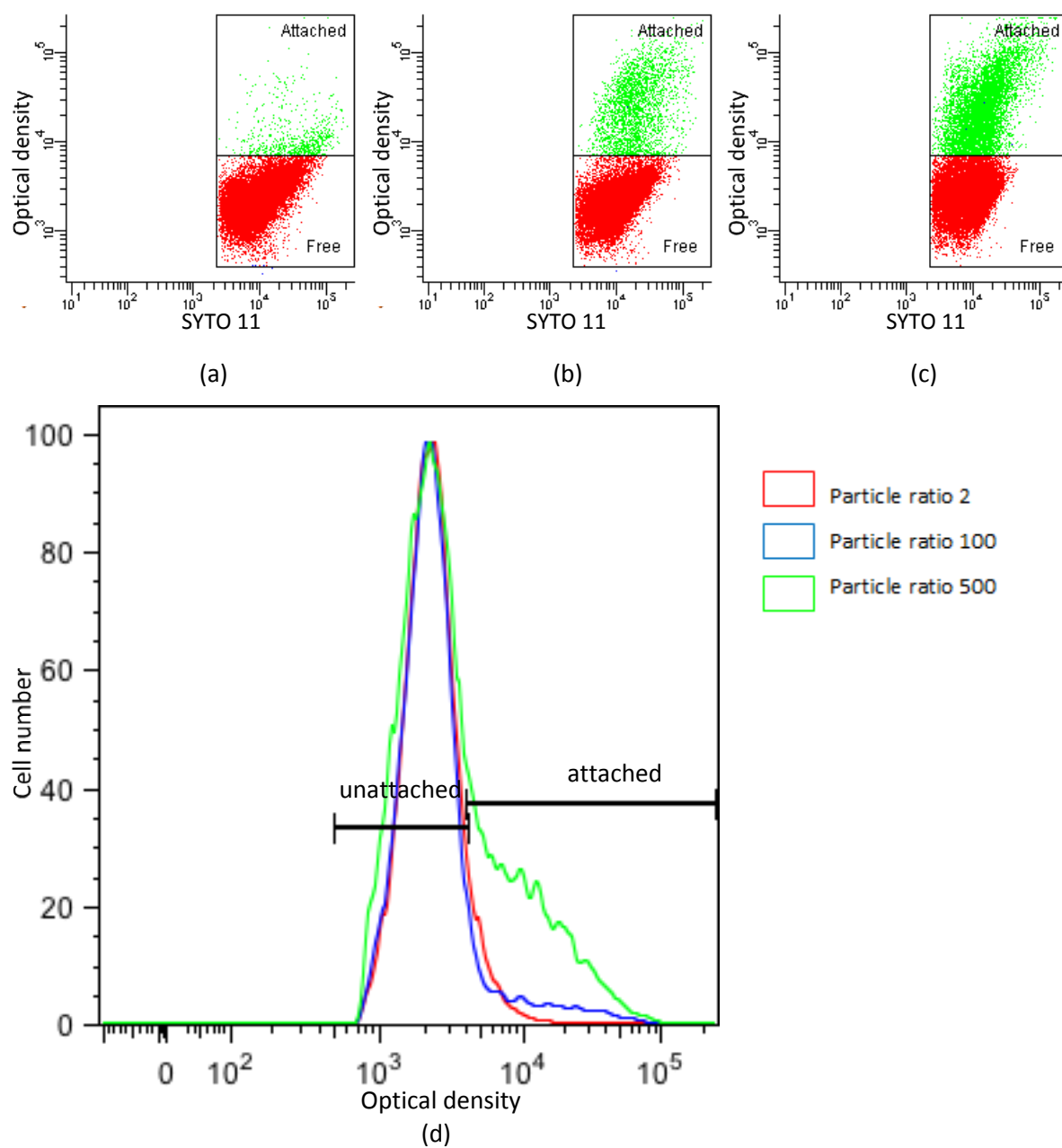


Figure D2-3. Strain #50 with Ca-Montmorillonite. (a) is the dot plot of particle ratio 2, (b) is of particle ratio 100 and (c) is of particle ratio 500. In (a), (b), and (c), each green dot shows one attached event while red dots show unattached events. (d) is the histogram with red, blue and green curve for particle ratio 2, 100 and 500, respectively. Gage limits were set and labeled.

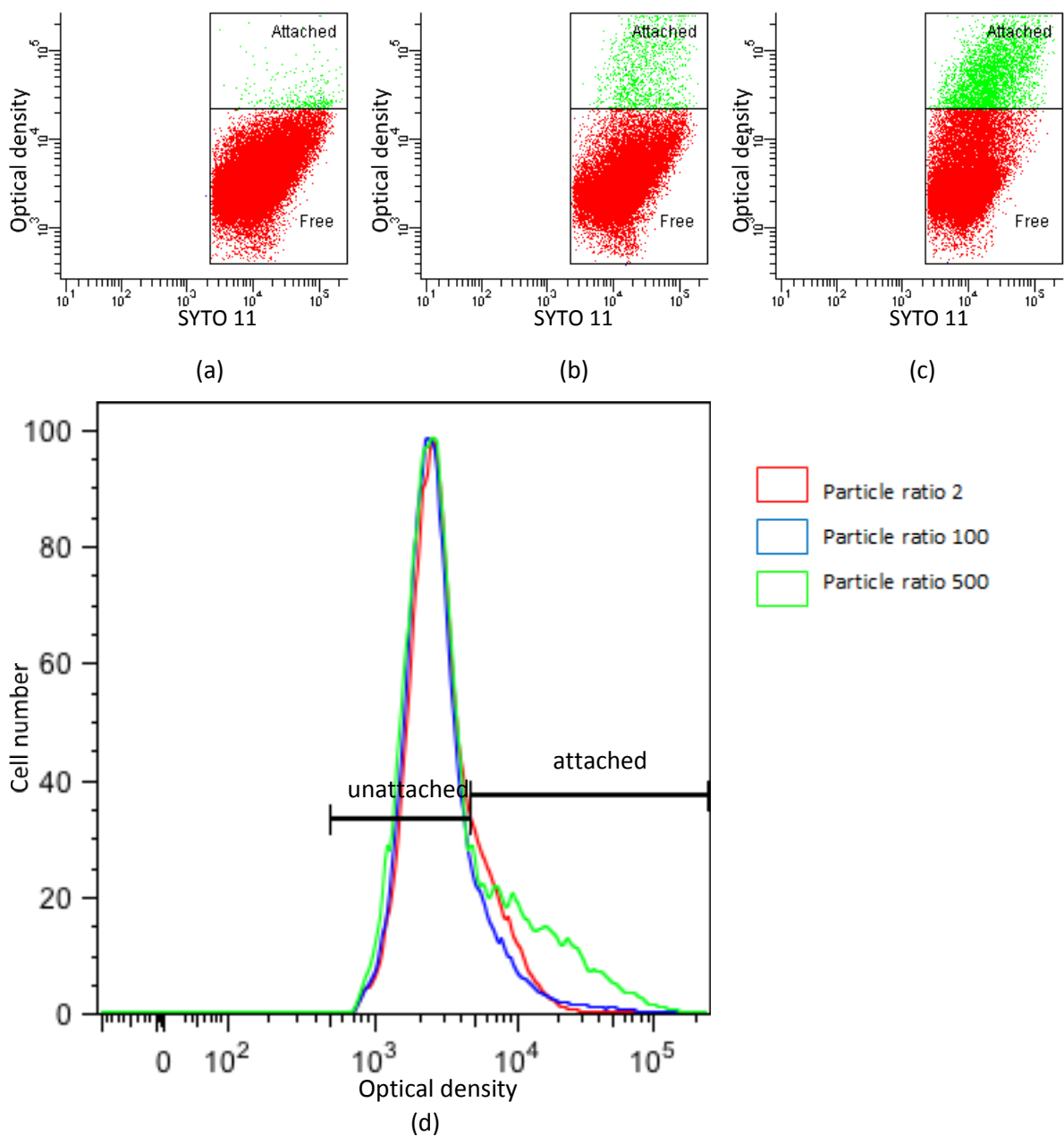


Figure D2-4. Strain #50 with Montmorillonite K-10. (a) is the dot plot of particle ratio 2, (b) is of particle ratio 100 and (c) is of particle ratio 500. In (a), (b), and (c), each green dot shows one attached event while red dots show unattached events. (d) is the histogram with red, blue and green curve for particle ratio 2, 100 and 500, respectively. Gage limits were set and labeled.

Appendix D3. Strain #89

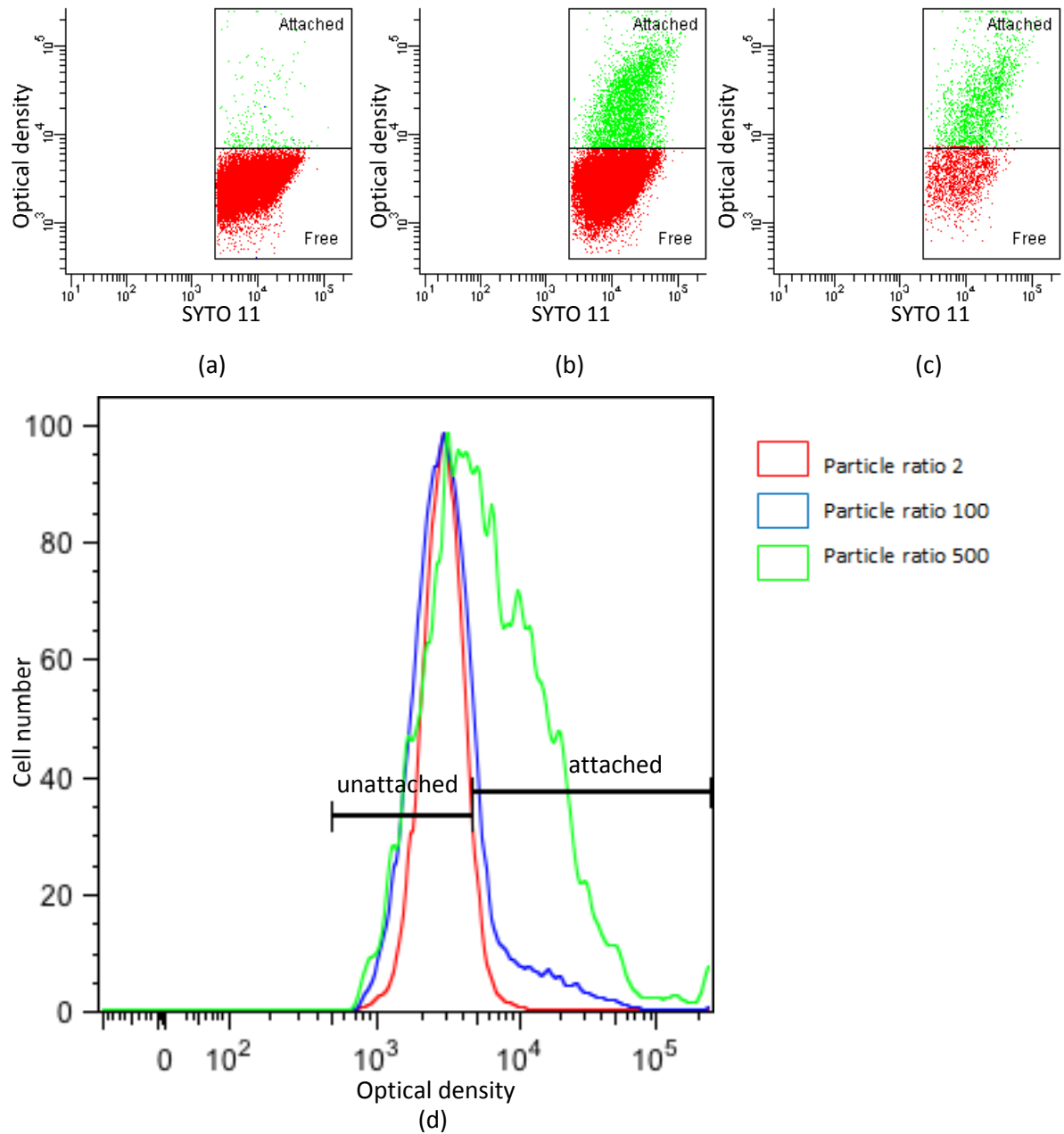


Figure D3-1. Strain #89 with Hectorite. (a) is the dot plot of particle ratio 2, (b) is of particle ratio 100 and (c) is of particle ratio 500. In (a), (b), and (c), each green dot shows one attached event while red dots show unattached events. (d) is the histogram with red, blue and green curve for particle ratio 2, 100 and 500, respectively. Gage limits were set and labeled.

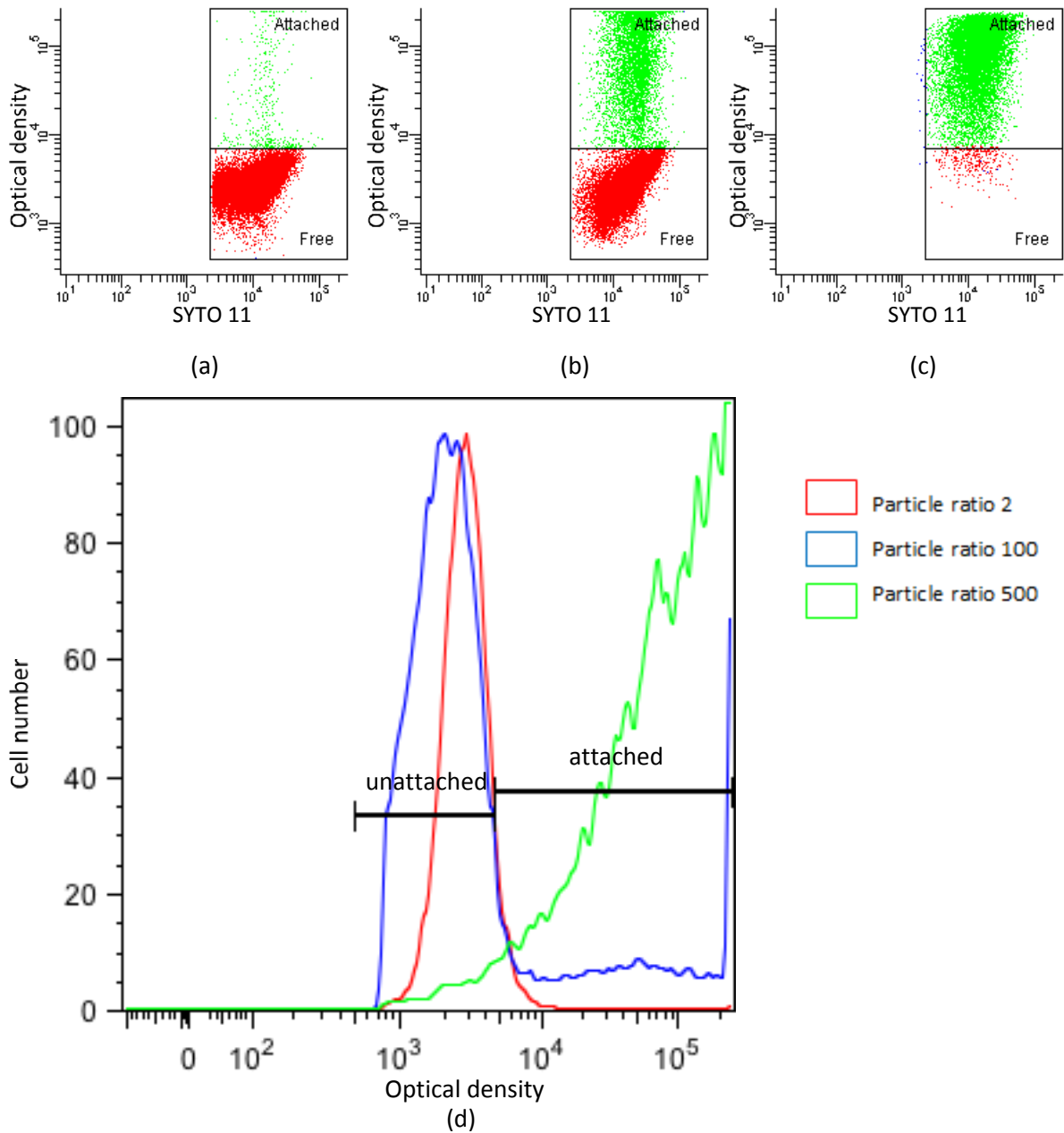


Figure D3-2. Strain #89 with Kaolin. (a) is the dot plot of particle ratio 2, (b) is of particle ratio 100 and (c) is of particle ratio 500. In (a), (b), and (c), each green dot shows one attached event while red dots show unattached events. (d) is the histogram with red, blue and green curve for particle ratio 2, 100 and 500, respectively. Gage limits were set and labeled.

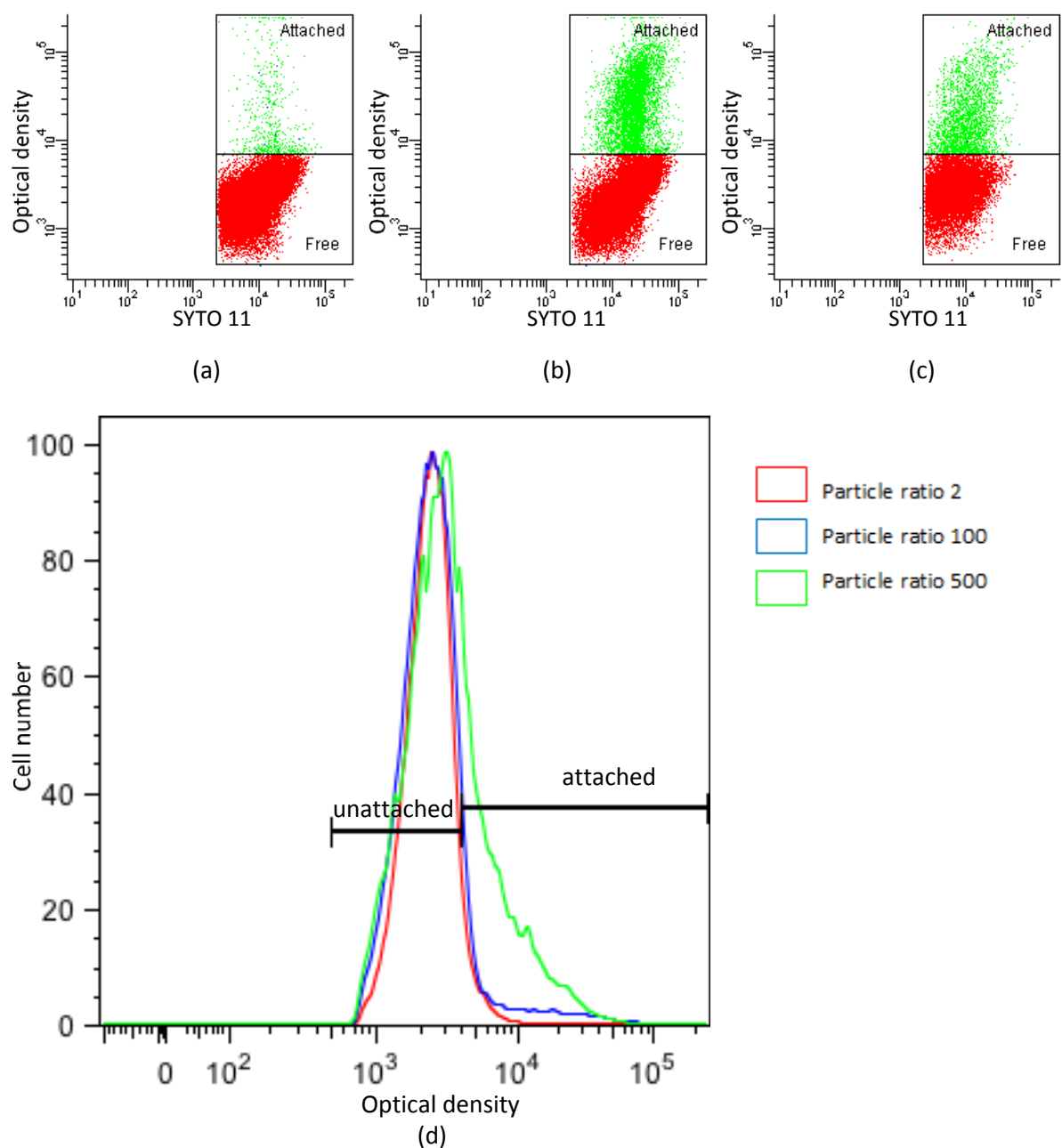


Figure D3-3. Strain #89 with Ca-Montmorillonite. (a) is the dot plot of particle ratio 2, (b) is of particle ratio 100 and (c) is of particle ratio 500. In (a), (b), and (c), each green dot shows one attached event while red dots show unattached events. (d) is the histogram with red, blue and green curve for particle ratio 2, 100 and 500, respectively. Gage limits were set and labeled.

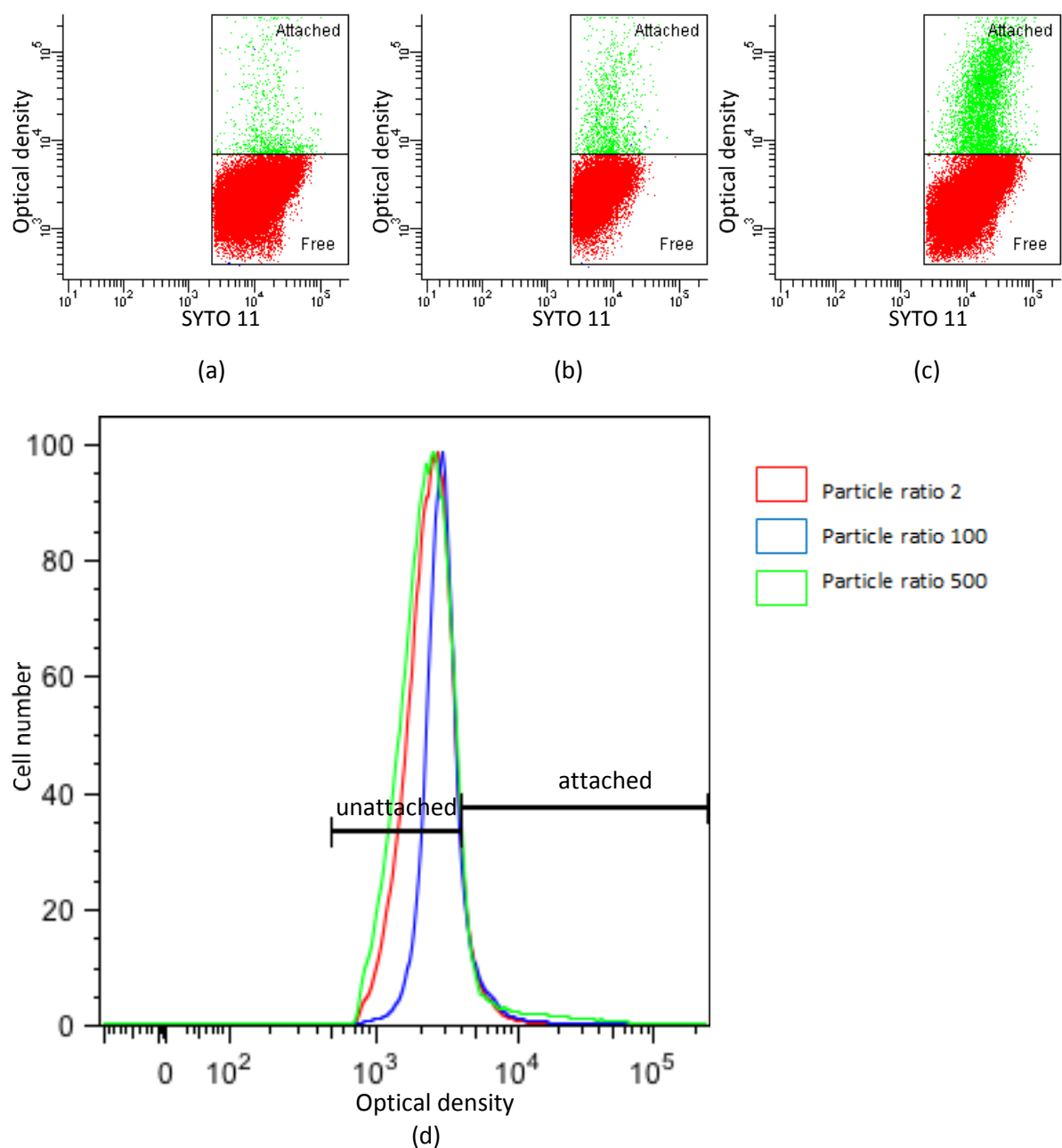


Figure D3-4. Strain #89 with Montmorillonite K-10. (a) is the dot plot of particle ratio 2, (b) is of particle ratio 100 and (c) is of particle ratio 500. In (a), (b), and (c), each green dot shows one attached event while red dots show unattached events. (d) is the histogram with red, blue and green curve for particle ratio 2, 100 and 500, respectively. Gage limits were set and labeled.

APPENDIX E. R CODE IN S STATISTICAL TESTS

APPENDIX E1. Statistical tests for data from the settling method

Table E1-1. Normality tests

```
#-----READ SETTLING DATA-----
#Examine normality(histogram and qqplot)
library(car)
qqPlot(setdata$Attachment.Ratio.ave,main="QQ.plot for settling data.(336 obs.)")
hist(setdata$Attachment.Ratio.ave,main="Hitstogram for settling data.(336 obs.)")
plot(setdata$Ratio,setdata$Attachment.Ratio.ave)
setdata$Attachment.Ratio.log <- log(setdata$Attachment.Ratio.ave)
hist(setdata$Attachment.Ratio.log,main="Hitstogram for settling data.(336 obs.)")

#Use log transformation.
hist(setdata$Attachment.Ratio.log)
qqPlot(setdata$Attachment.Ratio.log,main="QQ.plot for settling data(log transformed).(336 obs.)")
hist(setdata$Attachment.Ratio.trans,main="Hitstogram for settling data(log transformed).(336 obs.)")

#some plots
setdata$Ratio <- as.factor(setdata$Ratio)
qqplot(Ratio,Attachment.Ratio.ave,geom="point",data=setdata,colour=Strain,facets=Clay ~ .)
qqplot(Ratio, Attachment.Ratio.ave, geom="point", data=setdata, facets = Clay ~ Strain)
qqplot(Ratio,Attachment.Ratio.ave, data = setdata,facets =Clay ~ .,geom = "boxplot")
qqplot(Ratio,Attachment.Ratio.ave, data = setdata, facets =Strain ~ .,geom = "boxplot",
      binwidth = 0.1)
```

After comparisons, we used the untransformed data for the settling method.

Table E1-2. Three-ANOVA test and Tuckey's pairwise comparison test

```

#Three way ANOVA for settling data.

setdata$Ratio <- as.factor(setdata$Ratio)

set.lm1 <- lm(Attachment.Ratio.ave~Clay*Strain*Ratio,data=setdata)

anova(set.lm1)

plot(set.lm1$residuals)

set.lm2 <- lm(Attachment.Ratio.log~Clay*Strain*Ratio,data=setdata)

anova(set.lm2)

#Residual plots after fitting three way ANOVA model

delivery.res = setdata

delivery.res$M1.Fit = fitted(set.lm1)

delivery.res$M1.Resid = resid(set.lm1)

ggplot(delivery.res, aes(M1.Fit, M1.Resid, colour = Clay)) +
  geom_point() + xlab("Fitted Values") + ylab("Residuals") +
  facet_wrap( ~ Ratio)

delivery.res = setdata

delivery.res$M1.Fit = fitted(set.lm2)

delivery.res$M1.Resid = resid(set.lm2)

ggplot(delivery.res, aes(M1.Fit, M1.Resid, colour = Clay)) +
  geom_point() + xlab("Fitted Values") + ylab("Residuals") +
  facet_wrap( ~ Ratio)

```

Table E1-2 continued. Three-ANOVA test and Tukey's pairwise comparison test

```
delivery.res = setdata
delivery.res$M1.Fit = fitted(set.lm3)
delivery.res$M1.Resid = resid(set.lm3)
ggplot(delivery.res, aes(M1.Fit, M1.Resid, colour = Clay)) +
  geom_point() + xlab("Fitted Values") + ylab("Residuals") +
  facet_wrap( ~ Ratio)

##pairwise comparison on original data.
set.model1<-aov(Attachment.Ratio.ave~Clay*Strain*Ratio,data=setdata)
set.hsd1 = data.frame(TukeyHSD(set.model1, which = "Clay")$Clay)
set.hsd2 = data.frame(TukeyHSD(set.model1, which = "Strain")$Strain)
set.hsd3 = data.frame(TukeyHSD(set.model1, which = "Ratio")$Ratio)
set.hsd4 = data.frame(TukeyHSD(set.model1, which = "Clay:Strain")$"Clay:Strain")
set.hsd5 = data.frame(TukeyHSD(set.model1, which = "Clay:Ratio")$"Clay:Ratio")
set.hsd6 = data.frame(TukeyHSD(set.model1, which = "Strain:Ratio")$"Strain:Ratio")
set.hsd7 = data.frame(TukeyHSD(set.model1, which = "Clay:Strain:Ratio")$"Clay:Strain:Ratio")
set.hsd = data.frame(rbind(set.hsd1,set.hsd2,set.hsd3,set.hsd4,set.hsd5,set.hsd6,
  set.hsd7))
write.csv(set.hsd,"set.hsd.csv")
```

APPENDIX E2. Statistical tests for data from flow cytometry

Table E1-1. Normality tests

```
###-----READ FCM DATA-----
fcmdata <- read.csv(file.choose(),header=TRUE)
fcmdata <- subset(fcmdata,Clay != "Hectorite ")
table(fcmdata$Clay)
fcmdata$Clay <- as.character(fcmdata$Clay)
fcmdata$Clay <- as.factor(fcmdata$Clay)
levels(fcmdata$Clay)
str(fcmdata)
#some visudal displays
fcmdata$Ratio <- as.factor(fcmdata$Ratio)
qplot(Ratio, Attachment.Ratio,geom="point", data=fcmdata,colour=Strain,facets = Clay ~ .)
qplot(Ratio, Attachment.Ratio, geom="point", data=fcmdata, facets = Clay ~Strain)
qplot(Ratio,Attachment.Ratio, data = fcmdata,facets =Clay ~.,geom = "boxplot")
qplot(Ratio,Attachment.Ratio, data = fcmdata, facets =Strain ~ .,geom = "boxplot")
#Examine normality.(qq plot and histogram)
qqPlot(fcmdata$Attachment.Ratio,main="QQ.plot for FCM data.(324 obs.)")
hist(fcmdata$Attachment.Ratio,main="Hitstogram for FCM data.(324 obs.)")
#transform FCM data by log transformation.
ml <- boxcox.fit(fcmdata$Attachment.Ratio)
fcmdata$Attachment.Ratio.log <- log(fcmdata$Attachment.Ratio)
hist(fcmdata$Attachment.Ratio)
hist(fcmdata$Attachment.Ratio.log,main="Hitstogram for settling data(transformed).(324 obs.)")
qqPlot(fcmdata$Attachment.Ratio.log,main="QQ.plot for FCM data(transformed).(324 obs.)")
```

Natural log transformation was selected for flow cytometry data.

Table E2-2. Three-ANOVA test and Tuckey's pairwise comparison test

```

#three way ANOVA using log transformed data

fcm.lm2<-lm(Attachment.Ratio.log~Clay*Strain*Ratio,data=fcmdata)

anova(fcm.lm2)

qqPlot(fcm.lm2$residuals)

plot(fcm.lm2$residuals)

#Residual plots after fitting three way ANOVA model

delivery.res = fcmdata

delivery.res$M1.Fit = fitted(fcm.lm2)

delivery.res$M1.Resid = resid(fcm.lm2)

ggplot(delivery.res, aes(M1.Fit, M1.Resid, colour = Clay)) + geom_point() +
  xlab("Fitted Values") + ylab("Residuals")

ggplot(delivery.res, aes(M1.Fit, M1.Resid, colour = Clay)) +
  geom_point() + xlab("Fitted Values") + ylab("Residuals") +
  facet_wrap( ~ Ratio)

ggplot(delivery.res, aes(sample = M1.Resid)) + stat_qq()

delivery.hsd = data.frame(TukeyHSD(fcm.model1, which = "Clay")$Clay)

delivery.hsd$Comparison = row.names(delivery.hsd)

ggplot(delivery.hsd, aes(Comparison, y = diff, ymin = lwr, ymax = upr)) +
  geom_pointrange() + ylab("Difference in Mean Attachment Ratio by Clay")

delivery.res = fcmdata

delivery.res$M1.Fit = fitted(fcm.lm1)

delivery.res$M1.Resid = resid(fcm.lm1)

ggplot(delivery.res, aes(M1.Fit, M1.Resid, colour = Clay)) +
  geom_point() + xlab("Fitted Values") + ylab("Residuals") +
  facet_wrap( ~ Ratio)

```

Table E2-2 continued. Three-ANOVA test and Tukey's pairwise comparison test

```
##pairwise comparison on log transformed data.  
fcm.model1<-aov(Attachment.Ratio.log~Clay*Strain*Ratio,data=fcmdata)  
fcm.hsd1 = data.frame(TukeyHSD(fcm.model1, which = "Clay")$Clay)  
fcm.hsd2 = data.frame(TukeyHSD(fcm.model1, which = "Strain")$Strain)  
fcm.hsd3 = data.frame(TukeyHSD(fcm.model1, which = "Ratio")$Ratio)  
fcm.hsd4 = data.frame(TukeyHSD(fcm.model1, which = "Clay:Strain")$"Clay:Strain")  
fcm.hsd5 = data.frame(TukeyHSD(fcm.model1, which = "Clay:Ratio")$"Clay:Ratio")  
fcm.hsd6 = data.frame(TukeyHSD(fcm.model1, which = "Strain:Ratio")$"Strain:Ratio")  
fcm.hsd7 = data.frame(TukeyHSD(fcm.model1, which = "Clay:Strain:Ratio")$"Clay:Strain:Ratio")  
fcm.hsd = data.frame(cbind(fcm.hsd1,fcm.hsd2,fcm.hsd3,fcm.hsd4,fcm.hsd5,fcm.hsd6,  
fcm.hsd7))
```

APPENDIX E3. Statistical tests for method comparisons

Table E3-1. Normality tests

```
#-----merge two data sets to do method comparison-----

setdata2 <- read.csv(file.choose())

fcmdata2 <- read.csv(file.choose())

setdata2$Ratio <- as.factor(setdata2$Ratio)

fcmdata2$Ratio <- as.factor(fcmdata2$Ratio)

#The response is the difference of attachments ratio of the two methods.Examine the #normality of the
difference and find that the normality is not satisfied.

setdata2$diff <- fcmdata2$Attachment.Ratio-setdata2$Attachment.Ratio

qqPlot(setdata2$diff,ylab="Attachment.Ratio Difference",main="QQ-Plot of Attachment.Ratio Difference
between FCM and Settling Method")

hist(setdata2$diff,xlab="Attachment.Ratio Difference",main="Histogram of Attachment.Ratio Difference
between FCM and Settling Method")

#logdiff is the difference of log attachments ratio of the two methods.Examine the #normality of the log
difference and find that the normality is much better.

setdata2$logdiff <- fcmdata2$Attachment.Ratio.log-setdata2$Attachment.Ratio.log

qqPlot(setdata2$logdiff,ylab="Log Attachment.Ratio Difference",main="QQ-Plot of Log Attachment.Ratio
Difference between FCM and Settling Method")

hist(setdata2$logdiff,xlab="Log Attachment.Ratio Difference",main="Histogram of Log Attachment.Ratio
Difference between FCM and Settling Method")

#remove ratio 1 and ratio 2.Check the normality again.

setdata3 <- subset(setdata2,Ratio != 1 & Ratio != 2)

qqPlot(setdata3$logdiff,ylab="Log Attachment.Ratio Difference",main="QQ-Plot of Log Attachment.Ratio
Difference between FCM and Settling Method(Ratio 1 and 2 removed)")

hist(setdata3$logdiff,xlab="Log Attachment.Ratio Difference",main="Histogram of Log Attachment.Ratio
Difference between FCM and Settling Method(Ratio 1 and 2 removed)")
```

Table E3-2. Three-ANOVA test and Tuckey's pairwise comparison test

```

#some visual displays.

plot(setdata3$Clay,setdata3$logdiff,xlab="Clay",ylab="Log difference")

plot(setdata3$Strain,setdata3$logdiff,xlab="Strain",ylab="Log difference")

plot(setdata3$Ratio,setdata3$logdiff,xlab="Ratio",ylab="Log difference")

qplot(Ratio, logdiff, geom="point", data=setdata3, facets = Clay ~
Strain)

#three way ANOVA for the data after removed ratio 1 and ratio 2.

lm1 <-lm(setdata3$logdiff~Clay*Strain*Ratio,data=setdata3)

delivery.res = setdata3

delivery.res$M1.Fit = fitted(lm1)

delivery.res$M1.Resid = resid(lm1)

ggplot(delivery.res, aes(M1.Fit, M1.Resid, colour = Clay)) +geom_point() + xlab("Fitted Values") +
ylab("Residuals")

#pairwise comparison for the data after removed ratio 1 and ratio 2.

diff.model1<-aov(setdata3$logdiff~Clay*Strain*Ratio,data=setdata3)

diff.hsd1 = data.frame(TukeyHSD(diff.model1, which = "Clay")$Clay)

diff.hsd2 = data.frame(TukeyHSD(diff.model1, which = "Strain")$Strain)

diff.hsd3 = data.frame(TukeyHSD(diff.model1, which = "Ratio")$Ratio)

diff.hsd4 = data.frame(TukeyHSD(diff.model1, which = "Clay:Strain")$"Clay:Strain")

diff.hsd5 = data.frame(TukeyHSD(diff.model1, which = "Clay:Ratio")$"Clay:Ratio")

diff.hsd6 = data.frame(TukeyHSD(diff.model1, which = "Strain:Ratio")$"Strain:Ratio")

diff.hsd7 = data.frame(TukeyHSD(diff.model1, which = "Clay:Strain:Ratio")$"Clay:Strain:Ratio")

diff.hsd = data.frame(rbind(diff.hsd1,diff.hsd2,diff.hsd3,diff.hsd4,diff.hsd5,diff.hsd6,diff.hsd7))

write.csv(diff.hsd,"diff.hsd.csv")

```

APPENDIX E4. One sample t-tests

```
#t test for each clay.

t.test(subset(setdata3,Clay=="Kaolin")$logdiff)

t.test(subset(setdata3,Clay=="Ca-Mont")$logdiff)

t.test(subset(setdata3,Clay=="Mont K-10")$logdiff)

#t test for each strain.

t.test(subset(setdata3,Strain=="#31")$logdiff)

t.test(subset(setdata3,Strain=="#50")$logdiff)

t.test(subset(setdata3,Strain=="#89")$logdiff)

#t test for each ratio.

t.test(subset(setdata3,Ratio=="50")$logdiff)

t.test(subset(setdata3,Ratio=="100")$logdiff)

t.test(subset(setdata3,Ratio=="200")$logdiff)

t.test(subset(setdata3,Ratio=="500")$logdiff)

#t test for clay and strain combination

t.test(subset(setdata3,Strain=="#31" & Clay=="Kaolin")$logdiff)

t.test(subset(setdata3,Strain=="#31" & Clay=="Ca-Mont")$logdiff)

t.test(subset(setdata3,Strain=="#31" & Clay=="Mont K-10")$logdiff)

t.test(subset(setdata3,Strain=="#89" & Clay=="Ca-Mont")$logdiff)

t.test(subset(setdata3,Strain=="#89" & Clay=="Kaolin")$logdiff)

t.test(subset(setdata3,Strain=="#89" & Clay=="Mont K-10")$logdiff)
```

APPENDIX F. DATA TRANSFORMATIONS

APPENDIX F1. Original data distributions

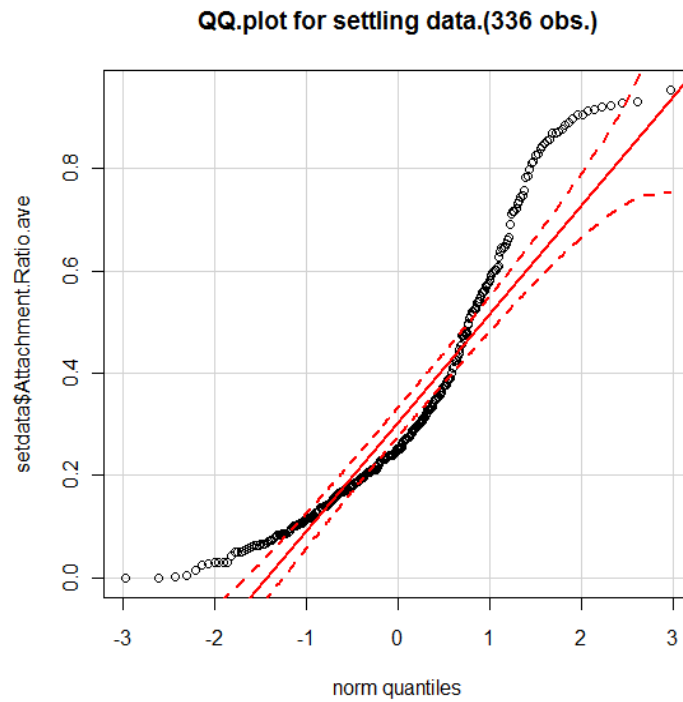


Figure F1-1. QQ plot of percent attached from the settling method. The dash line was not perfectly straight indicating that the distribution was non-normal.

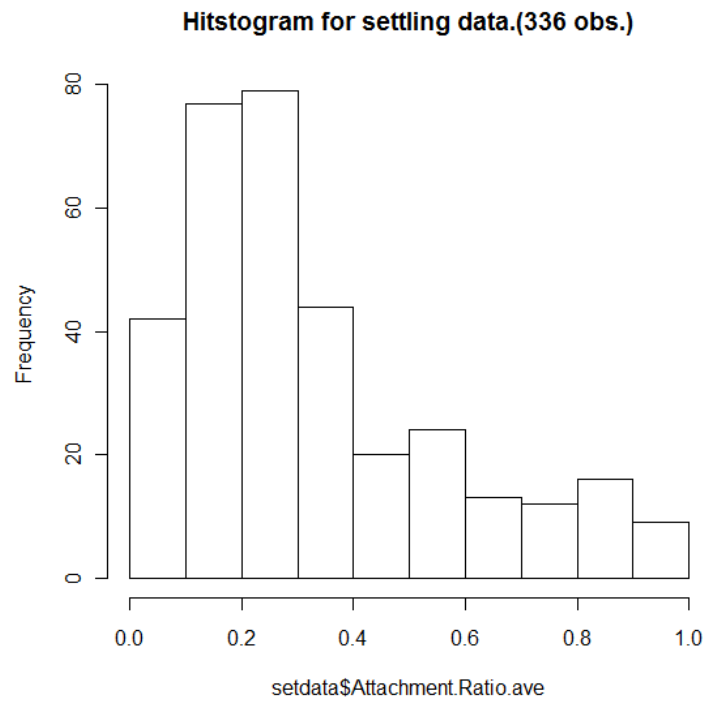


Figure F1-2. Histogram of attachment ratios from the settling method. The histogram indicated slightly right-skewed distribution.

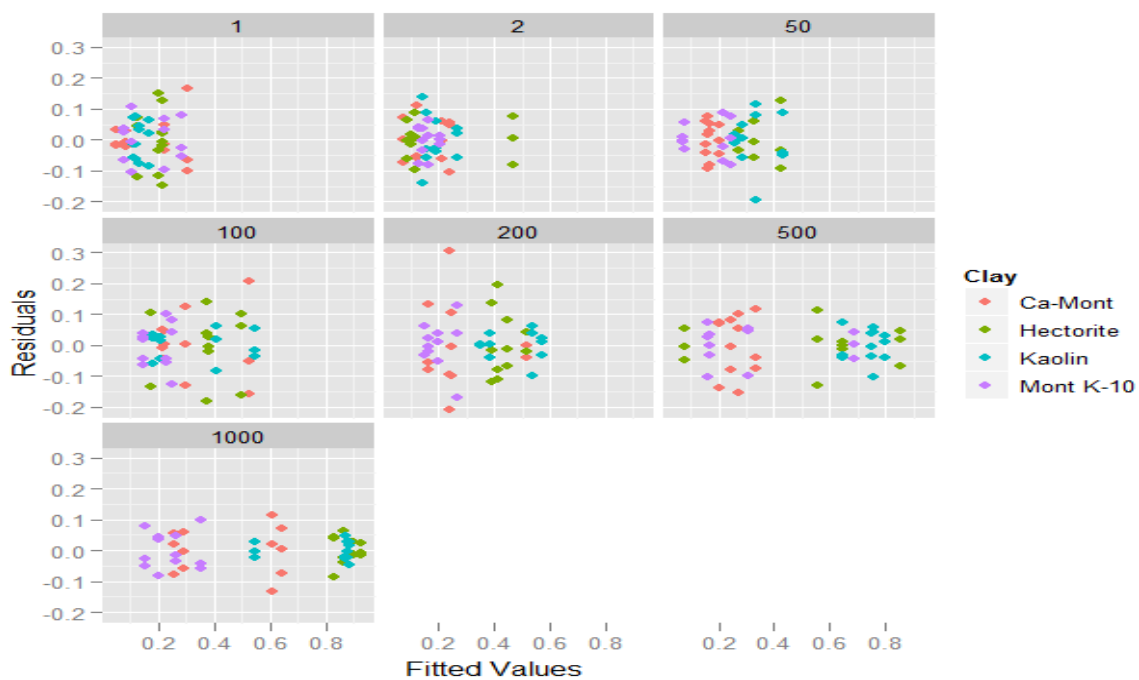


Figure F1-3. Scatter plots of residuals vs. fitted values of attachment ratios from the settling method. The plots for each kind of clay have different patterns which indicated that the attachment ratios from the settling method did not have a normal distribution.

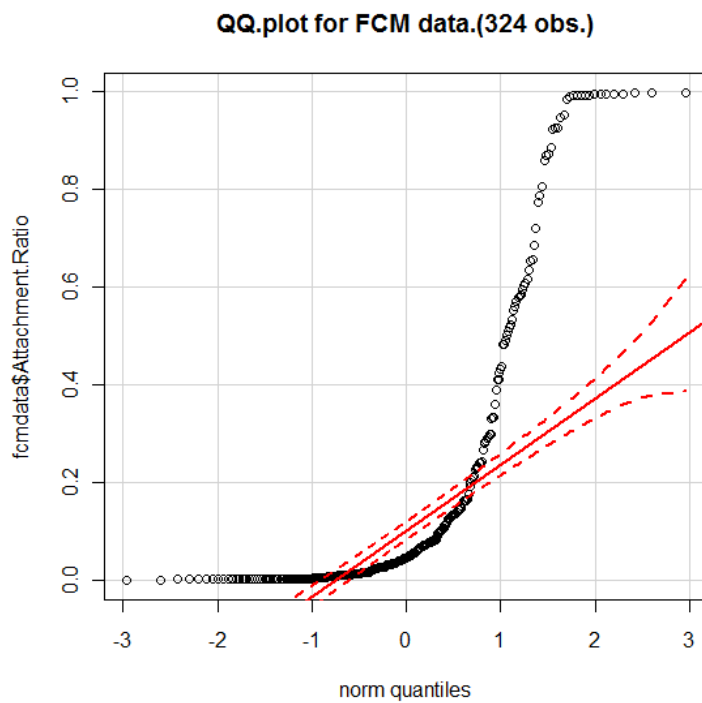


Figure F1-4. QQ plot of attachment ratios from flow cytometry. The dash line was far away from the reference line in red, which indicate that the attachment ratios from flow cytometry is not normal distribution.

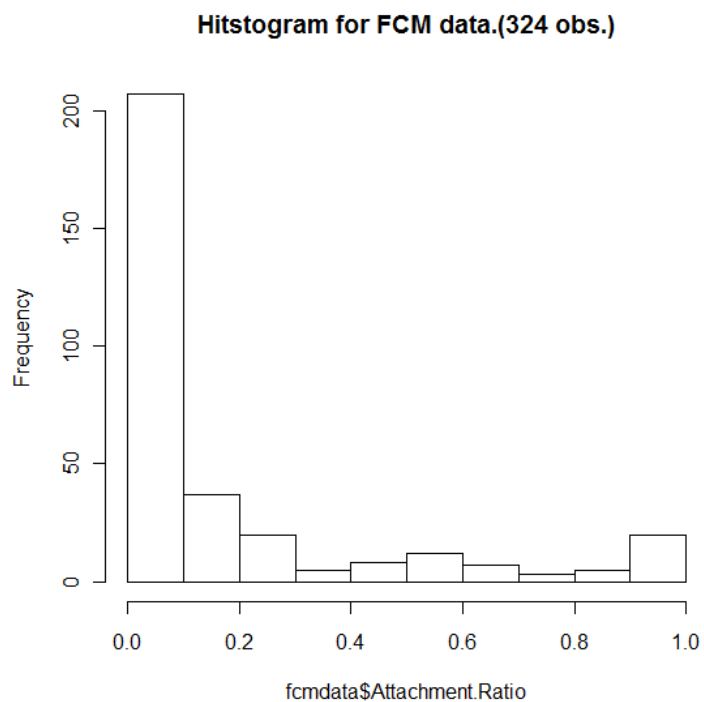


Figure F1-5. Histogram of attachment ratios from flow cytometry. The histogram showed that the attachment ratios rom flow cytometry was right-skewed.

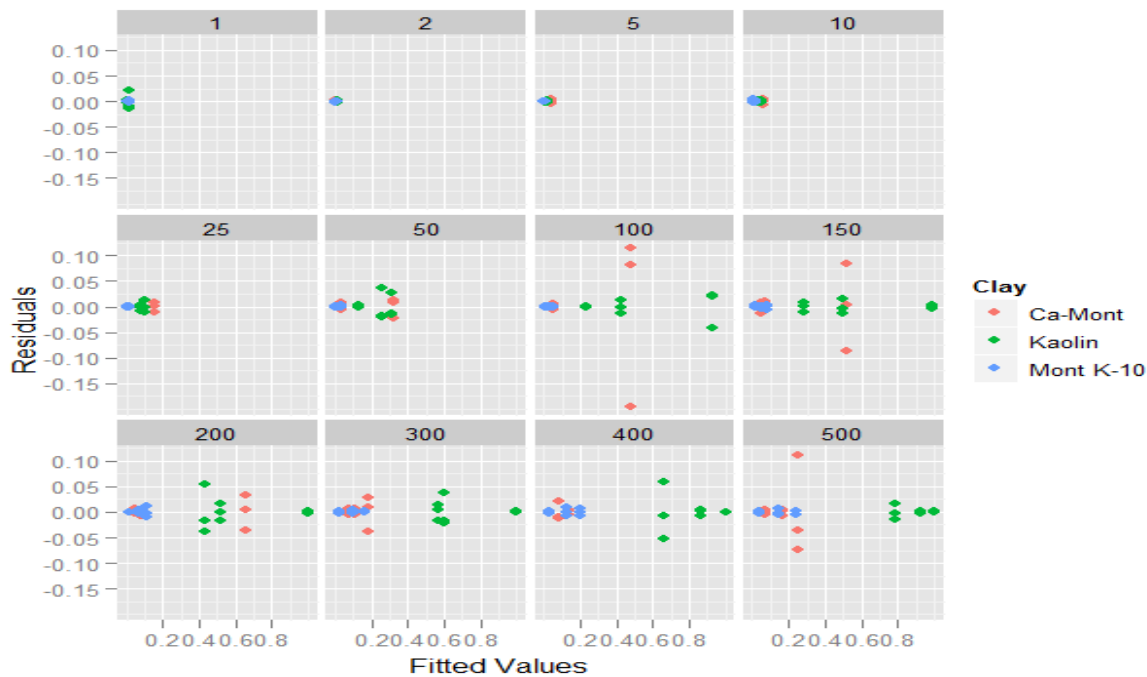


Figure F1-6. Scatter plot of residuals vs. fitted Values of attachment ratio from flow cytometry. The plots for each kind of clay have different patterns which indicated that the attachment ratios from flow cytometry did not have a normal distribution.

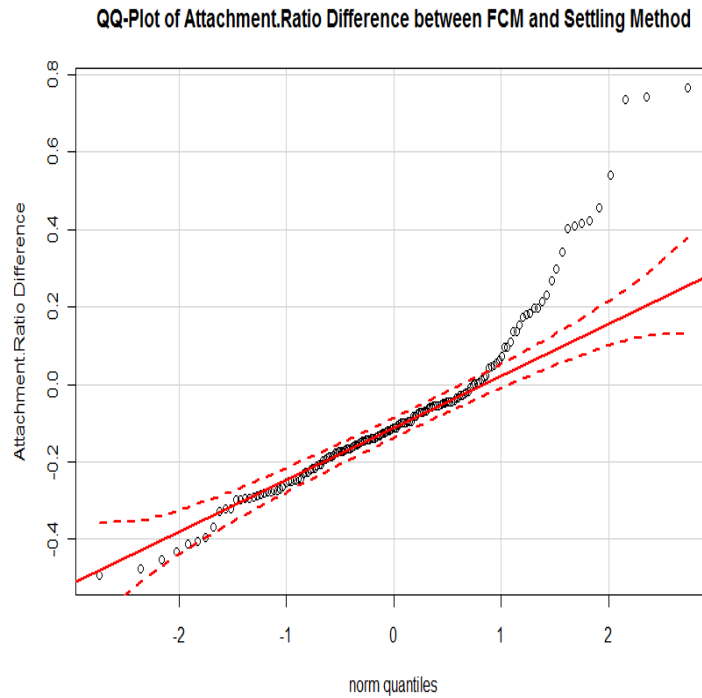


Figure F1-7. QQ plot of attachment ratio difference between flow cytometry and the settling method. The dash line was not perfectly straight indicating that the distribution was non-normal.

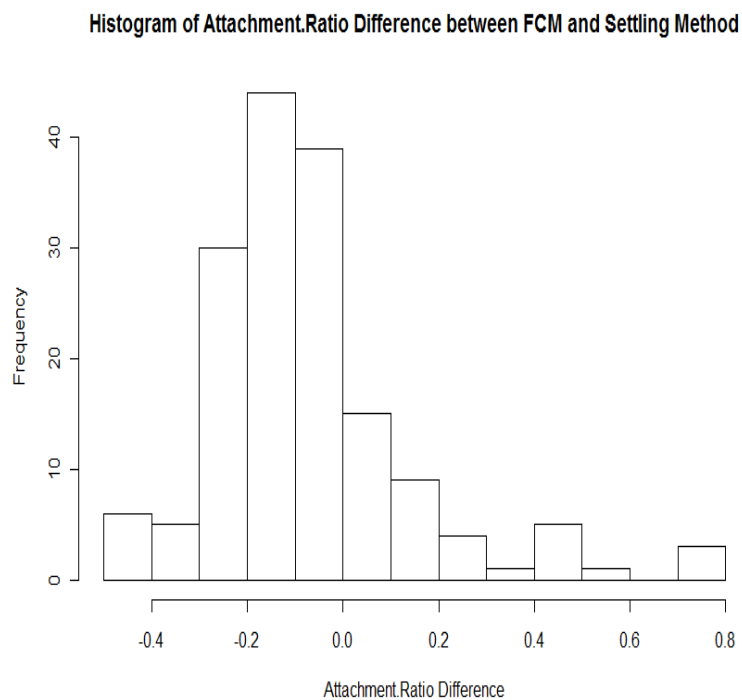


Figure F1-8. Histogram of attachment ratio difference between flow cytometry and the settling method. The histogram showed that the attachment ratios from flow cytometry was slightly right-skewed.

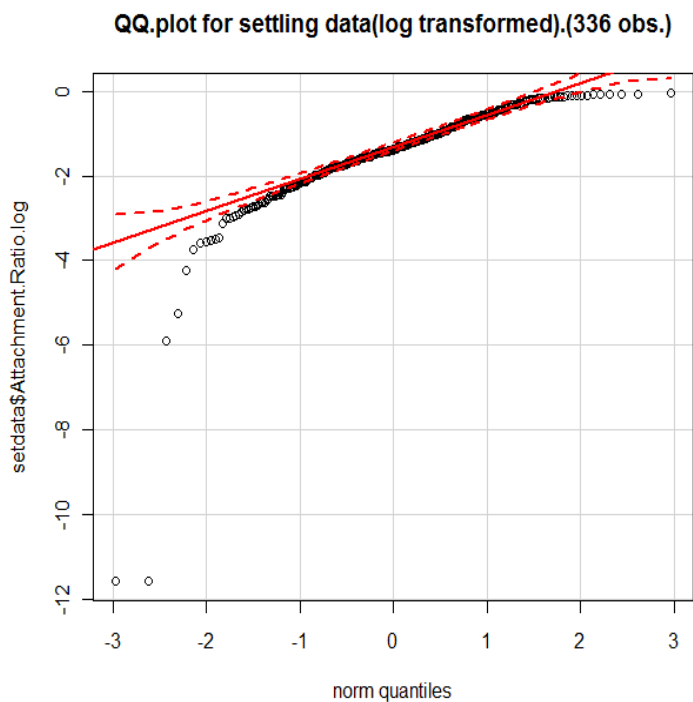
APPENDIX F2. Normality tests after transformations

Figure F2-1. QQ plot for natural log transformed attachment ratios from the settling method. The dash line was still not perfectly straight, which indicated that natural log transformation was not useful.

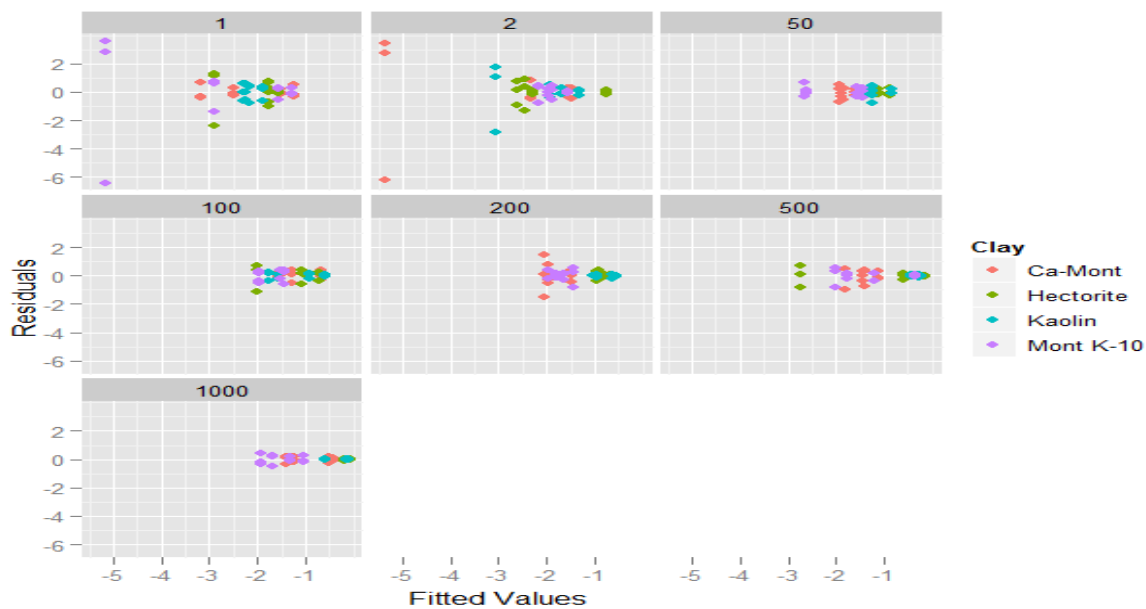


Figure F2-2. Scatter plot of residuals vs. fitted values for natural log transformed attachment ratios from the settling method. The plots for each kind of clay have different patterns which indicated that the natural log transformed attachment ratios from the settling method did not have a normal distribution.

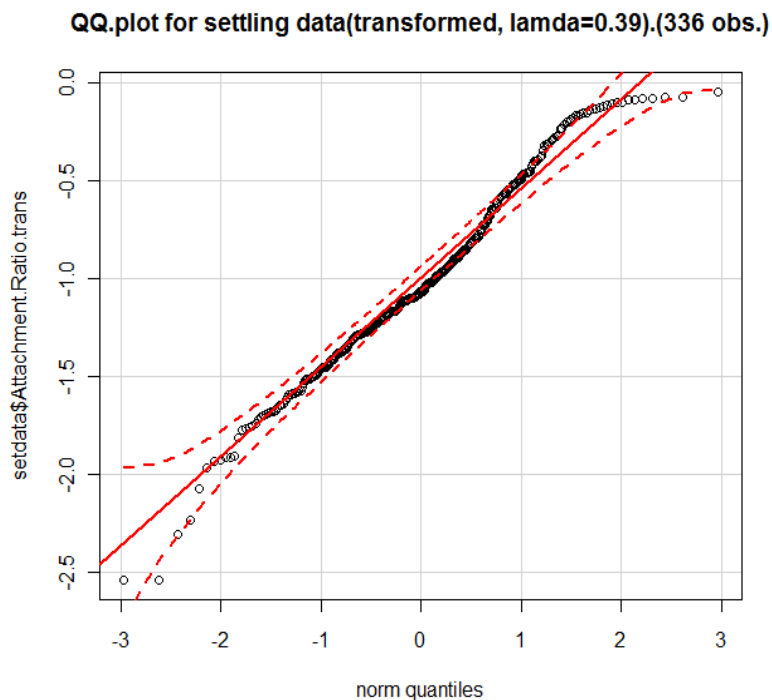


Figure F2-3. QQ plot of Box-cox transformed ($\lambda=0.39$) attachment ratios from the settling method. The dash line was still not perfectly straight, which indicated that natural log transformation was not useful.

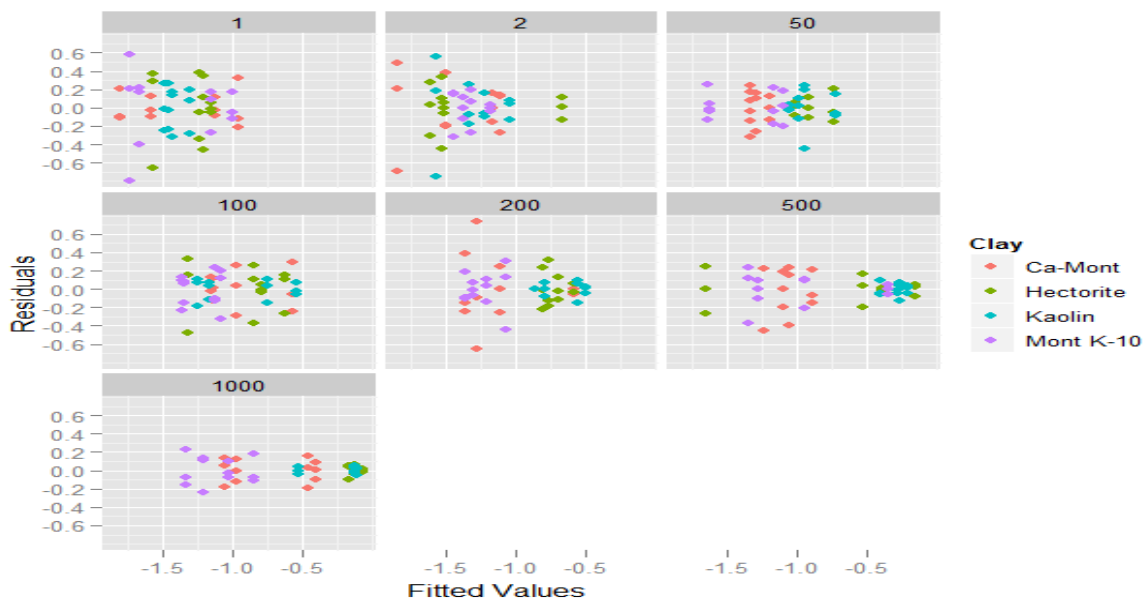


Figure F2-4. Scatter plot of residuals vs. fitted values for Box-cox transformed ($\lambda=0.39$) settling data. The plots for each kind of clay have different patterns which indicated that the natural log transformed attachment ratios from the settling method did not have a normal distribution.

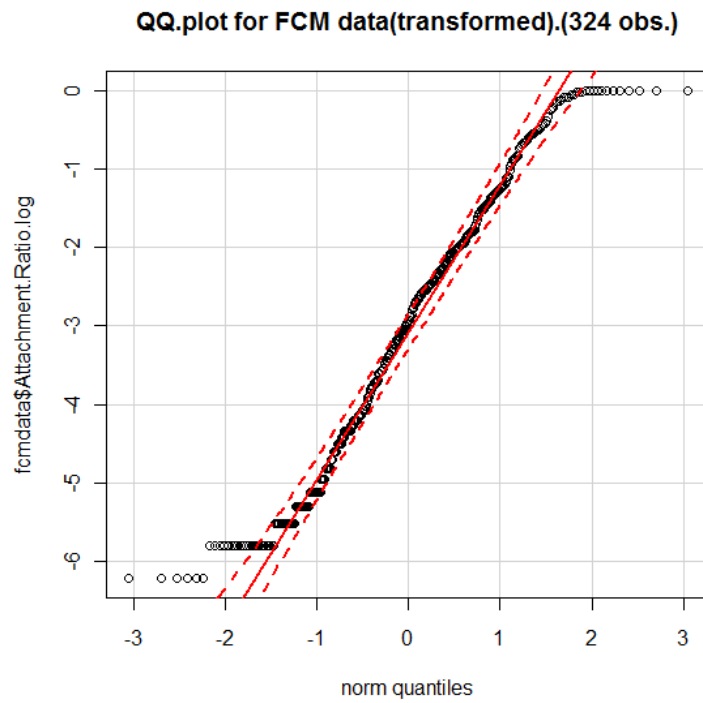


Figure F2-5. QQ plot of natural log transformed attachment ratios from flow cytometry. The dash line was straight, which indicated that the natural log transformation is suitable for the attachment ratios from flow cytometry.

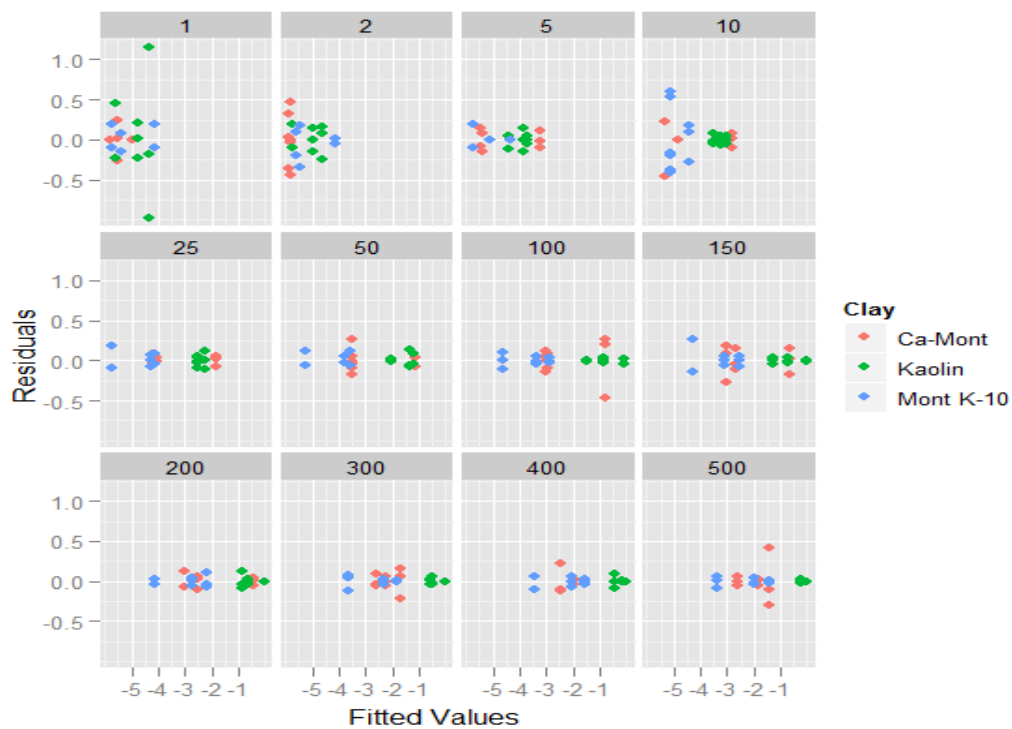


Figure F2-6. Scatter plot of residuals vs. fitted values for natural log transformed attachment ratios from flow cytometry. The plots have almost the same pattern, which indicated that the distribution of natural log transformed attachment ratios had a normal distribution.

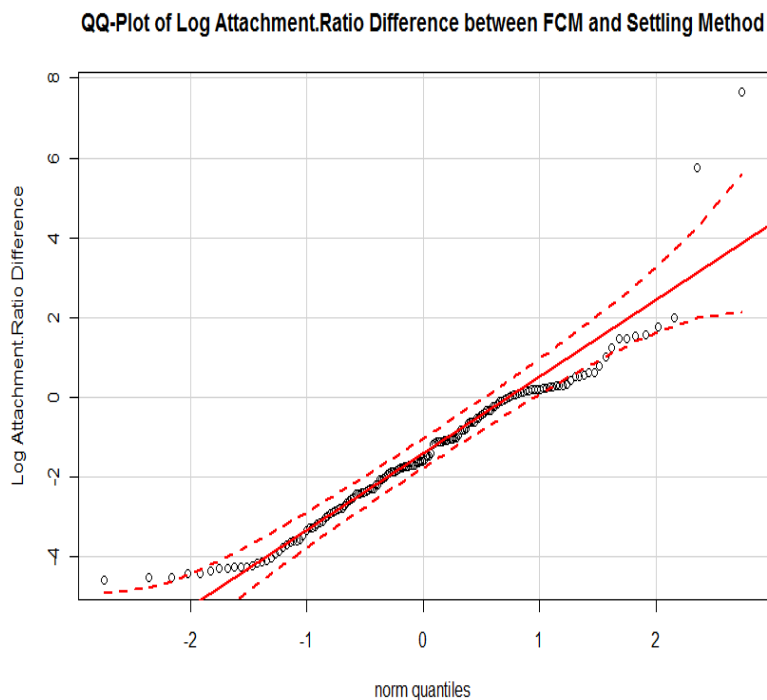


Figure F2-7. QQ plot of natural log transformed attachment ratio differences between flow cytometry and the settling method. The dash line was still not perfectly straight, which indicated that natural log transformation was not useful.

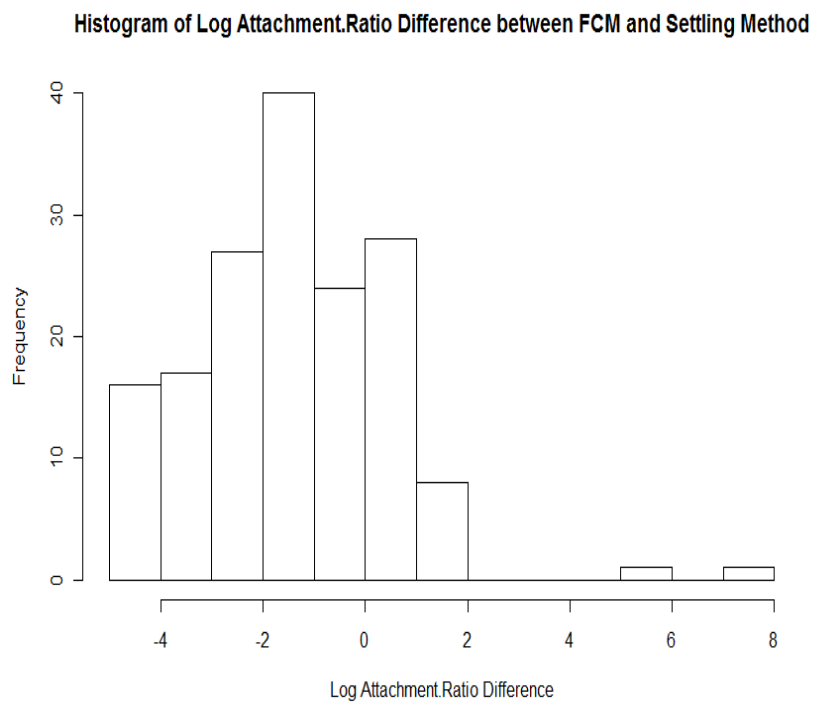


Figure F2-8. Histogram of natural log transformed attachment ratio differences between flow cytometry and the settling method. The histogram showed the distribution was still right-skewed.

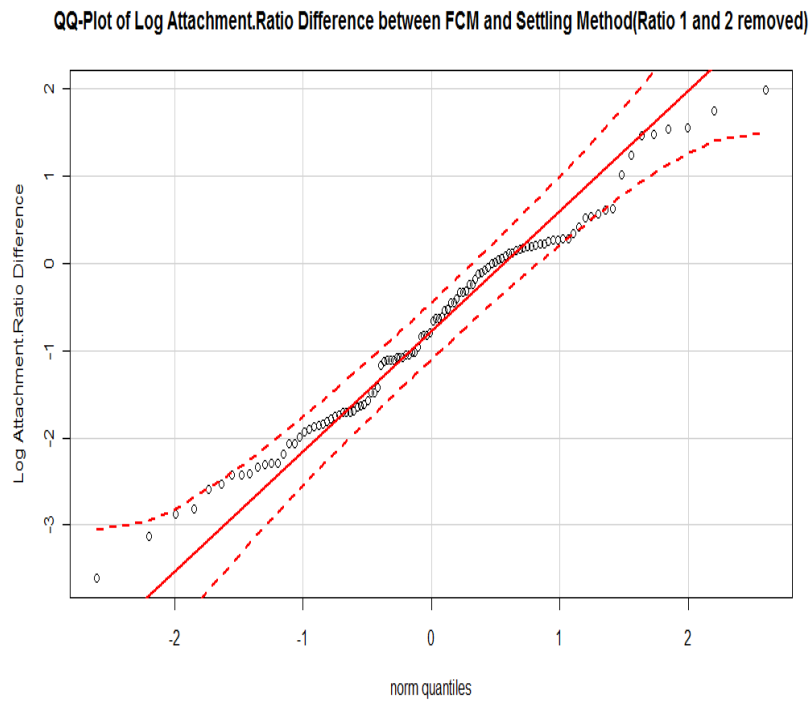


Figure F2-9. QQ plot of natural log transformed attachment ratio differences (surface area ratio 1 and 2 removed) between flow cytometry and the settling method. The dash line was within the reference range (red dash line), which indicated after removing surface area ratio 1 and 2, the distribution of natural log transformed attachment ratio difference was almost normal.

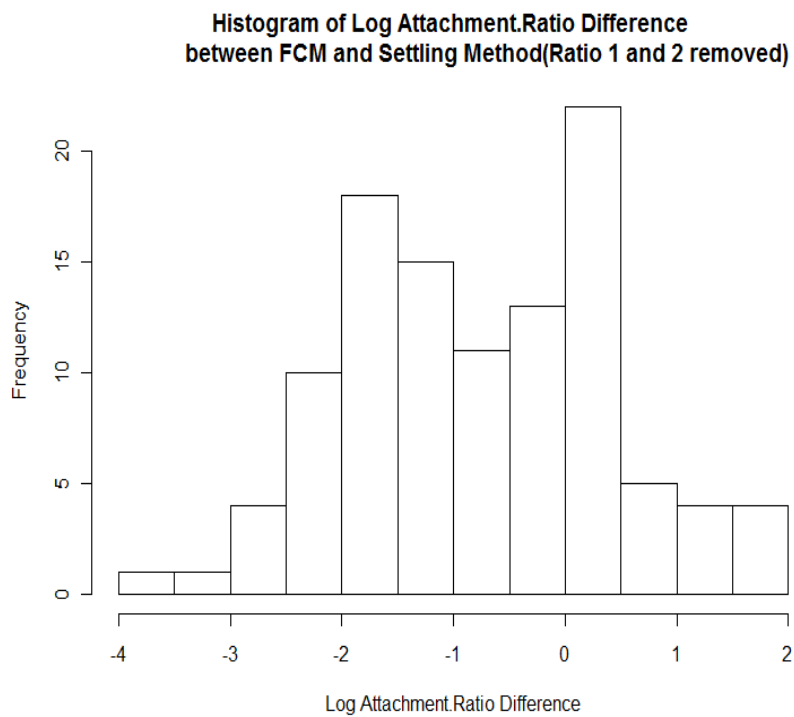


Figure F2-10. Histogram of natural log transformed attachment ratio differences (surface area ratio 1 and 2 removed) between flow cytometry and the settling method. The histogram indicated after removing surface area ratio 1 and 2, the distribution of natural log transformed attachment ratio difference was almost normal.

APPENDIX G. THREE-WAY ANOVA TEST RESULTS

APPENDIX G1. Results for natural log attachment ratios by flow cytometry

	Df	Sum Square	Mean Square	F-value	Pr (>F)
Clay type	2	195.29	97.644	2790.469	$< 2.2 \times 10^{-16}$
Strain	2	73.20	36.601	1045.987	$< 2.2 \times 10^{-16}$
Surface area ratio	11	624.13	56.739	1621.472	$< 2.2 \times 10^{-16}$
Clay type: Strain	4	31.08	7.769	222.027	$< 2.2 \times 10^{-16}$
Clay type: Surface area ratio	22	2254.41	2.473	70.672	$< 2.2 \times 10^{-16}$
Strain: Surface area ratio	22	21.31	0.968	27.676	$< 2.2 \times 10^{-16}$
Clay type: Strain: Surface area ratio	44	21.28	0.484	13.818	$< 2.2 \times 10^{-16}$

APPENDIX G2. Results for attachment ratios by the settling method

	Df	Sum Square	Mean Square	F-value	Pr (>F)
Clay type	3	3.0762	1.02540	142.4468	$< 2.2 \times 10^{-16}$
Strain	3	0.1253	0.04175	5.8001	0.000779
Surface area ratio	6	7.0592	1.17653	163.4417	$< 2.2 \times 10^{-16}$
Clay type: Strain	9	0.8058	0.08954	12.4381	6.022×10^{-16}
Clay type: Surface area ratio	18	2.8876	0.16042	22.2859	$< 2.2 \times 10^{-16}$
Strain: Surface area ratio	18	0.9560	0.05311	7.3781	7.948×10^{-15}
Clay type: Strain: Surface area ratio	54	2.2593	0.04184	5.8121	$< 2.2 \times 10^{-16}$

APPENDIX G3. Results for natural log attachment ratio difference between flow cytometry and the settling method

	Df	Sum Square	Mean Square	F-value	Pr (>F)
Clay type	2	55.349	27.6747	168.0975	$< 2.2 \times 10^{-16}$
Strain	2	39.600	19.7998	120.2649	$< 2.2 \times 10^{-16}$
Surface area ratio	3	8.194	2.7315	16.5910	2.711×10^{-8}
Clay type: Strain	4	15.588	3.8971	23.6771	1.611×10^{-12}
Clay type: Surface area ratio	6	4.006	0.6677	4.0555	0.0014756
Strain: Surface area ratio	6	5.390	0.8984	5.4569	0.0001067
Clay type: Strain: Surface area ratio	12	7.640	0.6367	3.8674	0.0001443

**APPENDIX H. PAIRWISE COMPARISONS BETWEEN DIFFERENT
SURFACE AREA RATIOS**

Method	Comparison	Difference	95% Confidence Interval		p-value
			Lower Limit	Upper Limit	
Settling method (untransformed)	2--1	0.01249478	-0.0390342	0.0640237	0.991176963
	50-1	0.07805425	0.0265253	0.1295832	0.000212333
	100-1	0.13638352	0.0848546	0.1879125	3.07E-12
	200-1	0.1828113	0.1312823	0.2343403	0
	500-1	0.3014646	0.2499356	0.3529936	0
	1000-1	0.42824918	0.3767202	0.4797781	0
	50-2	0.06555948	0.0140305	0.1170884	0.003671463
	100-2	0.12388874	0.0723598	0.1754177	2.50E-10
	200-2	0.17031652	0.1187876	0.2218455	5.88E-15
	500-2	0.28896982	0.2374409	0.3404988	0
	1000-2	0.4157544	0.3642254	0.4672834	0
	100-50	0.05832926	0.0068003	0.1098582	0.015355401
	200-50	0.10475705	0.0532281	0.156286	1.27E-07
	500-50	0.22341035	0.1718814	0.2749393	0
	1000-50	0.35019493	0.298666	0.4017239	0
	200-100	0.04642778	-0.0051012	0.0979567	0.107975979
	500-100	0.16508108	0.1135521	0.21661	9.88E-15
	1000-100	0.29186566	0.2403367	0.3433946	0
	500-200	0.1186533	0.0671243	0.1701823	1.47E-09
	1000-200	0.24543788	0.1939089	0.2969668	0
1000-500	0.12678458	0.0752556	0.1783135	9.20E-11	
Flow cytometry (natural log transformed)	2--1	-0.200873	-0.369102	-0.032644	0.005932
	5--1	0.5459936	0.377765	0.7142224	5.31E-14
	10--1	0.9627628	0.794534	1.1309916	0
	25-1	1.6129859	1.444757	1.7812147	0
	50-1	2.3101083	2.14188	2.4783371	0
	100-1	2.8900399	2.721811	3.0582687	0
	150-1	3.0880155	2.919787	3.2562443	0
	200-1	3.2940347	3.125806	3.4622635	0
	300-1	3.4127984	3.24457	3.5810272	0
	400-1	3.5674846	3.399256	3.7357134	0
	500-1	3.6872185	3.51899	3.8554473	0
	5--2	0.7468667	0.578638	0.9150955	0
	10--2	1.1636359	0.995407	1.3318647	0
	25-2	1.8138589	1.64563	1.9820877	0
50-2	2.5109814	2.342753	2.6792102	0	

Flow cytometry (natural log transformed)	100-2	3.0909129	2.922684	3.2591417	0
	150-2	3.2888885	3.12066	3.4571173	0
	200-2	3.4949077	3.326679	3.6631365	0
	300-2	3.6136714	3.445443	3.7819002	0
	400-2	3.7683577	3.600129	3.9365865	0
	500-2	3.8880916	3.719863	4.0563204	0
	10--5	0.4167692	0.24854	0.584998	1.62E-12
	25-5	1.0669923	0.898763	1.2352211	0
	50-5	1.7641147	1.595886	1.9323435	0
	100-5	2.3440463	2.175817	2.5122751	0
	150-5	2.5420219	2.373793	2.7102507	0
	200-5	2.7480411	2.579812	2.9162699	0
	300-5	2.8668048	2.698576	3.0350336	0
	400-5	3.021491	2.853262	3.1897198	0
	500-5	3.1412249	2.972996	3.3094537	0
	25-10	0.6502231	0.481994	0.8184519	0
	50-10	1.3473455	1.179117	1.5155743	0
	100-10	1.9272771	1.759048	2.0955059	0
	150-10	2.1252527	1.957024	2.2934815	0
	200-10	2.3312719	2.163043	2.4995007	0
	300-10	2.4500356	2.281807	2.6182644	0
	400-10	2.6047218	2.436493	2.7729506	0
	500-10	2.7244557	2.556227	2.8926845	0
	50-25	0.6971224	0.528894	0.8653512	0
	100-25	1.277054	1.108825	1.4452828	0
	150-25	1.4750296	1.306801	1.6432584	0
	200-25	1.6810488	1.51282	1.8492776	0
	300-25	1.7998125	1.631584	1.9680413	0
	400-25	1.9544987	1.78627	2.1227275	0
	500-25	2.0742326	1.906004	2.2424615	0
	100-50	0.5799316	0.411703	0.7481604	4.88E-15
	150-50	0.7779072	0.609678	0.946136	0
	200-50	0.9839264	0.815698	1.1521552	0
	300-50	1.1026901	0.934461	1.2709189	0
	400-50	1.2573763	1.089147	1.4256051	0
	500-50	1.3771102	1.208881	1.545339	0
	150-100	0.1979756	0.029747	0.3662044	0.007298
	200-100	0.4039948	0.235766	0.5722236	7.52E-12
	300-100	0.5227585	0.35453	0.6909873	7.79E-14
	400-100	0.6774447	0.509216	0.8456735	0
500-100	0.7971786	0.62895	0.9654075	0	
200-150	0.2060192	0.03779	0.374248	0.004073	
300-150	0.3247829	0.156554	0.4930117	6.99E-08	
400-150	0.4794691	0.31124	0.6476979	8.26E-14	

Flow cytometry (natural log transformed)	500-150	0.599203	0.430974	0.7674318	0
	300-200	0.1187637	-0.049465	0.2869925	0.456825
	400-200	0.2734499	0.105221	0.4416787	1.30E-05
	500-200	0.3931838	0.224955	0.5614126	2.78E-11
	400-300	0.1546862	-0.013543	0.322915	0.104833
	500-300	0.2744202	0.106191	0.442649	1.18E-05
	500-400	0.1197339	-0.048495	0.2879627	0.44357

APPENDIX I EXAMPLE OF ORIGINAL DOT PLOTS FROM FLOW CYTOMETRY WITH CONTROLS

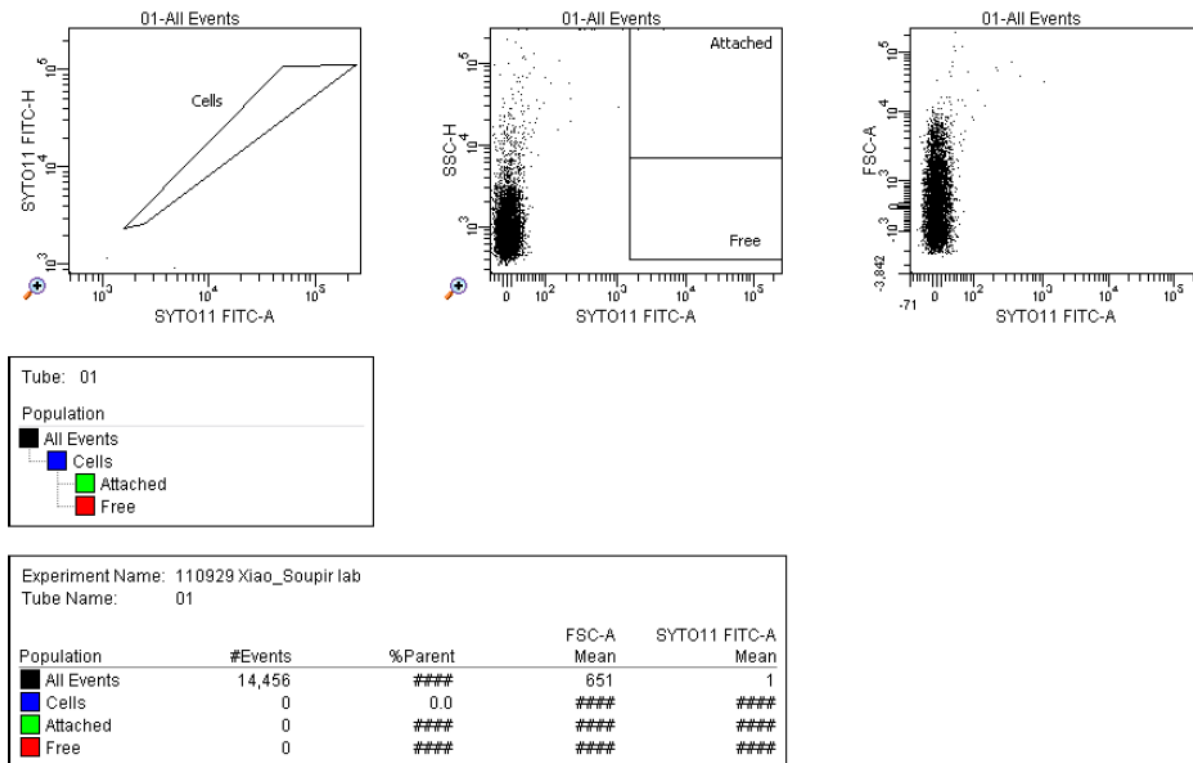


Figure I-1. Dot plot of PBS only from flow cytometry.

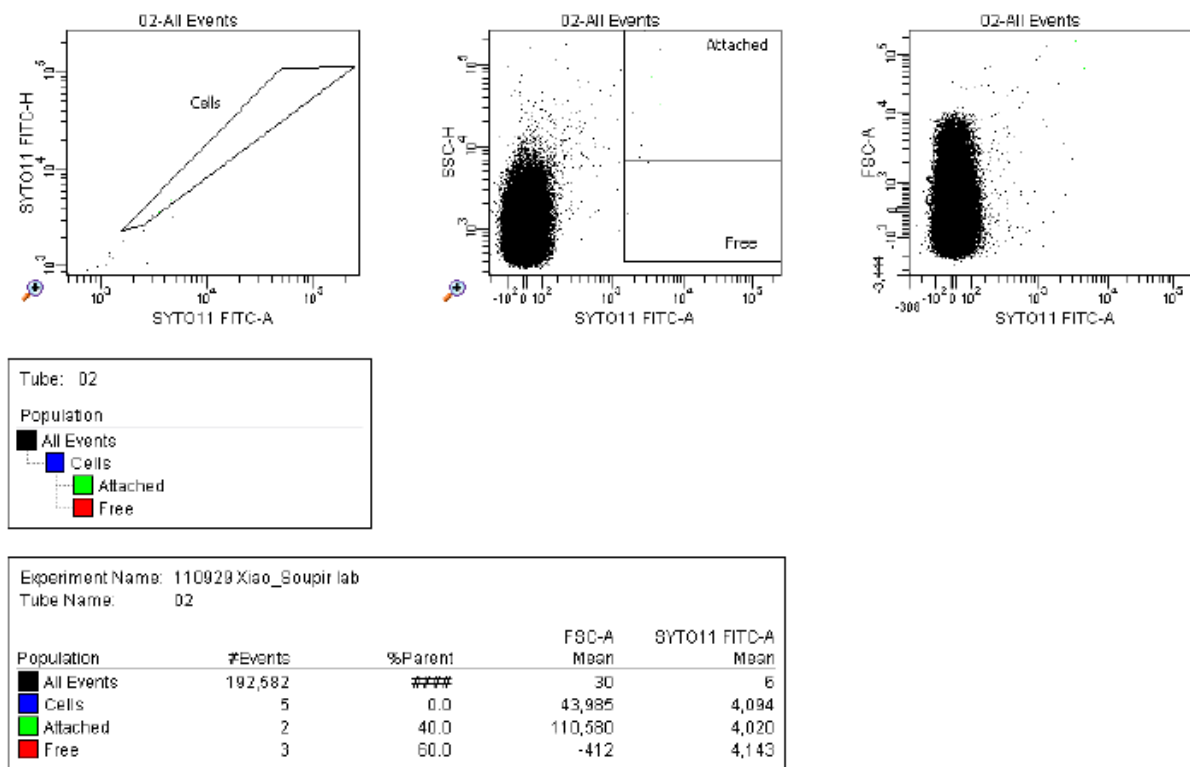


Figure I-2. Dot plot of PBS with SYTO 11 from flow cytometry.

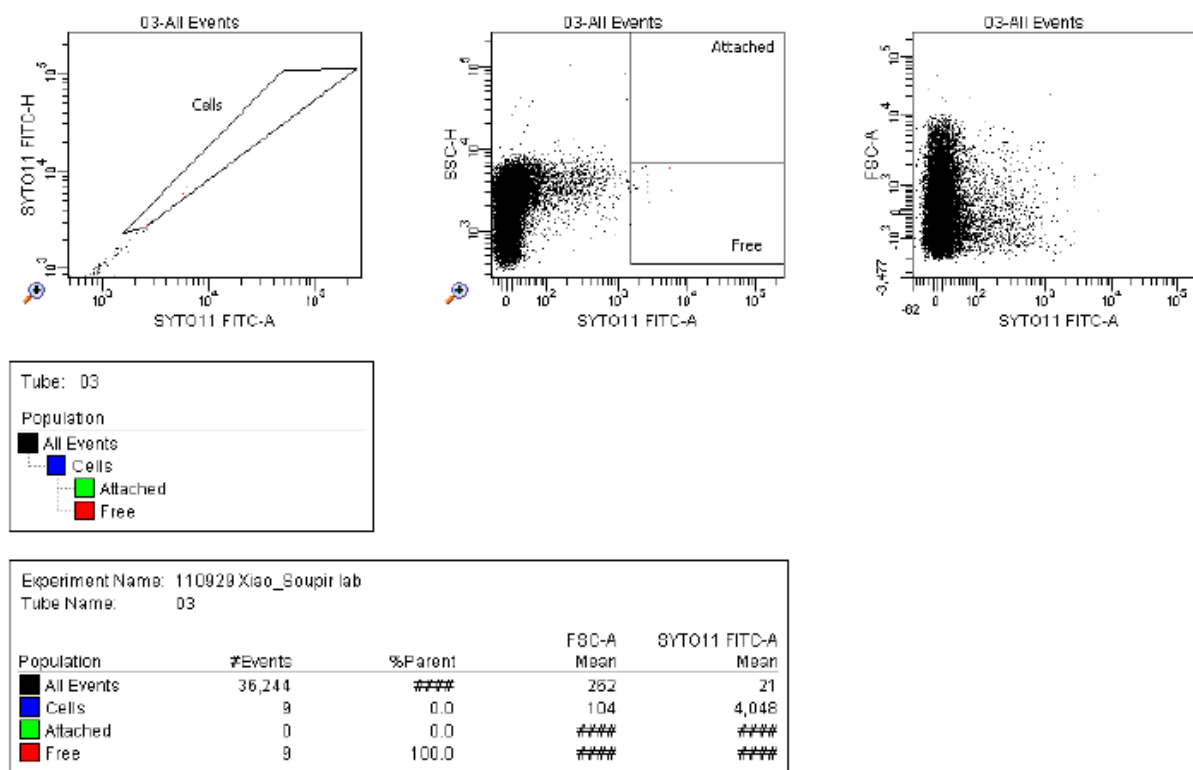


Figure I-3. Dot plot of PBS and strain #31 at 10^7 CFU ml^{-1} from flow cytometry.

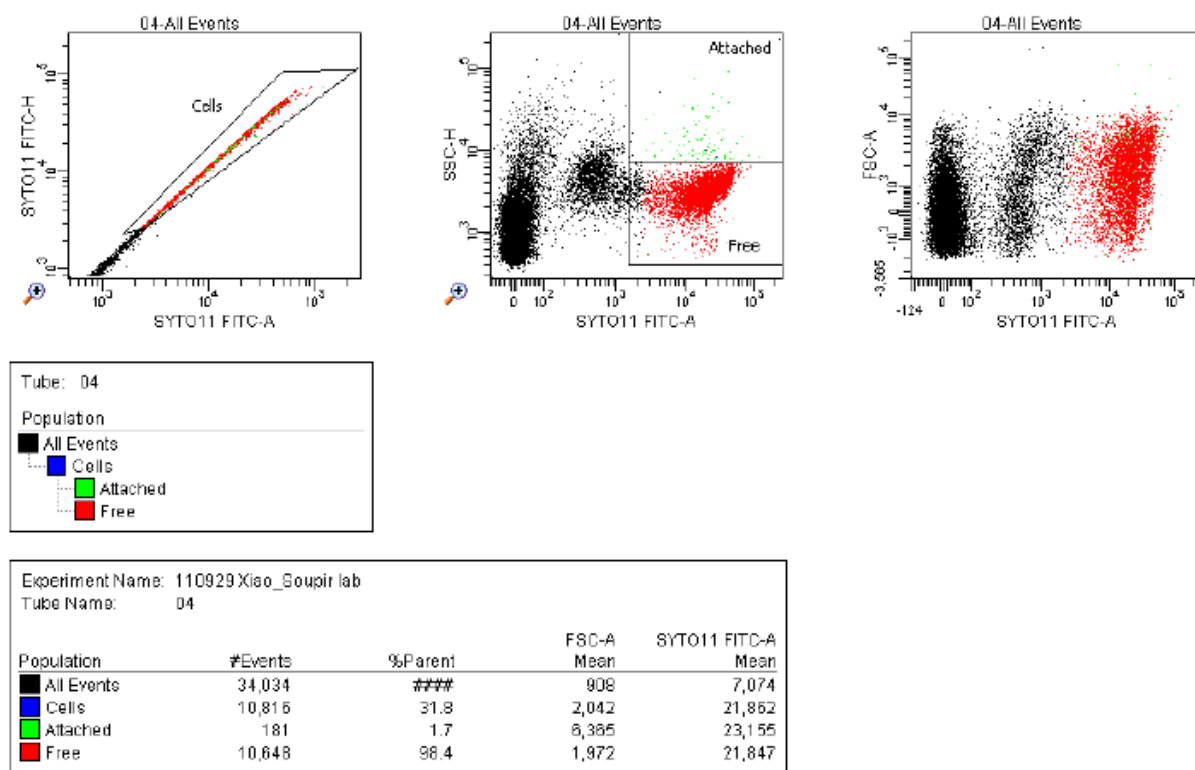


Figure I-4. Dot plot of PBS, strain #31 at 10^7 CFU ml⁻¹, and SYTO 11 from flow cytometry.

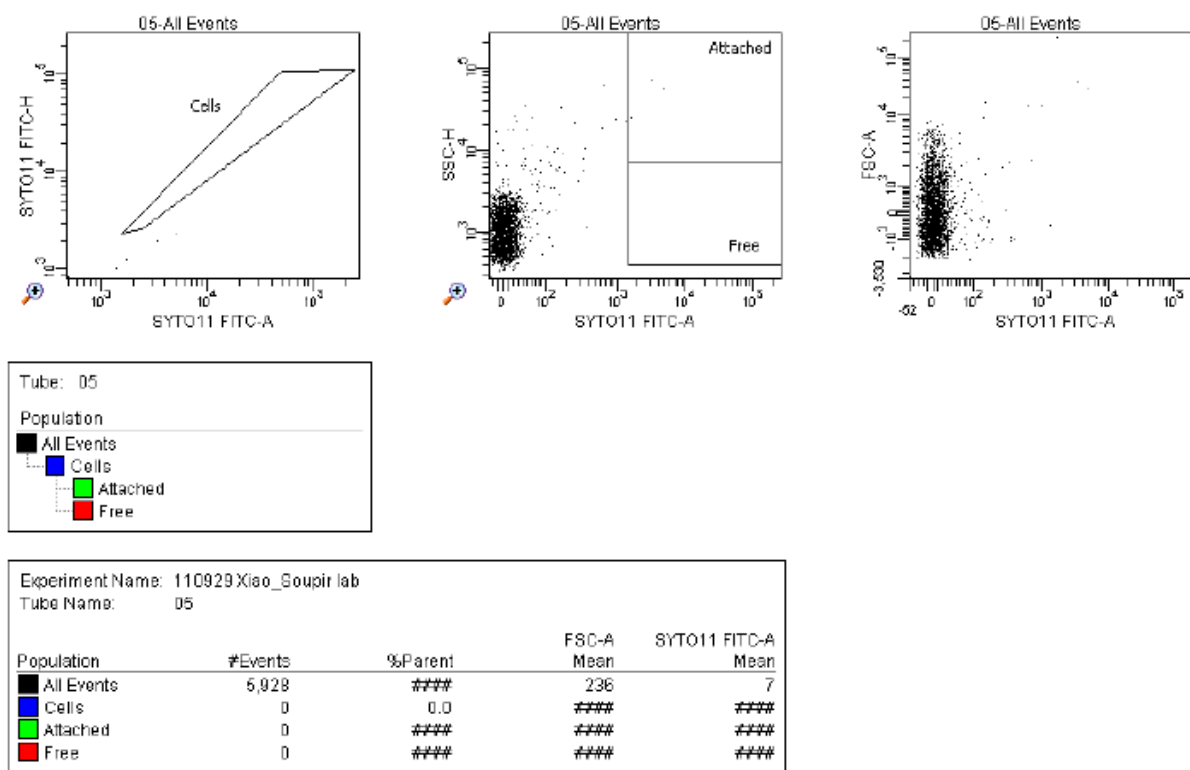


Figure I-5. Dot plot of PBS and Ca-Montmorillonite at $8 \times 10^{-4} \text{ g L}^{-1}$ from flow cytometry.

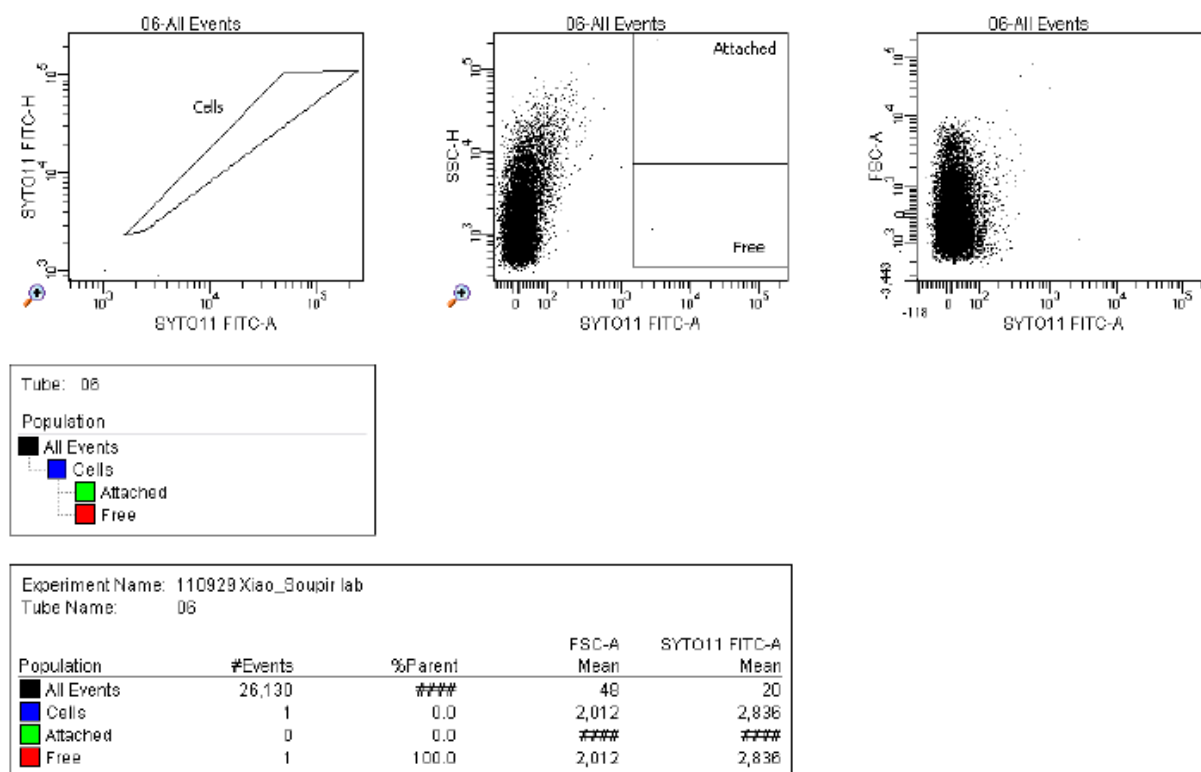


Figure I-6. Dot plot of PBS, Ca-Montmorillonite at $8 \times 10^{-4} \text{ g L}^{-1}$, and SYTO 11 from flow cytometry.

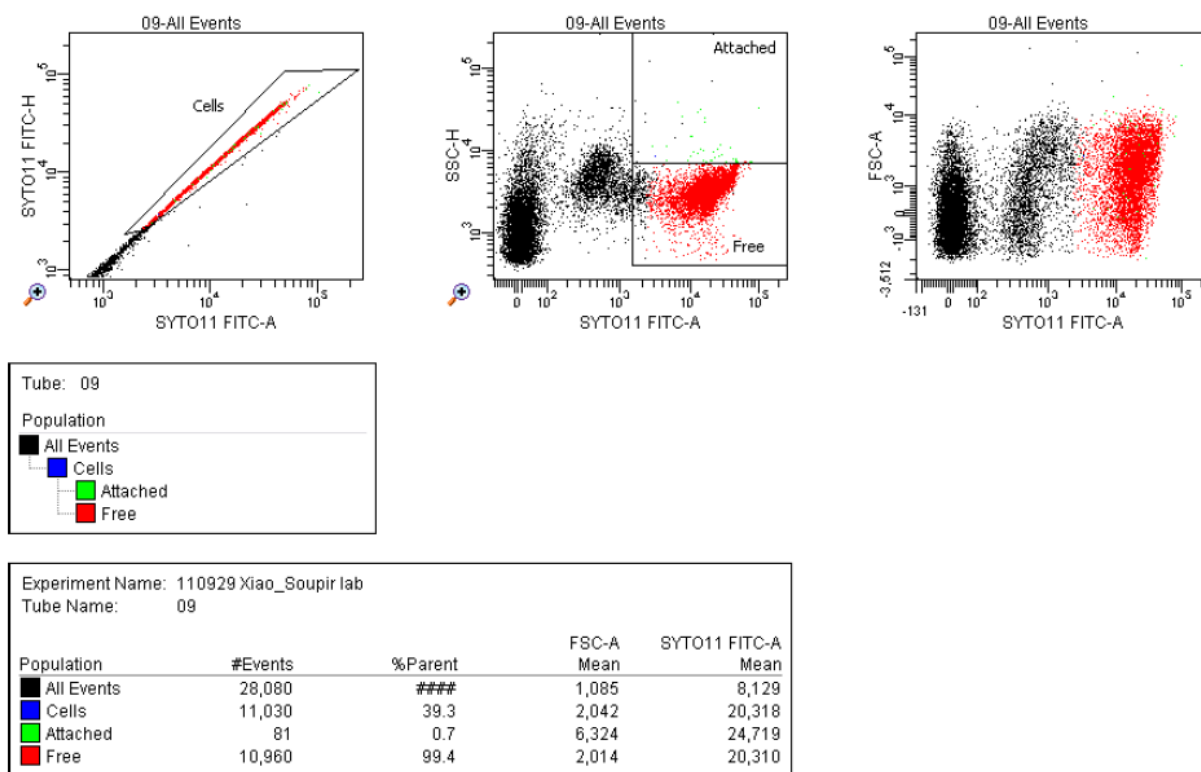


Figure I-7. Dot plot of PBS, strain #31 at 10^7 CFU ml⁻¹, Ca-Montmorillonite at 8×10^{-4} g L⁻¹, and SYTO 11 from flow cytometry (surface area ratio 1).

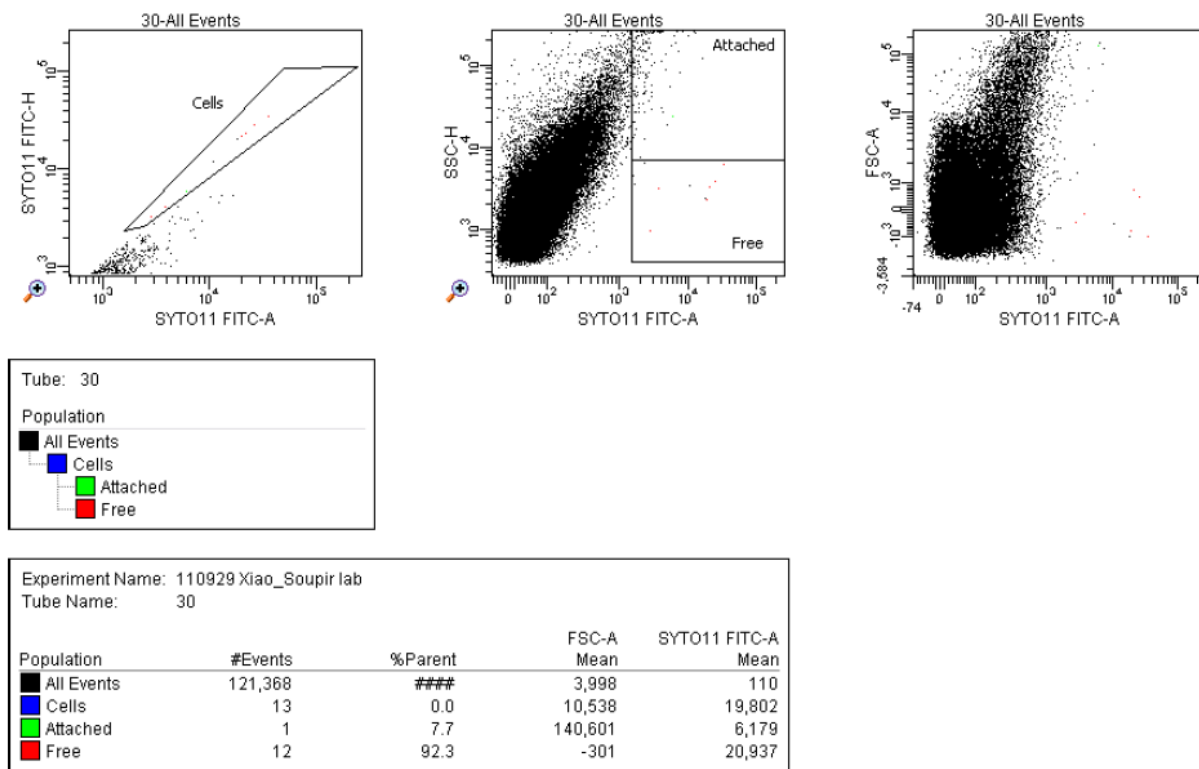


Figure I-8. Dot plot of PBS and Ca-Montmorillonite at $4 \times 10^{-2} \text{ g L}^{-1}$ from flow cytometry.

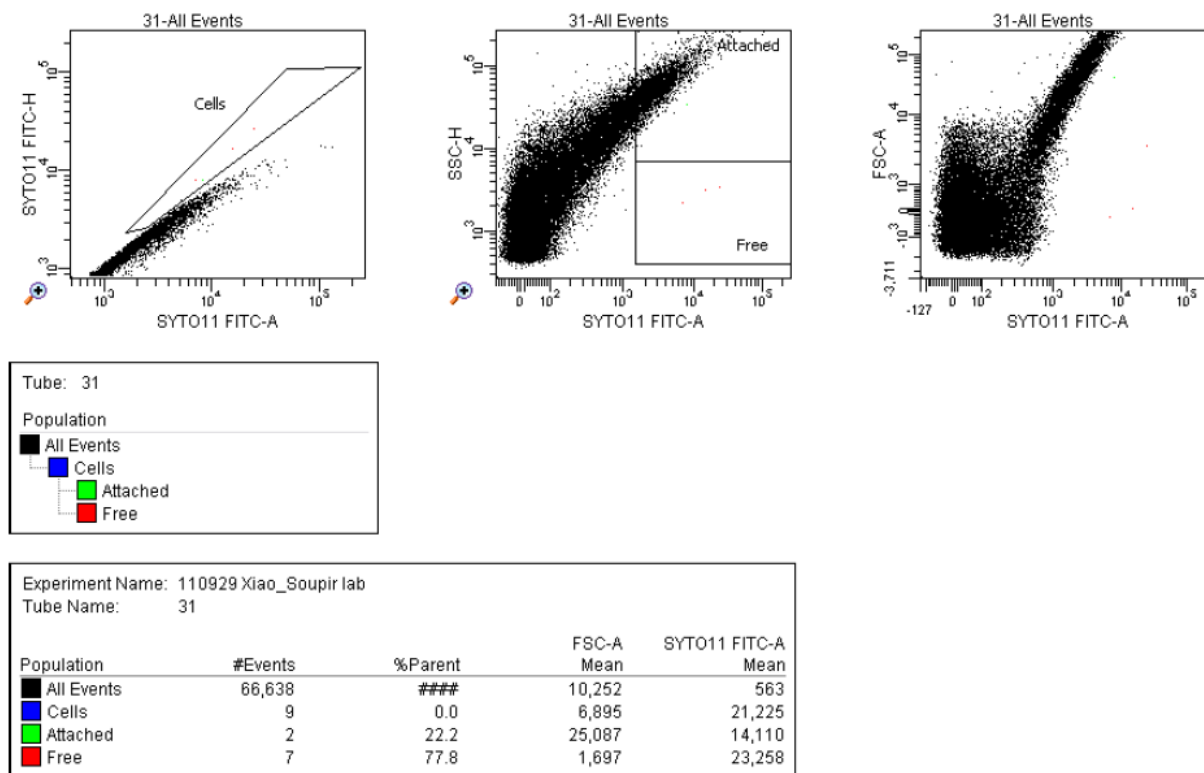


Figure I-9. Dot plot of PBS, Ca-Montmorillonite at $4 \times 10^{-2} \text{ g L}^{-1}$, and SYTO 11 from flow cytometry.

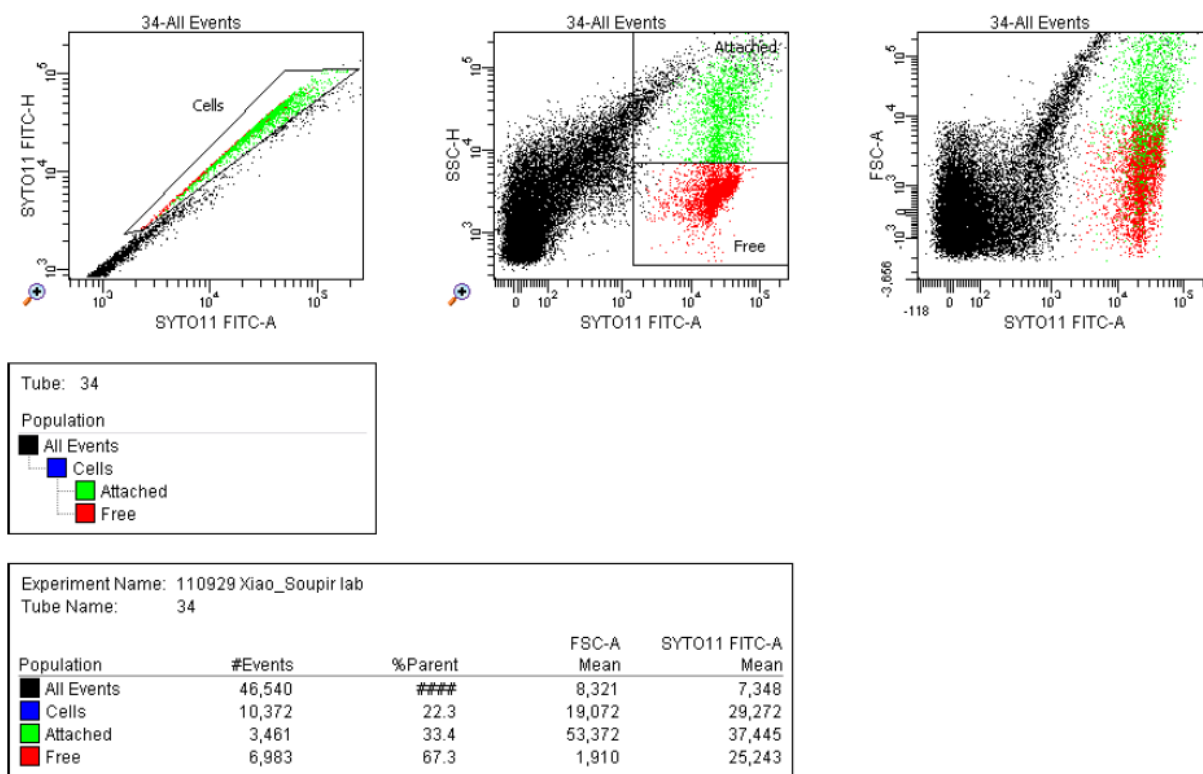


Figure I-10. Dot plot of PBS, strain #31 at 10^7 CFU ml⁻¹, Ca-Montmorillonite at 4×10^{-2} g L⁻¹, and SYTO 11 from flow cytometry (surface area ratio 50).